

Morten Droas

# Stability and lifespan analysis of nanofiltration membrane in binary solution – pilot project

Master's thesis

Trondheim, 15<sup>th</sup> June 2019

1. Supervisor: Prof. Cynthia Hallé, Ph.D. (NTNU, Norway)
2. Supervisor: Prof. Dr.-Ing. P. U. Thamsen (TUB, Berlin)

Norwegian University of Science and Technology

Faculty of Engineering (IV)

Department of Civil and Environmental Engineering



**NTNU – Trondheim**  
Norwegian University of  
Science and Technology

# 1 Abstract

This thesis focuses on the separation of fat contained in the roe solvent extract from the salt and other low molecular weight contaminants. In particular, polar lipids containing omega-3 fatty acids shall be obtained from the extract. They are used as important dietary supplements. The separation is carried out by a laboratory scale nanofiltration test with the winding module DuraMem®300. The applied process conditions were 25 bar, 30 °C and 6.01 L/min (retentate flux). The solvent used consisted of 70 wt.% ethanol and 30 wt.% water.

In this pilot project tests have shown a polar lipids rejection of about 80 % after a stabilization time period during which permeate flux decreases of 30 % was observed. The tests showed that there was a relationship between temperature and rejection and flux observed in the module. The extent of the solvent influence (e.g. by ethanol content) on the performance of the module should be determined in subsequent tests.

This work proves that the desalination of the retentate can be achieved by this type of nanofiltration and that important elements can be enriched in the retentate at the same time.

## 2 Acknowledgement

In the following I would like to thank all those who have contributed significantly to the success of this work. First and foremost, I would like to thank my professor Cynthia Hallé for her support and mentoring of my master thesis, as well as her supervision and co-organization in Trondheim. Also, my thank goes to Professor Dr.-Ing. Paul Uwe Thamsen for his support from the TUB and the attendance of this thesis. Of course, I would like to thank the Norwegian University of Science and Technology (NTNU) Trondheim and the Technische Universität Berlin (TUB).

Furthermore, I would like to thank the cooperation network Nordic Water Network, which is supported by the Federal Ministry of Education and Research and by the German Academic Exchange Service (DAAD). In particular, I would like to thank Markus Fischer, who supported this cross-university project with his excellent organization and communication.

I would like to express another big thanks to the company Artic Nutrition AS and its employees, with whose cooperation this master's thesis was created. I would like to mention the following by name: Ole Arne Eiksund, Hogne Hallaråker, Per Christian Sæbø, Daniele Mancinelli, Marte Frida Grønnevet, Sirgun Lindhom Knardal and Marius Nystøl. During this cooperation I gained a great insight into this company and a lot of practical experience in working on this pilot project. The support of Daniele Mancinelli deserves a special mention! Through his tireless work in the laboratory, answering all my questions and not least as a good friend in Ørsta, he has made a significant contribution to the successful and joyful realization of this work. Above all, I would like to take this opportunity to thank him and his wife Stina Jakobsen once again for their all-embracing support in Norway and for hosting me for the time in Ørsta - especially through you both I was able to spend a great and unforgettable time in Norway!

At this point I would also like to thank my girlfriend Marnie and my friends, especially Katharina Hellmund and her husband Dr. Markus Hellmund for their professional and friendly support in writing this work. For the linguistic corrections and academic hints, I would like to thank Anna Barkhoff in particular.

Finally, this work and the whole stay in Norway would not have been possible without my parents Maike and Michael as well as my grandmother Waltraud. Through their trust and loving support throughout all this time, they have laid the foundation for my career and this thesis. Many thanks for everything!

### 3 Statutory declaration

“I herewith declare that I have composed the present thesis myself and without use of any other than the cited sources and aids. Sentences or parts of sentences quoted literally are marked as such; other references with regard to the statement and scope are indicated by full details of the publications concerned. The thesis in the same or similar form has not been submitted to any examination body and has not been published. This thesis was not yet, even in part, used in another examination or as a course performance. Furthermore, I declare that the submitted written (bound) copies of the present thesis and the version submitted on a data carrier are consistent with each other in contents.” (Goethe-University, 2018)

Trondheim, 13-06-2019

Signature: .....

A handwritten signature in blue ink, appearing to read 'Morten D. Ross', is written over a dotted line.

## 4 Table of content

1	Abstract .....	1
2	Acknowledgement.....	2
3	Statutory declaration .....	3
4	Table of content.....	4
5	List of abbreviations.....	6
6	Table of figures .....	7
7	Table of tables .....	8
8	Introduction .....	9
9	Literature review .....	11
9.1	Process overview .....	11
9.1.1	Composition of fish roe.....	12
9.1.2	Desalination.....	13
9.1.3	Nanofiltration .....	14
9.2	Filtration theory .....	17
9.2.1	Membrane theory .....	17
9.2.2	Membrane fouling .....	20
9.2.3	Membrane types and module overview.....	21
9.2.4	Process control .....	23
9.2.5	Spiral-wound module .....	24
10	Material and methods .....	27
10.1	The pilot plant .....	27
10.1.1	DuraMem®300 .....	27
10.1.2	Pilot plan .....	28
10.1.3	Modes of operation.....	33
10.1.4	Solvent composition.....	34
10.1.5	Feed composition .....	35
10.1.6	Calculations .....	38
10.2	Experimental plan .....	40
10.3	Sampling and analytical methods .....	42
10.3.1	Sampling points and schedule .....	42
10.3.2	UHPLC.....	43
10.3.3	Dry matter analysis.....	43
10.3.4	Solvent test – cleaning approach.....	44
10.4	Source of error .....	44
10.4.1	Error analysis of important measurement methods.....	45

11	Results and discussion.....	48
11.1	Stability analysis .....	48
11.1.1	Stability of rejection .....	48
11.1.2	Stability of permeate flux .....	53
11.2	Lifespan analysis.....	62
11.3	Membrane fouling and cleaning .....	67
11.4	Cleaning approaches .....	68
11.5	Swelling .....	70
11.6	Case study for production (multi-stage test).....	72
11.6.1	Calculation of starting material (9 kg) – first stage.....	72
11.6.2	Product analysis.....	73
11.6.3	Conductivity .....	74
11.6.4	Calculations for simulation – 100 kg assumed start material per batch.....	75
11.6.5	Energy consumption and cost estimation for laboratory scale.....	78
12	Conclusion and recommendation .....	81
13	Future work .....	82
14	List of references .....	83
15	Appendix .....	87
15.1	Tables/Data .....	87
15.2	Figures.....	99

## 5 List of abbreviations

### **A**

A - Membrane surface .....	17
A_active - Active membrane area .....	19

### **D**

DF - Diafiltration test .....	40
DHA - Docosahexaenoic acid .....	9
DM - Dry matter .....	37

### **E**

EPA - Eicosatetraenoic acid .....	13
-----------------------------------	----

### **I**

i - Component one .....	18
-------------------------	----

### **J**

j - Component two .....	18
J - Mass flux .....	17
J_0 - Initial mass flux (permeate) .....	53

### **L**

LPM - Liter per minute .....	19
------------------------------	----

### **M**

m - Mass .....	17
M - Permeate mass flow .....	18
MWCO - Molecular weight cut off .....	27

### **N**

NC - Normal condition .....	40
NF - Nanofiltration .....	15

### **O**

OSN - Organic solvent nanofiltration .....	55
--	----

### **P**

P - Permeability .....	18
PL - Polar lipids .....	12
PTFE - Polytetrafluoroethylene .....	82

### **R**

R_i - Rejection of component i .....	18
RC - Recirculation test .....	40

### **S**

S - Solvent test .....	40
SD - Standard deviation .....	46

### **T**

T - Temperature test .....	40
t - time of flow .....	17
t_operation - Time of operation .....	19
TMP - Transmembrane pressure difference .....	14

### **U**

UV - Ultraviolet .....	43
------------------------	----

### **V**

V_s - Amount of filtrated material .....	19
--	----

### **W**

w - Mass fraction .....	18
-------------------------	----

## 6 Table of figures

Figure 1: Extraction process order in general. ....	11
Figure 2: Composition of fish roe (Artic Nutrition AS, 2018).....	12
Figure 3: Shape of phospholipid. ....	13
Figure 4: C18 saturated Phosphatidylcholin. ....	13
Figure 5: Hierarchy of pressure-driven membrane processes.....	15
Figure 6: Representation of membrane function.....	17
Figure 7: Influence of concentration polarization and fouling compared.....	21
Figure 8: Structure of different asymmetric organic membranes.....	22
Figure 9: General performance of cross flow filtration.....	23
Figure 10: General structure of a spiral-wound module. ....	24
Figure 11: Cleaning approaches for membranes.....	25
Figure 12: Permeate flux over time - reversible and irreversible layering.....	26
Figure 13: Plant design for recirculation mode. ....	29
Figure 14: Legend for recirculation mode.....	30
Figure 15: Plant design for diafiltration mode. ....	32
Figure 16: Dehomogenized mixed fish roe with solvent. ....	35
Figure 17: Microfiltration setup in laboratory scale.....	36
Figure 18: Particles retained by microfiltration in laboratory scale.....	37
Figure 19: Example of an analysis result of UHPLC.....	38
Figure 20: Schematic illustration of experimental plan under NC (25 bar, 30 °C, 6.01 L/min). .....	41
Figure 21: Results of rejection in recirculation mode with feed. ....	49
Figure 22: Results of rejection in the first stage diafiltration mode with feed.....	50
Figure 23: Results of rejection in temperature tests with feed in recirculation mode.....	51
Figure 24: Results of rejection in diafiltration mode for multi-stage diafiltration.....	52
Figure 25: Results of flux conditioning in recirculation mode with solvent.....	53
Figure 26: Results of flux in recirculation mode with feed (0.5 %). ....	54
Figure 27: Results of flux in average in recirculation mode with feed (0.5 %). ....	55
Figure 28: Increased feed concentration during recirculation mode with feed.....	56
Figure 29: Results of flux in first stage diafiltration with feed. ....	57
Figure 30: Results of flux in temperature tests with 0.3 % dry matter in feed. ....	59
Figure 31: Results of permeate mass flow over time in temperature tests with feed.....	60
Figure 32: Flux performance of multi-stage diafiltration with feed.....	61
Figure 33: Approximated lifespan of the first module in recirculation and diafiltration mode with feed. ....	62
Figure 34: Lifespan analysis of 1. & 2. module based on permeate mass flow of PL and solvent. .....	63
Figure 35: Decrease of rejection in lifespan of both moduls with feed. ....	65
Figure 36: Rejection over flux change in the lifespan of both moduls with feed. ....	66
Figure 37: Permeate mass flow over lifespan of the 1. module (solvent and feed). ....	67
Figure 38: Example of cleaning performance in recirculation test. ....	68
Figure 39: Cleaning performance during first stage diafiltration test. ....	69
Figure 40: Swelling effect observed in permeate mass flow performance. ....	71
Figure 41: Conductivity results of multi-stage diafiltration test (case study) with feed.....	74
Figure 42: Calculated results of case study with assumed starting material of 100 kg per batch in the first stage of diafiltration. ....	77
Figure 43: Rejection over permeate mass flow in the lifespan of the moduls with feed. ....	99



## 7 Table of tables

Table 1: Error deviation of mixing solvent used.	45
Table 2: Standard deviation of UHPLC analysis exemplified with DF07, RC02 and T02.	46
Table 3: Error distribution of methods.	47
Table 4: Multi-stage test – designation.	72
Table 5: Overview – material calculations for laboratory scale in multi-stage diafiltration mode.	73
Table 6: External analysis results of the last diafiltration stage.	73
Table 7: Data for conductivity analysis of multi-stage diafiltration tests with feed in laboratory scale.	75
Table 8: Overview – material calculations for assumed scale up in multi-stage diafiltration mode.	75
Table 9: Calculated results for the scale up simulation of multi-stage diafiltration tests.	76
Table 10: Overview over the operation effort for case study in laboratory scale.	79
Table 11: Cost overview of the case study in laboratory scale.	80
Table 12: Overview of the experimental plan.	87
Table 13: Pipette accuracy (1 ml) with pure water.	88
Table 14: Measurement results from sampling – RC01.	88
Table 15: Measurement results from – RC02.	89
Table 16: Measurement results from sampling – RC03.	89
Table 17: Measurement results from sampling – DF01.	90
Table 18: Measurement results from sampling – DF02.	90
Table 19: Measurement results from sampling – DF03.	90
Table 20: Measurement results from sampling – DF04.	91
Table 21: Measurement results from sampling – DF05.	91
Table 22: Measurement results from sampling – DF06.	91
Table 23: Measurement results from sampling – DF07.	92
Table 24: Measurement results from sampling – T01.	92
Table 25: Measurement results from sampling – T02.	92
Table 26: Measurement results from sampling – T03.	92
Table 27: Measurement results from sampling – DF08.	93
Table 28: Measurement results from sampling – DF09.	93
Table 29: Measurement results from sampling – DF10.	93
Table 30: Measurement results from sampling – DF11.	93
Table 31: UHPLC-results of RC01.	93
Table 32: UHPLC-results of RC02.	94
Table 33: UHPLC-results of RC03.	95
Table 34: Conductivity data of the diafiltration test.	96
Table 35: Measurement value deviation of the UHPLC exemplified with DF07, RC02 and T02.	97
Table 36: Test results of laboratory test - basis for calculations.	98

## 8 Introduction

A balanced diet is very important for human health. But many people are lacking essential ingredients during the day (Bundestag, 2005), so that nutrition deficiencies can occur regarding these substances. This can lead to various health consequences. In addition, some people need an increased intake of certain substances from their diet, which they cannot absorb through their daily food alone. An example of this is patients suffering from the skin disease psoriasis vulgaris. Here, omega-3-rich nutritional supplements can help to control this disease (Otterlei, 2018). Furthermore, omega 3 fatty acids have anti-inflammatory effects and protect against various neurological and metabolic diseases (Parmet, 2019).

The company Artic Nutrition, for example, developed a product which is rich in omega-3 fatty acids – such as docosahexaenoic acid (DHA). This omega-3 fatty acid is particularly found in cold water fish and is extracted from the fish roe.

The quality of the extracted fats is very important and is determined by the lowest possible proportion of heavy metals, other fat types, proteins and contaminants. Furthermore, the lowest possible salt content is desired. This is produced in the conventional process by means of a thermal or chemical desalination process through crystallization. Since the quality of the omega-3 fatty acids can be reduced by this type of heat treatment, an alternative desalination process using nanofiltration is being tested in this project.

The membrane module to be tested in this thesis was selected by a previous screening test (Zefikj, 2017). It was found that the DuraMem®300 has the best rejection with high ethanol content in the feed and the lowest standard deviation. As a result, this membrane was recommended for further pilot testing using full scale nanofiltration membrane module.

The main objective of this work is to test the stability and lifetime of the membrane module DuraMem®300 for the isolation of phospholipid from fish roe. To reach this main objective, four specific objectives were identified:

1. Explore the membrane module behavior in binary ethanol-water solution.
2. Evaluate the rejection and permeate mass flow performance using different feed concentration of phospholipid and temperature.
3. Investigate the cleaning procedure of the membrane module.
4. Estimate the cost and energy requirement for the production of phospholipid using DuraMem®300.

In general, the test has been carried out with conditions as close as possible to the current industrial process. Even though it is not possible to make an exact comparison with a full-scale plant (Reisman, 2008). Data of rejection and flux will be provided more consistent with the industrial scale by cross-flow filtration regarding to Tsibranska & Saykova (2013).

In principle, a first impression of fouling or other types of phenomenon, which can occur in a long-term use of the module, will be obtained and evaluated.

The following hypotheses are formulated and will be evaluated at the end of this thesis:

- Permeate flow provides a stable flux.
- Rejection will be stable
- Sodium passes through the membrane and magnesium and calcium will be retained in the retentate; product quality will increase.
- The module can work for a longer period of time without significant fouling.

This thesis starts with a literature review presenting the basic theories on membranes, processes, process types and the module type used. This is followed by the chapter "material and methods" in which the pilot plant with its components, operating modes and materials used is presented at the beginning. After an overview of the experiments carried out, the methods for analysis and data measurement are presented. At the end of this chapter, possible sources of error are analyzed in more detail. The results and discussion chapter presents the data evaluation of flux stability, rejection and process parameters. The lifetime of the module is estimated and further aspects such as membrane blocking, and cleaning applications are investigated. Subsequently, a case study will be explained, and the resulting product will be analyzed. An estimation of the costs of this case study will follow. Finally, the results will be summarized, and an outlook is given.

## 9 Literature review

In this chapter, theoretical basics about omega-3 fatty acids and membrane filtration will be presented as a basis for following chapters.

### 9.1 Process overview

In this section, the general process for the extraction of omega-3 fatty acids from fish roe is described. This pilot project will be placed in the following process structure at the end.

The general extraction process is illustrated in Figure 1.

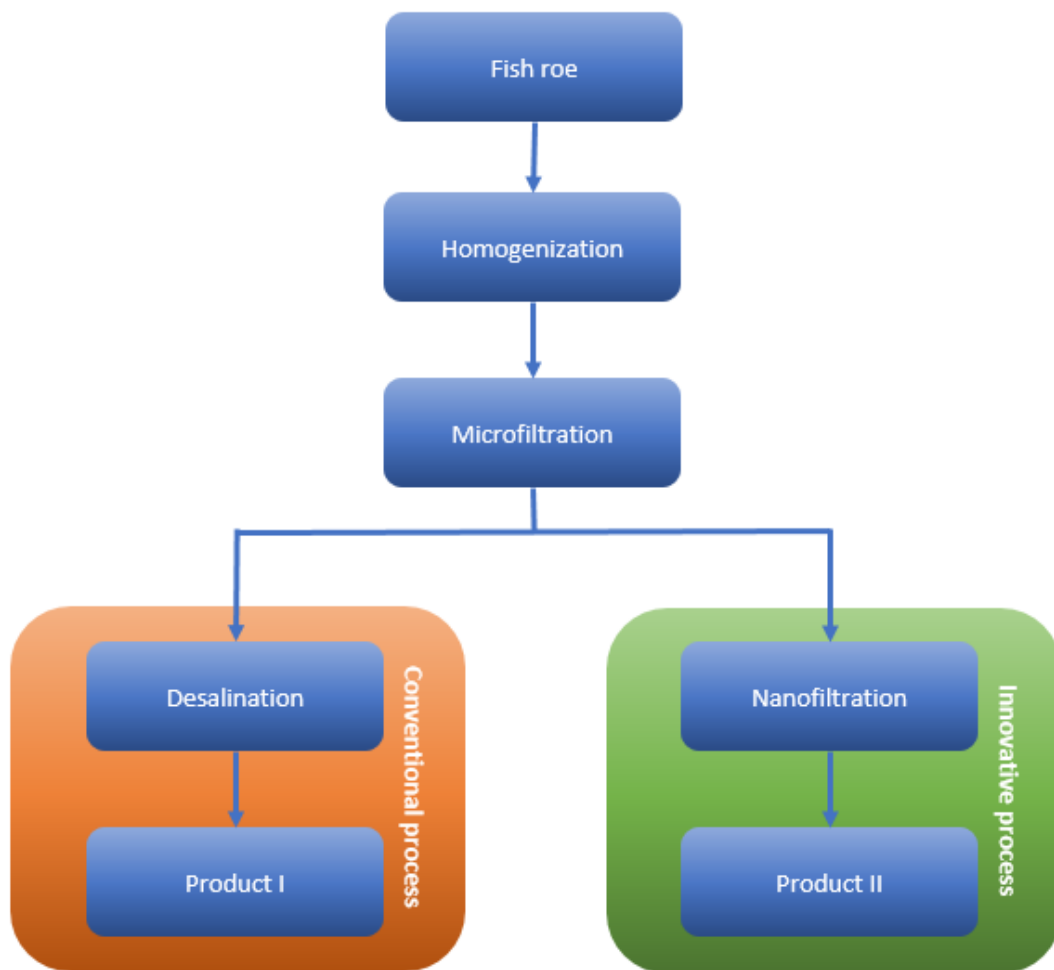


**Figure 1: Extraction process order in general.**

The first step is to homogenize the selected roe followed by microfiltration as second step – these process steps will be described in Chapter 10.1.5.1. In the conventional process currently in use, the mixture will be desalinated. This desalination process is called crystallization, which is described in Chapter 9.1.2 and an extract of fish roe is obtained.

The process step investigated in this thesis for the treatment of the mixture is the application of nanofiltration as an alternative desalination process. In the following chapters, composition of fish roe used and differences between desalination and nanofiltration processes are explained.

### 9.1.1 Composition of fish roe

In this section, fish roe composition and important components will be explained, to understand the material used in the process.

The immature fish roe can be purchased from the fish industry and transformed to produce nutritional supplements. The composition of the fish roe used is shown in Figure 2.

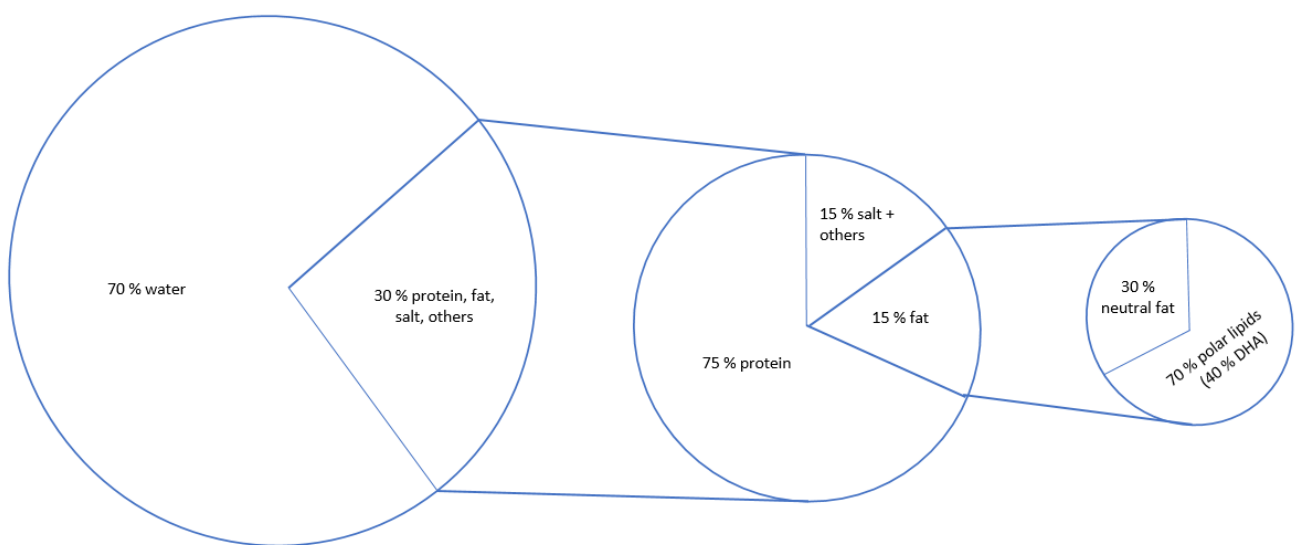


**Figure 2: Composition of fish roe (Artic Nutrition AS, 2018).**

The fish roe consists of approximately 70% water and 30% proteins, fats, salts and other substances. They are divided into 75 % proteins, 15 % salts and other substances, as well as 15 % fats. The fat content consists of 30 % neutral fat and 70 % polar lipids (PL), of which 40 % are DHA. These DHA shall mainly be obtained from the fish roe.

Two types of lipids are existing, namely neutral and polar lipids. The latter differ from the neutral lipids by a greater polarity. Furthermore, both groups usually have a hydrophobic characteristic, i.e. they are difficult to dissolve in water. In fats, oils and other organic solvents, however, these substances can usually be dissolved very well (lipophilic characteristic) (Ulrih, Gmajner, & Raspor, 2009).

Phospholipids belong to polar lipids. They have a hydrophobic hydrocarbon tail and a hydrophilic head (see Figure 3). Through this phosphorous group the phospholipids are able to bound to water and other polar molecules like ethanol. The hydrocarbon compound of the tail

is apolar and forms hydrophobic bonds to fats, because there is no possibility for repulsive interaction between uncharged molecules (Goss & Schwazenbach, 2003).

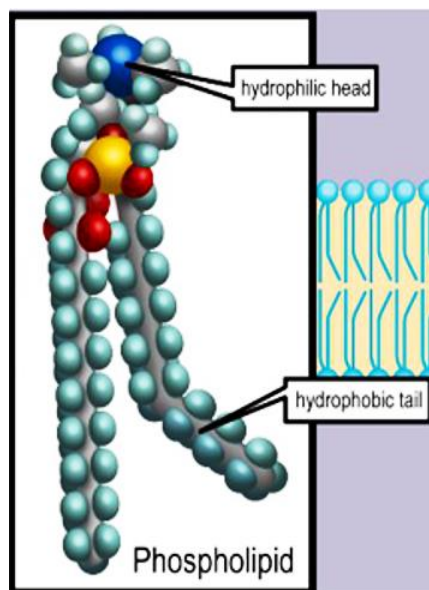


**Figure 3: Shape of phospholipid.**

Omega-3 fatty acids are unsaturated fatty acids which are essential for human body and cannot be produced independently. These include the two omega-3 fatty acids docosahexaenoic acid (DHA) and eicosatetraenoic acid (EPA), which are mostly found in fatty fish.

A molecule, which gives an impression of the average molecule from the polar lipids rejected, is given in Figure 4 (designed with ChemDraw Professional 16.0). The molecular weight is around 834 g/mol.

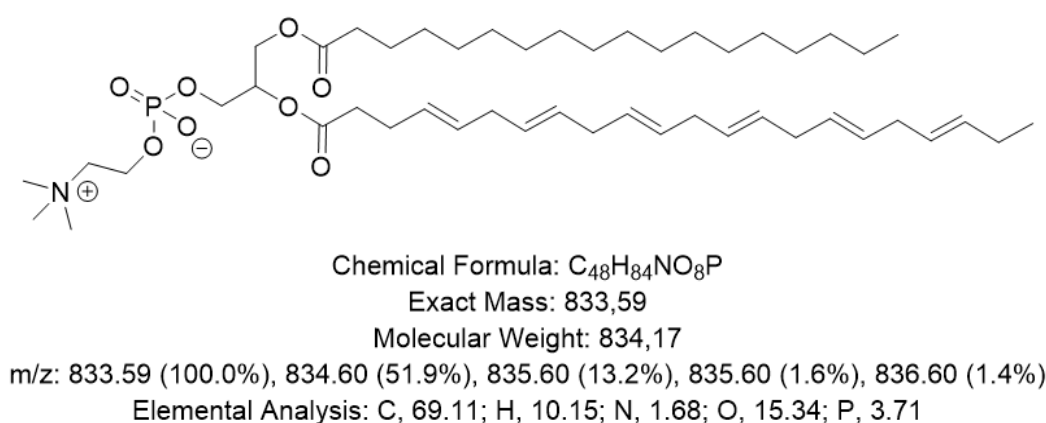


**Figure 4: C18 saturated Phosphatidylcholin.**

### 9.1.2 Desalination

The currently used desalination process got great importance to the best possible desalination of the extract in order to improve the taste component and compatibility through minimum salt

content of sodium ( $\text{Na}^+$ ) and chloride ( $\text{Cl}^-$ ). The microfiltered mixture is filled into a rotary evaporator and heated under the addition of pure ethanol. This makes use of two effects that reduce the water content of the mixture. On one hand, heating the mixture makes the liquid evaporate, that water leaves the system and the mixture is further concentrated. On the other hand, the addition of pure ethanol reduces the water content of the mixture, too. Since salts can dissolve much better in water than in ethanol, the reduction of the water content in the salty mixture causes precipitation of the salt molecules – the salt crystallizes out. The remaining mixture is then filtered again to remove the salt crystals. This process separates sodium, chloride as well as calcium ( $\text{Ca}^{2+}$ ) and magnesium ( $\text{Mg}^{2+}$ ) from the product. Furthermore, this type of desalination of omega-3 fatty acids EPA and DHA are subjected to an additional thermal stress which can negatively influence their quality (Pike & Jackson, 2010). In order not to influence the product quality negatively, the desired nutrients should be strained as little as possible by heat or oxygen. It is therefore being considered to replace desalination using evaporation of residual water (conventional process) by nanofiltration (innovative process) through a membrane; which is explained in the next chapter.

### **9.1.3 Nanofiltration**

Nanofiltration got its name from the fact that a significant rejection of components is only achieved from a molecular weight higher than 200 kg/kmol. This molecular weight corresponds approximately with a molecule size of 1 nm. The usual transmembrane pressure difference (TMP; see chapter 9.2.1) is between 3 and 30 bar (Melin & Rautenbach, 2007).

Nanofiltration membranes are ion selective and can retain polyvalent anions or cations whereas monovalent anions or cations are more likely to pass through the membrane (see Figure 5 regarding to Crittenden et al. (2012)).

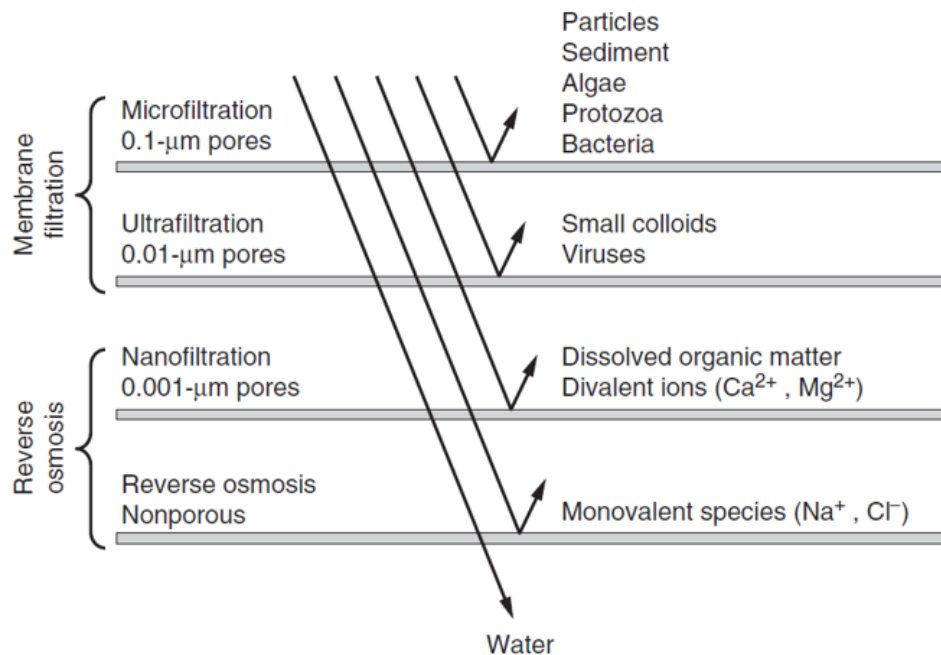


**Figure 5: Hierarchy of pressure-driven membrane processes.**

As a result, nanofiltration can serve as an alternative desalination process without exposing the entire mixture to additional thermal stress due to evaporation.

On one hand, removing monovalent species of ions is desired. On the other hand, an increased magnesium and calcium content can further increase the quality of the desired product, as these substances are important and often in demand for a healthy nutrition. E.g. magnesium deficiency can lead to serious consequences such as heart attacks (Li, et al., 2011), whereas calcium deficiency can lead to symptoms of hypocalcemia (Larsen, 1999).

Based on serial investigations of numerous nanofiltration (NF) membranes the rejection of anions increases in the order  $\text{NO}_3^-$ ,  $\text{Cl}^-$ ,  $\text{OH}^-$ ,  $\text{SO}_4^{2-}$ ,  $\text{CO}_3^{2-}$ . The rejection of cations increases in the order  $\text{H}^+$ ,  $\text{Na}^+$ ,  $\text{K}^+$ ,  $\text{Ca}^{2+}$ ,  $\text{Mg}^{2+}$ ,  $\text{Cu}^{2+}$  (Melin & Rautenbach, 2007). Because of electrostatic interactions higher charged ions are more prevented by passing the membrane. As soon as an ion species is retained by the semipermeable membrane, a requirement for the occurrence of the Donnan effect is fulfilled. This effect results in an uneven distribution of the ion concentration on the retentate side and the permeate side (Melin & Rautenbach, 2007). If the non-permeating ion species is more concentrated on the retentate side, the permeating ions will compensate this imbalance. Therefore, the ions that have passed into the permeate may diffuse back through the membrane to the retentate side. This ion exchange restores the electrochemical



equilibrium. The net charge is removed from the system and the sum of the equivalent concentrations is balanced on both sides. This ion movement creates a particle flow in the opposite direction to the diffusion. Furthermore, larger ions that do not diffuse through the membrane can cause smaller, equally polar ions on the same side to move more strongly into the permeate to compensate for the potential difference, resulting in a lower rejection of this component.

Due to the different concentration distribution (difference in activity) on both sides of the membrane, the solvent flows back from the permeate into the retentate. This is related to the target to dilute the concentrated components in the retentate. Thus, a concentration equilibrium will be achieved. This process is based on the effect of the osmotic pressure against the direction of diffusion (Kraume M., Membranverfahren, 2014).

## 9.2 Filtration theory

Firstly, the basics of filtration theory will be presented. Afterwards, membrane fouling, different membrane types, modes of operation and, in particular, the winding module used in this paper will be discussed.

### 9.2.1 Membrane theory

According to Melin & Rautenbach (2007) a membrane is generally described as follows:

"Membranes are flat, partially permeable structures that are permeable to at least one component of a fluid – a liquid or a gas – contacting them, but impermeable to others."

The task of most membranes to mechanically separate substances from each other is based on this description. Figure 6 illustrates the general use of a cross flow membrane (Melin & Rautenbach, 2007).

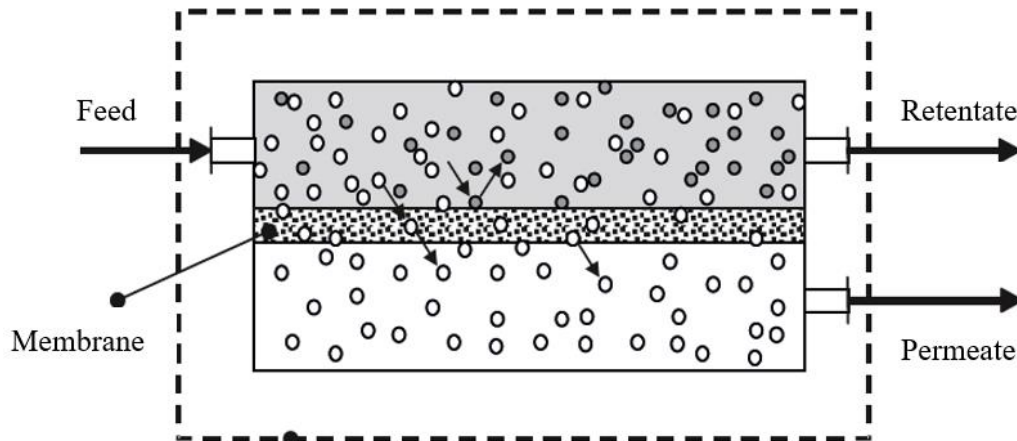


Figure 6: Representation of membrane function.

This membrane usually has at least one inlet for the fluid to be separated (feed) and at least two outlets; one outlet for the separated substance (permeate) and one outlet for the retained substance (retentate). Some particles are passed through the membrane, others not. This may be due to different sizes, concentrations, polarities or other material properties.

The material flow which flows through the active membrane surface over time is called mass flux  $J$  [ $\text{kg}/\text{m}^2\text{s}$ ] and is composed of the corresponding mass  $m$  [ $\text{kg}$ ], the membrane surface  $A$  [ $\text{m}^2$ ] through which the material flows and the corresponding time of the flow  $t$  [ $\text{s}$ ]:

$$J = \frac{m}{A * t} \quad (9.1)$$

The advantage of this formula is that the value of  $J$  does not directly depend on the size of the considered system. Thus, an area-specific assessment of the mass flow can be made. If, on the

other hand, two systems with the same mass flows (mass flux) are compared, the system with the larger membrane area will also enable a larger mass transport (Crittenden et al., 2012). Thus, the flux can be understood as the efficiency of a membrane.

Furthermore, the permeate mass flow  $M$  [kg/s] can be used to visualize the absolute value of mass which was produced. It results from the multiplication of the flux  $J$  with the corresponding membrane area  $A$ :

$$M = \frac{m}{t} = J * A \quad (9.2)$$

Another important parameter in filtration technology is the separating efficiency of a membrane. One of the underlying properties is the selectivity of the membrane, which is the ability to distinguish between the components of a mixture. The selectivity can be defined by the mass fractions of permeate (P) and feed (F) as follows (Melin & Rautenbach, 2007):

$$S_{ij}|_w = \frac{w_{iP}/w_{jP}}{w_{iF}/w_{jF}} = \frac{w_{iP}/(1 - w_{jP})}{w_{iF}/(1 - w_{jF})} \quad (9.3)$$

The mass fractions  $w$  of components  $i$  and  $j$  are used for the permeate and the feed in this equation.

In order to measure the selectivity of a membrane filtration with regard to one component – in this thesis polar lipids – the rejection  $R_i$  is used:

$$R_i = \frac{w_{iF} - w_{iP}}{w_{iF}} \quad (9.4)$$

Here, the mass fraction of the component  $i$  that is to be investigated in the feed and in the permeate is used to determine the rejection of this component.

Permeability parameter  $P$  can be used for the transmittance of a membrane:

$$P = \frac{J}{TMP} = \frac{m}{t * A * TMP} \quad (9.5)$$

In addition to the flux  $J$ , this contains the transmembrane pressure difference  $TMP$ .

The transmembrane pressure difference  $TMP$  is the pressure difference between the feed side and the permeate side, which is used as the driving force for the separation process of pressure-driven membrane processes. It can be generated by a vacuum on the permeate side or, as is often the case, by an overpressure on the feed side.

For better comparability the amount of filtrated material through the module the specific volume ( $V_s$ ) [L/m<sup>2</sup>] is used to provide certain charts with dependency of time.

$$V_s = \frac{t_{operation} * LPM}{A_{active}} \quad (9.6)$$

For this operation time  $t_{operation}$  is multiplied with LPM in [L/min] and divided by the active membrane area  $A_{active}$ . LPM describes the amount of liquid per minute flowing through a cross section – in this case the amount of retentate produced from the module.

### 9.2.2 Membrane fouling

All components of the mixture to be separated are transported convectively and diffusively to the membrane surface from the core flow of the feed. During permeation, at least one component is strongly retained due to the selectivity of the membrane. In the stationary operating state, this component must be transported back into the core flow. In the immediate environment of the membrane surface, the flow is very slow, so that this re-transport only occurs by diffusion. The requirement for diffusive transport is a concentration gradient, i.e. an increase in concentration for the retained component and a drop in concentration for the preferred permeating component at the membrane (Crittenden et al., 2012, p. 334). The formation of these concentration sections is called concentration polarization. This can lead to a deterioration of the separation result, as the driving force for the preferentially permeating component is reduced and that of the retained component is increased as a result of the change in concentration at the membrane surface (Crittenden et al., 2012, p. 1368). The former means that the total flux decreases. The latter means that the desired component is lost to the permeate.

During operation, substances which reduce the flux and thus worsen the filtration results are deposited on the membrane over time. A distinction is made between two types of deposition: fouling and scaling.

In scaling, the retentate is concentrated above the solubility limit of a substance dissolved in the feed, so that it precipitates and blocks the membrane (Crittenden et al., 2012, p. 1376). Especially with winding modules, it is a challenge to rinse the crystal sludge out of the module. Therefore, scaling should be avoided by certain methods such as removal or stabilization of the substances or their chemical transformation, so that the saturation concentration is never reached for the dissolved substance.

The term fouling describes in principle the flux decrease by membrane blocking, which is produced mainly by extracellular substances and proteins, which form a slime layer when accumulated and block the pores. A distinction can be made between biofouling and colloid fouling. In both cases, a cover layer builds up on the membrane surface, so that the performance of the membrane is no longer determined just by the membrane resistance, but the system cover layer/membrane influences the performance of the module. Thus, the top layer stands for a further resistance, which has to be overcome during permeation. On the other hand, the top layer on the membrane also increases the rejection of certain components.

Figure 7 shows an assessment of the influence of fouling on permeate flow according to Kraume (2014). It can be seen that fouling can influence the permeate flow significantly more than concentration polarization.

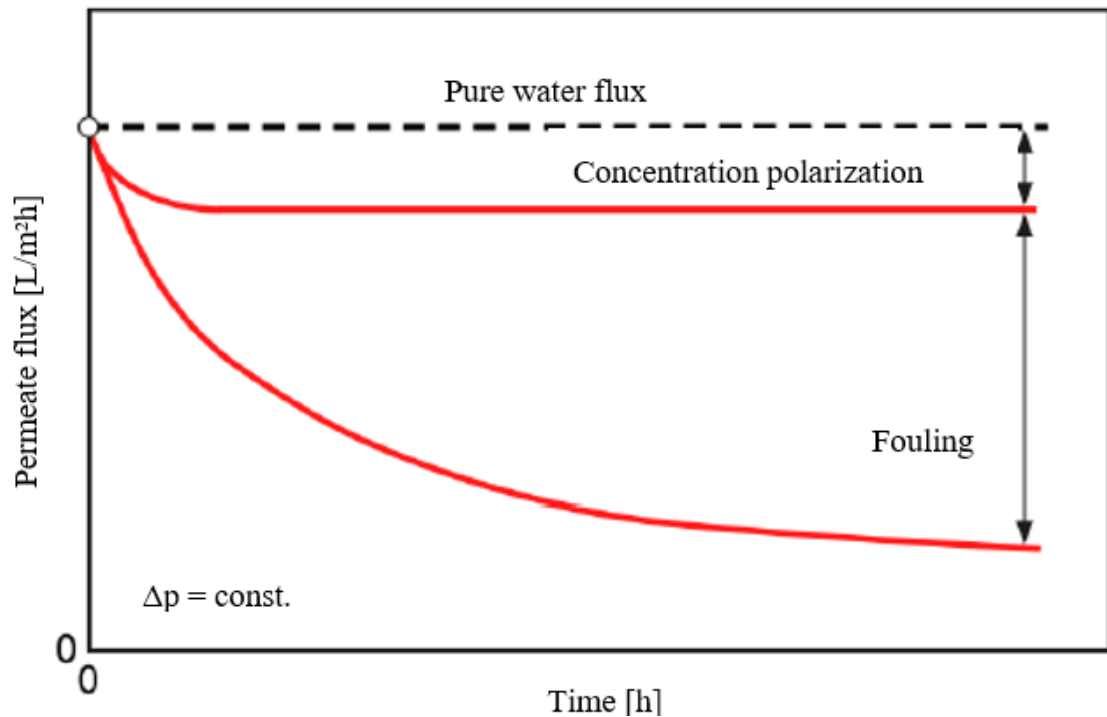


**Figure 7: Influence of concentration polarization and fouling compared.**

Biofouling is a special type of fouling. Small microorganisms accumulate on the membrane and form an extracellular polymeric substance with a slimy consistency. This biofilm is unavoidable during filtration with water and can lead to a permeate drop of up to 10 % (Melin & Rautenbach, 2007). This drop is mainly caused by an increase in concentration polarization, a decrease in transmembrane pressure and an increase in frictional resistance.

### 9.2.3 Membrane types and module overview

Membranes can be divided into synthetically produced and biological membranes. The aim is to synthetically reproduce the properties of biological membranes, as their effectiveness is considered to be ideal. There are both liquid and solid synthetic membranes, with the solid membranes, which occur most frequently, being organic or inorganic. Inorganic membranes are always porous. Organic membranes can be porous or non-porous. In morphology, symmetric membranes can always be assigned to porous membranes, while asymmetric membranes can also be non-porous. In this case, it is a so-called solution-diffusion membrane. Asymmetric membranes can be produced synthetically by a composite process and a phase inversion process.

In the composite process, the membranes are composed of different polymers; therefore, these membranes are also called composite asymmetric membranes. Usually a thin, homogeneous polymer layer is applied to a microporous supporting layer. The desired properties of the different membrane layers can be better adapted.

In the phase inversion process, on the other hand, only a single polymer is used for production. These so-called integral asymmetric membranes are produced by precipitation of the polymer from a homogeneous solution. The transition between the substructure and the active separation layer is continuous, and both layers consist of the same material; however, they have different pore sizes (Melin & Rautenbach, 2007).

Figure 8 (Melin & Rautenbach (2007); California Patentnr. 3,133,132, (1964)) shows the difference between the two manufacturing variants.

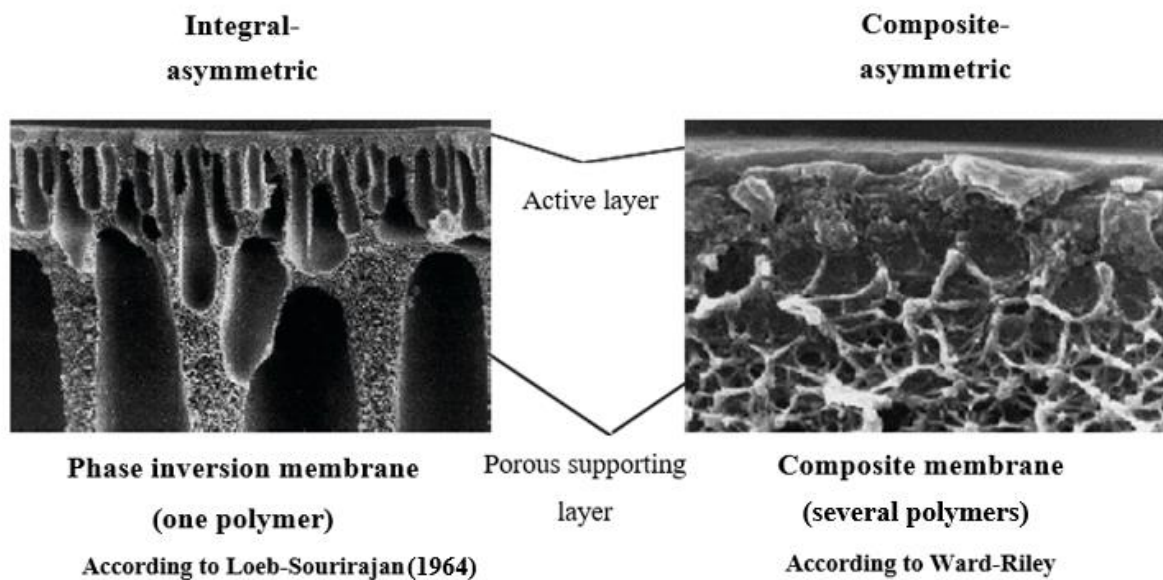


**Figure 8: Structure of different asymmetric organic membranes.**

In general, two types of membranes can be distinguished: the pore membrane and the "tight" solution diffusion membrane. The pore membrane is defined as having a mostly porous structure so that particles can be transported through the membrane as a result of convective flow. A pure solution diffusion membrane, on the other hand, is "tight", so that the transport through this type of membrane is exclusively diffusive.

In most cases, this type of membrane has an asymmetrical structure. It has a dense layer (solution diffusion membrane) and a porous supporting layer (pore membrane), which gives the actual active separation layer the required stability. The separation-active layer should be as thin as possible in order to enable the lowest possible diffusion path. It should be ensured that this separation layer has no flaws or small pores, as these leaks can already impair the separation efficiency of the membrane (Kraume, 2014).

## 9.2.4 Process control

There are two types of process control in filtration processes: dead-end filtration and cross-flow filtration (Kraume, 2014). In dead-end filtration, the fluid flows orthogonally against the filter. The liquid will pass through the filter and the suspension particles form a filter cake on the membrane, which grows over time and must be separated. From this fact it follows that such a process is a discontinuous process. The process control used in this thesis is cross-flow filtration, which is described in more detail in the following chapter.

### 9.2.4.1 Cross flow filtration

Cross flow filtration was developed to avoid the frequent and cost-intensive replacement of membrane modules after fouling. This makes it possible to implement a continuous process with a longer lifespan. In this process, the mixture flows parallel to the membrane surface. The permeate is separated transversely to the flow direction, as shown in Figure 9 (Kraume M., 2012).

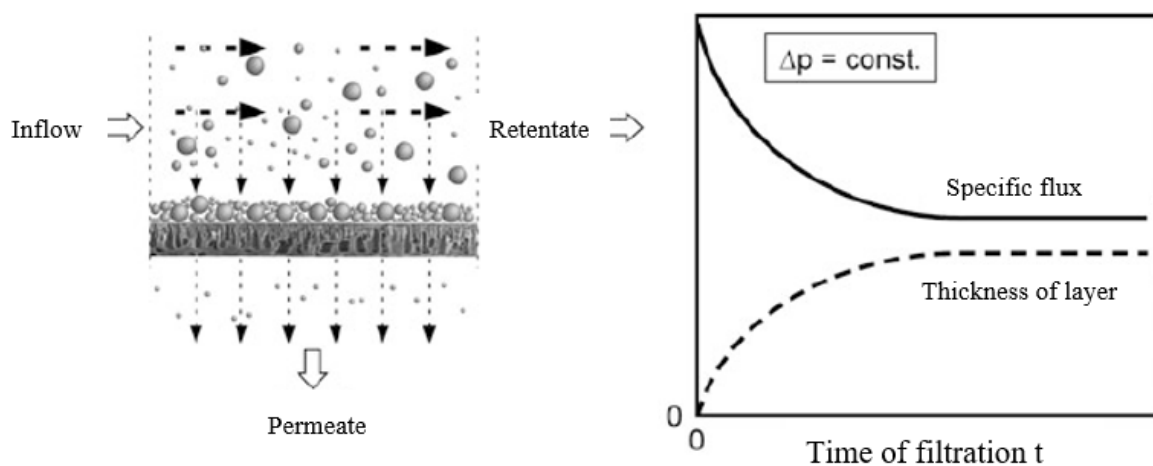


**Figure 9: General performance of cross flow filtration.**

This transverse flow generates shear and uplift forces on the membrane surface, which return the particles deposited on the membrane back to the core flow, except for a thin particle base layer. Ideally, the thickness of the top layer converges to a constant value, so that the specific filtrate flux also assumes a constant value. In fact, however, the technical application shows a gradual decrease in the specific filtrate flow over time. Reasons for this are, for example, fine particles blocking the particle top layer or the filter medium (Kraume M., 2012).

The composition and thickness of this particle base layer vary with the operating conditions and can significantly increase the overall flow resistance. Nevertheless, this type of process control leads to the avoidance of larger cover layers, which can significantly increase the resistance. It



is therefore important to have as high an overflow velocity as possible along the membrane surface – this requires a relatively high energy input.

### 9.2.5 Spiral-wound module

The process control of cross-flow filtration described above can be implemented in the form of a spiral-wound module. This will now be further explained.

The spiral-wound module in Figure 10 (Melin & Rautenbach, 2007) consists of one or more membrane layers, each of which is wound spirally around a permeate collecting tube with a net-like spacer. The membrane pocket consists of several membranes between which a spacer for permeate removal is incorporated. On one side the membrane layer is connected to the perforated permeate collecting tube – the other sides are closed. The feed flows in at the end face and flows axially through the module, while the permeate flows spirally inside the porous permeate spacer to the collection tube.

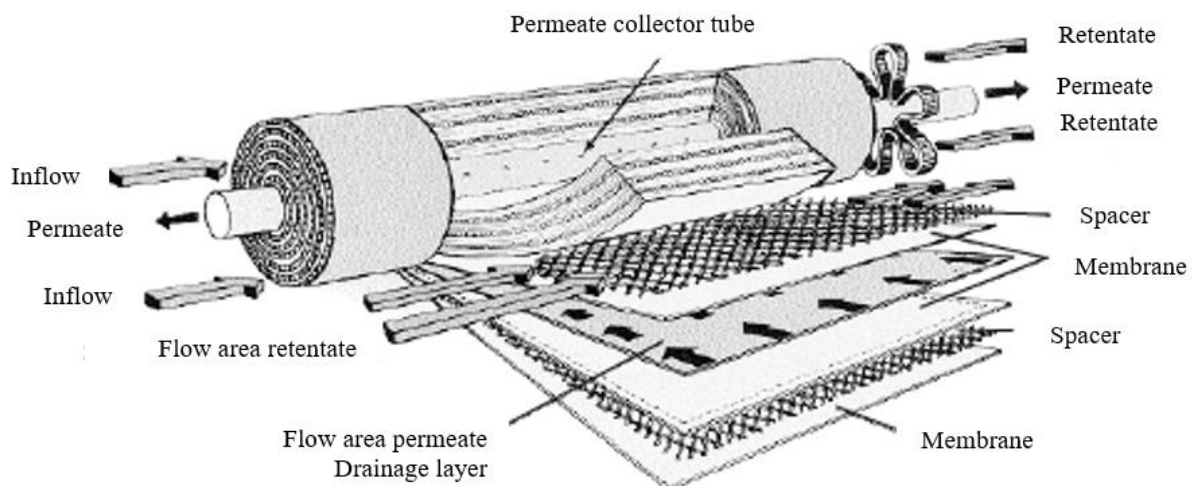


**Figure 10: General structure of a spiral-wound module.**

In general, very high packing densities ( $< 1000 \text{ m}^3/\text{m}^2$ ) can be attributed to the winding modules (Karger & Hoffmann, 2013, p. 168). However, this also results in a relatively poor module cleanability, which is reinforced by the spacers incorporated on the feed side, and a relatively high pressure drop. This can compress the membrane winding in the axial direction and narrow the feed and permeate (Melin & Rautenbach, 2007, p. 174). Furthermore, the feed-side spacers not only have the task of ensuring the distance between the membranes, but they also have a positive effect on the mass transfer as well as on the flow shape. The spacers allow a better control of the concentration polarization by increasing the turbulence even at relatively low flow velocities (Kraume M., 2014, pp. 4-8). This not only leads to better mixing, but also has a positive effect on the shear forces that occur to remove the surface layer.

### 9.2.5.1 Cleaning options – Winding module

In general, it is very difficult to remove the crystal sludge produced by the scaling from the winding modules only by shear forces (Karger & Hoffmann, 2013). Also, the removal of the top layer created by the fouling is only possible to a limited extent. The top layer increases the thickness of the active separation layer and changes the nominal pore diameter of the membrane (Kraume M., 2012).

Usually in membrane processes, cleaning methods like backwashing or chemical cleaning as shown in Figure 11 (Melin & Rautenbach, 2007, p. 858) are used to recover the flux. This example is operating at constant TMP.

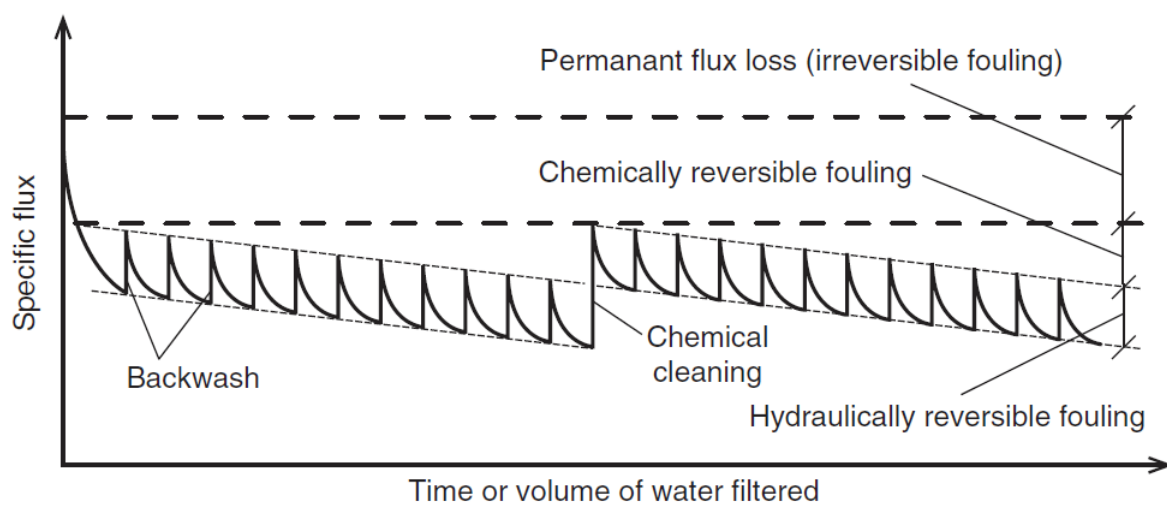


**Figure 11: Cleaning approaches for membranes.**

Flux loss, which can be recovered by backwashing is called hydraulically reversible fouling. In this case, mainly large particles occurring during cake formation, can be removed. During chemical cleaning, small particles – clogging within the membrane matrix and due to slow adsorption – can be dissolved and removed (Melin & Rautenbach, 2007, p. 858). This type of fouling is called chemically reversible fouling.

Since backwashing is not possible in some cases and chemical cleaning does not promise success in some cases, one of the few possibilities for cleaning a winding module is to exploit the hydrodynamics. Due to high overflow speeds, correspondingly high shear forces can be exerted on the surface layer so that it can be removed in the overflow direction. The top layer can consist of two layers – one reversible and the other irreversible (Crittenden et al., 2012, p. 857). The reversible top layer can be removed by appropriate shear forces. The irreversible top layer usually consists of many small particles, which are attached closely to the membrane and

cannot be detached from the membrane surface by hydrodynamically generated mechanical forces alone.

In cross-flow filtration, a simplified assumption can be made that a purely reversible top layer is formed. After a running-in phase, in which the permeate flow initially decreases as a result of the build-up of the top layer, a stationary state occurs in which the mass flow of the particles transported to the top layer corresponds exactly to the mass flow that corresponds to the particles transported away again by diffusive or dynamic effects (see Figure 12 (Kraume M., 2012, p. 305)). Increasing temperature causes an increase in transmembrane pressure difference and feed flow. The value of stationary permeate flow can be increased by reducing the feed concentration (Kraume M., 2012).

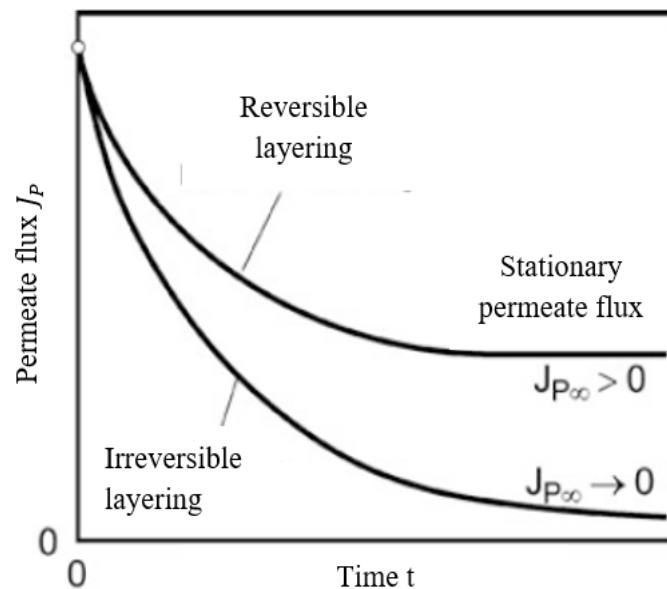


**Figure 12: Permeate flux over time - reversible and irreversible layering.**

Due to the feed spacers, shear force increasing turbulences can be generated even at low flow velocities in order to remove most of the reversible cover layer. In reality, however, there is usually always a certain decrease in permeate flow and irreversible formation of the cover layer. This is caused, for example, by fine particulates blocking the top layer of the particles or the filter medium (Kraume M., 2012, p. 304).

## **10 Material and methods**

This chapter presents the materials and methods used in the series of experiments. Essential laboratory equipment and routine work steps will be described.

### **10.1 The pilot plant**

This chapter briefly introduces the main features of the pilot plant and its general mode of operation. First, the membrane module used will be presented, then the pilot plant will be described. After explaining the modes of operation, used liquids will be introduced, before general calculations will follow.

#### **10.1.1 DuraMem®300**

DuraMem®300 from Evonik Resource Efficiency GmbH was the selected module (Evonik Resource Efficiency GmbH, 2017). It consists of an organic modified polyimide and has an integral asymmetric structure. The membrane has a molecular weight cut off (MWCO) of 300 Da, with an apolar surface that can tolerate a maximal pressure of 60 bar and a maximal temperature of 50 °C. It can be classified as a synthetic, solid, organic, non-porous and asymmetric-phase-inverse membrane. The module has an active membrane area of 0.11 m<sup>2</sup> and is typically operated at a feed flow of 150 L/h.

In this study, the module is operated at a pressure of 25 bar, a temperature of 30 °C and an LPM (Liter of retentate Per Minute) of 6.01 L/min.

##### **10.1.1.1 Preparation of the module**

Before a new module was used in the process, it was cleaned from the preservatives. The system (without module) was filled with three liters of ethanol (99.95%) and flushed at low pumping speed. The ethanol was then discharged, and the system was filled up to the top mark of the tank with solvent (see Chapter 10.1.6.3). The membrane module was then inserted into the intended module housing of the system and operated for a few minutes at a pump speed of 1 % until the entire system, including the membrane module, was filled with solvent. The pump was then stopped, and the membrane was allowed to condition for a few hours.

### **10.1.2 Pilot plan**

In general, this pilot plant is designed to pump the desired mixture, which will be separated, into the corresponding membrane module by a pump. The liquid passes through a heat exchanger, which ensures the desired temperature of the mixture. The selected membrane module can be inserted into the device provided for this purpose and retentate and permeate can be discharged using outgoing pipe and tube connections. The plant can be operated in recirculation mode or in diafiltration mode. The schematic design of the pilot plant in general for recirculation is shown in Figure 13.

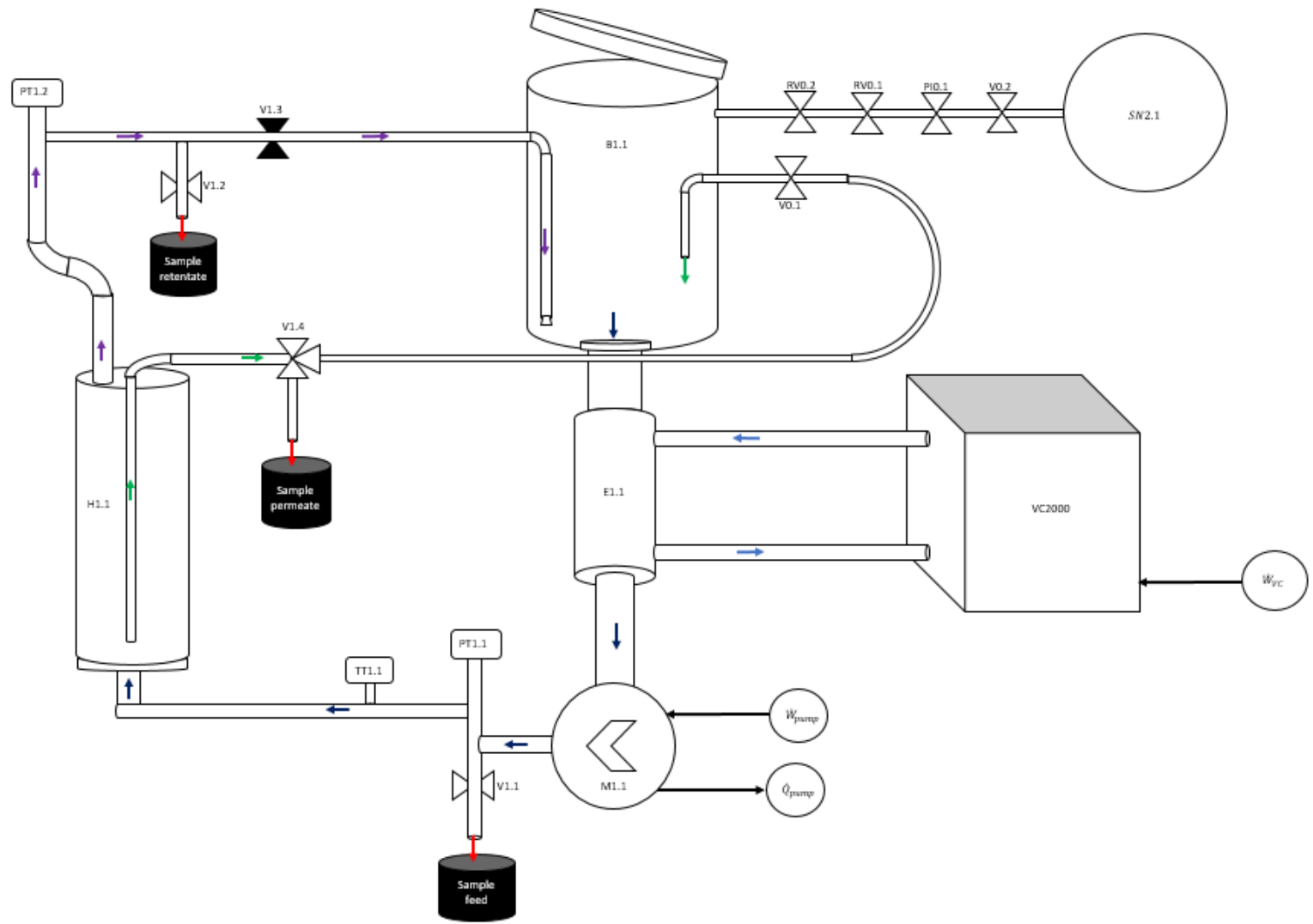







Figure 13: Plant design for recirculation mode.

<b>Legend:</b>		
B1.1	Tank	10l hold up volume
M1.1	Pump	High pressure membrane piston pump Pressure and circulation pump
VC2000	VarioCool [LAUDA]	Temperature control and generator for E1.1
SN2.1	Nitrogen storage	Stores and presses $N_2$ into the tank.
E1.1	Heat exchanger	Multitube heat exchanger to heat or cool the feed
H1.1	Membrane housing	Housing for 1x1812 spiral wound module
PT1.1	Pressure sensor	Measures system pressure and pressure drop
PT1.2	Pressure sensor	Measures system pressure and pressure drop
TT1.1	Temperature sensor	Measures temperature of feed
V1.1	Valve	Drain valve to empty the membrane housing by gravity
V1.2	Valve	Outlet valve for retentate sample
V1.3	Valve	Ball valve to control the pressure
V1.4	Valve	"L"-valve to sample permeate
V0.1	Valve	Valve to open / close permeate flow into tank
V0.2	Valve	Inlet valve for external $N_2$ supply
RV0.1	Valve	Low pressure regulation valve
RV0.2	Valve	Safety relief valve to avoid overpressure of the tank
PIO.1	Valve	Pressure regulation for $N_2$
	Permeate	
	Retentate	
	Feed	
	Sampling	
	Heating/Cooling	

**Figure 14: Legend for recirculation mode.**

In the following, the main components of the pilot plan are presented, and the process is briefly described.

The feed is filled into the tank (B1.1), which has a hold up volume of 10 l and a lockable lid. After the feed has been filled into the tank, the pump (M1.1) is put into operation. It is a high-pressure membrane piston pump. It feeds the feed from the tank through a heat exchanger E1.1 into the membrane housing (H1.1) where the membrane module is located. The heat exchanger is regulated by the VC2000 VarioCool [LAUDA]. The pipe between tank and pump is encased in a heat exchanger. The VC2000 can feed water into the heat exchanger at a predetermined temperature. This enables heat to be transferred to or from the feed. A temperature sensor TT1.1 and a pressure sensor PT1.1 are installed between the pump and the membrane housing. These two sensors measure the temperature of the feed entering the module and the corresponding pressure in front of the membrane housing. Furthermore, there is a valve (V1.1) shortly after the pump, which can be used for emptying the membrane housing by gravity or for sampling the feed.

The feed is pumped by the pump from below into the membrane module where the nanofiltration is performed.

In the membrane housing, the feed flows over the membrane surface. The mixture is divided into retentate and permeate. The retentate does not pass through the membrane, but the permeate does. At the housing outlet, the retentate and permeate are removed from the module by different outlets. The retentate flows through a second pressure sensor PT1.2. The second pressure value can be used to determine the pressure drop within the module using the first pressure value at the input of the module. Furthermore, the TMP can be determined by this.

After the pressure sensor, another valve is installed for the sampling of the retentate. This is followed by the ball valve (V1.2) for manual adjustment of the TMP. At the end of this pipe, the retentate flows back into the tank and is mixed using a rotating nozzle that serves as a dispenser.

The permeate flows out of the membrane module via an "L"-valve (V1.4) through which samples can be taken. The "L"-valve leads the permeate back into the tank if no sample is taken. The retentate and permeate are mixed again in the tank and kept as free of oxygen as possible by a connected pipe to a nitrogen storage (SN2.1). After a sample has been taken, the nitrogen can be added to the system through this pipe to extend the lifespan of the phospholipids. This supply pipe is equipped with different safety and regulation valves (V0.2, RV0.1, RV0.2, PI0.1).

Figure 15 shows the test setup for the diafiltration mode. The legend can be taken from Figure 14. The permeate outlet is led into a separate container using the valve V1.4 and no longer back into the tank. This container stands on a scale that measures the weight of permeate produced over time. Samples for the retentate are taken from the tank into which it is returned and mixed. In this case, the retentate can be considered as a feed for the next cycle. In addition, a diafiltration pump is connected to the tank, which can pump pure ethanol from a reservoir into the tank as required to ensure a certain solution equilibrium and reduce the negative effects of concentrating the fat components of the mixture (see Chapter 9.2.2).



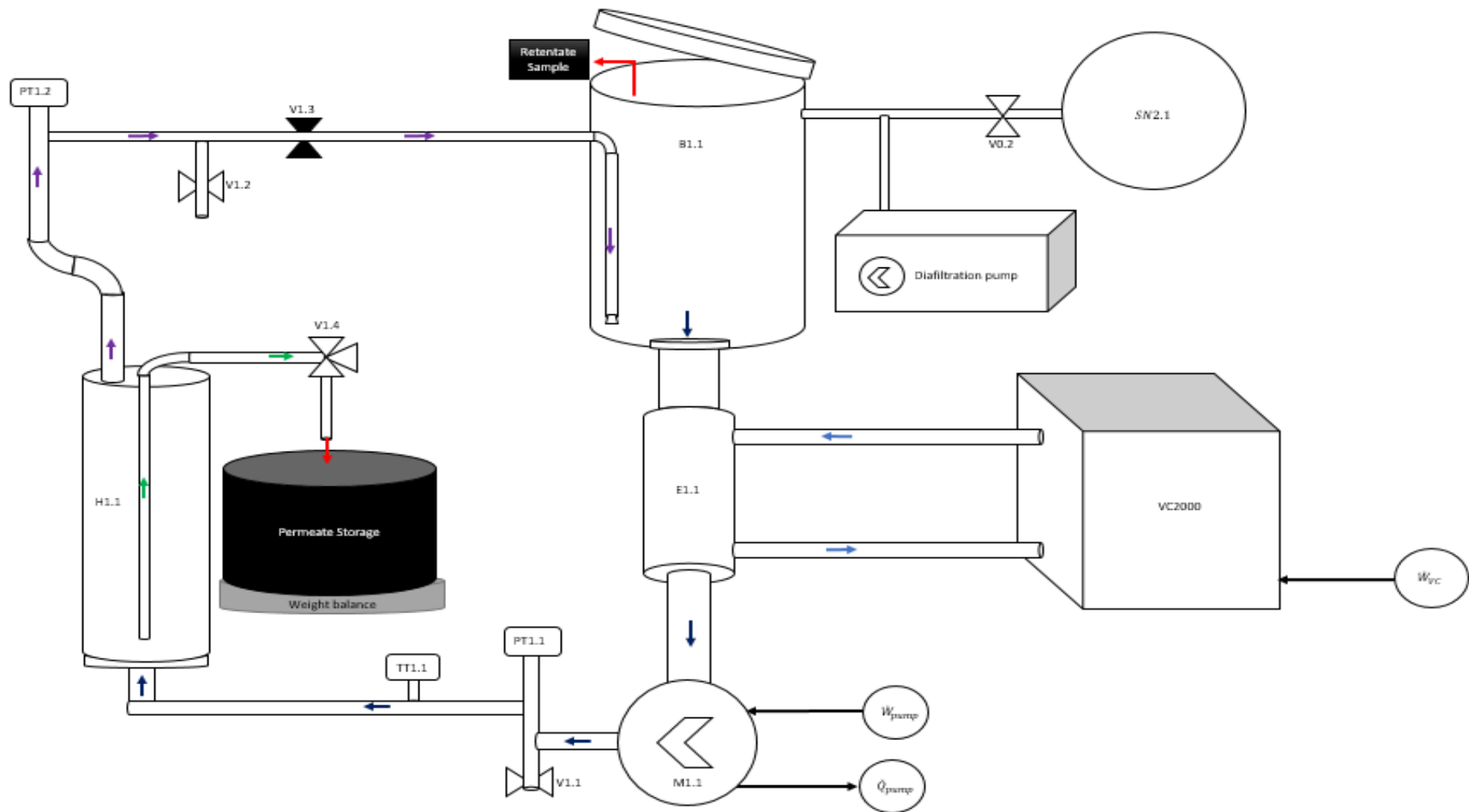


Figure 15: Plant design for diafiltration mode.

### **10.1.3 Modes of operation**

Two operating modes of this system are presented below. In one variant, both membrane output flows are fed back into the tank, in the other the permeate mass flow is collected separately.

#### **10.1.3.1 Mode of operation: Recirculation**

The recirculation term used here is defined as follows:

Recirculation means that both retentate and permeate are transported back into the feed tank and mixed there without a significant reduction of the total mass. Thus, there is no controlled concentration of the retentate.

The recirculation mode was used to study how the module performances developed over time and its lifespan without the influence of the variation of the concentration in the retentate during the tests. This allows the influence of continuous operation on the membrane to be studied. It can be determined whether a deterioration of the separation performance is caused by a long operation of the module itself. Furthermore, the lifespan at low concentration loading can be investigated.

During the recirculation process, samples of retentate and permeate could be taken at regular intervals without significant reduction of the total mass. A schematic illustration of the plant design for the recirculation mode is shown in Figure 13.

In summary, the advantage of this operation mode is the marginal change and impact of the concentration on the membrane performance. The disadvantage is that collecting permeate and retentate in the same tank does not produce any product (e.g. extract). Therefore, this mode is only used in laboratory scale for removing impact factors for analyzing membrane performance over time. It will not be used in product manufacturing.

#### **10.1.3.2 Mode of operation: Diafiltration**

The diafiltration term that is used here is defined as follows:

Diafiltration is a process in which the permeate that is produced is removed from the system and the retentate is returned to the feed tank. There is no mixing of these streams – as a result, the retentate is concentrated over time. This causes a change in the concentration of certain substances in the system; some substances are removed from the system through the permeate, others cannot permeate the membrane and remain in the retentate.

The diafiltration mode allows to add pure ethanol to the feed tank by a separate pipe. This mode of operation serves to produce a kind of extract by concentrating the retentate, which can be

processed into a product in the further course of the process. The undesirable substances like salts and heavy metals have been removed from the mixture by the permeate and by adding pure ethanol, precipitation of the phospholipids from the mixture can be largely prevented; this would otherwise lead to clogging of the membrane and loss of the fats. In addition, the water content in the retentate must not be reduced too quickly, because salt molecules still present could crystallize and lead to scaling.

In summary, this operation mode is used to manufacture an extract under industry-related conditions. The challenge in this operation mode is to balance the water-ethanol mixture adequately and to avoid precipitation of substances.

#### **10.1.4 Solvent composition**

The used solvent is a mixture of 30 wt.% water in ethanol. It is used to dissolve both the salts contained in the roe extract and the fatty acids to be extracted. Fats can be dissolved well in ethanol. Salts are soluble in water. When this mixture is mixed together, there is an effect that should be considered in order to obtain a correct mixture: volume contraction.

##### **10.1.4.1 Volume contraction**

Volume contraction is the effect that occurs when two substances are mixed, and the total volume produced is less than the sum of the initial volumes. The corresponding volume difference is called excess volume and is negative when the volume is reduced; correspondingly positive when the volume is increased, which can also occur.

Due to the formation of additional binding forces (e.g. hydrogen bonds) between the molecules, they occupy a smaller space than before, resulting in a volume reduction/contraction (Schrader, 2016). This effect also occurs with the mixture of ethanol and water. For this reason, the dimensions and units were usually traced back to the mass in grams or kilograms and, in most cases, a volume representation was omitted; e.g. quantities for the mixing of the solvent (see Table 1).

### 10.1.5 Feed composition

In this chapter the process of producing the feed used is described. The fish roe was homogenized and microfiltered, before it was concentrated to an extract in the rotary evaporator and frozen.

#### 10.1.5.1 Homogenization

In order to extract as much as possible of the fats. The fish roe was homogenized in the extraction solvent. The fish roe shells were broken by mechanical force, e.g. a mixer, and the corresponding contents were released. After the homogenization the mixture was allowed to decant. The separated roe shells tend to precipitate to the bottom of the vessel. A white layer was formed on top of the solid fraction, which consists mainly of proteins. On top is the solvent with water, ethanol as well as the extracted solutes (salts and various fats, etc.) (See Figure 16).



**Figure 16: Dehomogenized mixed fish roe with solvent.**

This mixture was passed on to microfiltration.

### 10.1.5.2 Microfiltration

Like nanofiltration (Chapter 9.1.3), microfiltration is also a pressure-driven process. On a laboratory scale (see Figure 17), microfiltration is achieved by exploiting gravity and a vacuum on the permeate side. The microfiltration of the extract was performed with a paper filter (MUNKTELL, 2018).



**Figure 17: Microfiltration setup in laboratory scale.**

The operating range is normally between 0.3 and 3 bar TMP (Kraume M., 2014). The left side of Figure 17 shows the main components of the laboratory microfiltration application. These are a glass container with a connection device for vacuum generator and corresponding gum attachment, as well as a coarse ceramic filter cylinder and the selected microfiltration paper filter. This is stabilized during the process with a specially manufactured metallic cylinder. The selected microfiltration filter had a pore diameter between 1-2  $\mu\text{m}$ .

The membrane was used in a dead-end filtration configuration (see Chapter 9.2.4). A filter cake formed on the membrane surface. This cake retained bacteria and larger proteins, but also – as a result of adsorption of smaller substances on the larger particles – was able to retain certain viruses (Crittenden, et al., 2012, p. 822). An example of the particles retained at the membrane surface on a laboratory scale is shown in Figure 18.



**Figure 18: Particles retained by microfiltration in laboratory scale.**

Following the conventional process, the microfiltered mixture is then added to the desalination process (see Chapter 9.1.2).

In this case, at laboratory scale, the permeate produced was concentrated in a rotary evaporator and frozen for storage. The desired feed was later produced from the roe extract (dry matter - DM) – as described below.

### **10.1.5.3 Feed production**

To produce the feed, a certain amount of roe extract is added to the solvent so that the desired dry mass fraction is present in the mixture. The calculation for this is described in Chapter 10.1.6.4.

During the mixing and further handling of the feed, it should be noted that a too high ethanol content in the mixture can cause the salt contained in the extract to crystallize in the solution. It should also be noted that an excessively high-water content can cause the fats to precipitate. To ensure that all components are dissolved in the solvent, a dry mass of 0.3 % to 0.5 % were selected for the fractions used in the test series.

Before the feed is added to the tank, it is microfiltered again. This allows to filter smaller proteins and peptides, which passed through the filter during the first microfiltration (see Chapter 10.1.5.2), because they tend to agglomerate during the concentration, freezing and reheating to produce the feed. During the feed production some salts did not solve in the dilution solvent and were removed during the second filtration. Finally, the filtration stage prevents dust and environmental contaminants from being transported into the pilot plant.

## 10.1.6 Calculations

In this chapter the calculations our of measured results will be explained on examples to show the basis for interpretations of results.

### 10.1.6.1 Rejection

The rejection was calculated with Formula 9-4. Each sample was taken in a sampling vessel and analyzed by the Ultra High Performance Liquid Chromatography (UHPLC) – average values are given in Tables 14-33 in the Appendix. A typical analysis result is shown in Figure 19.

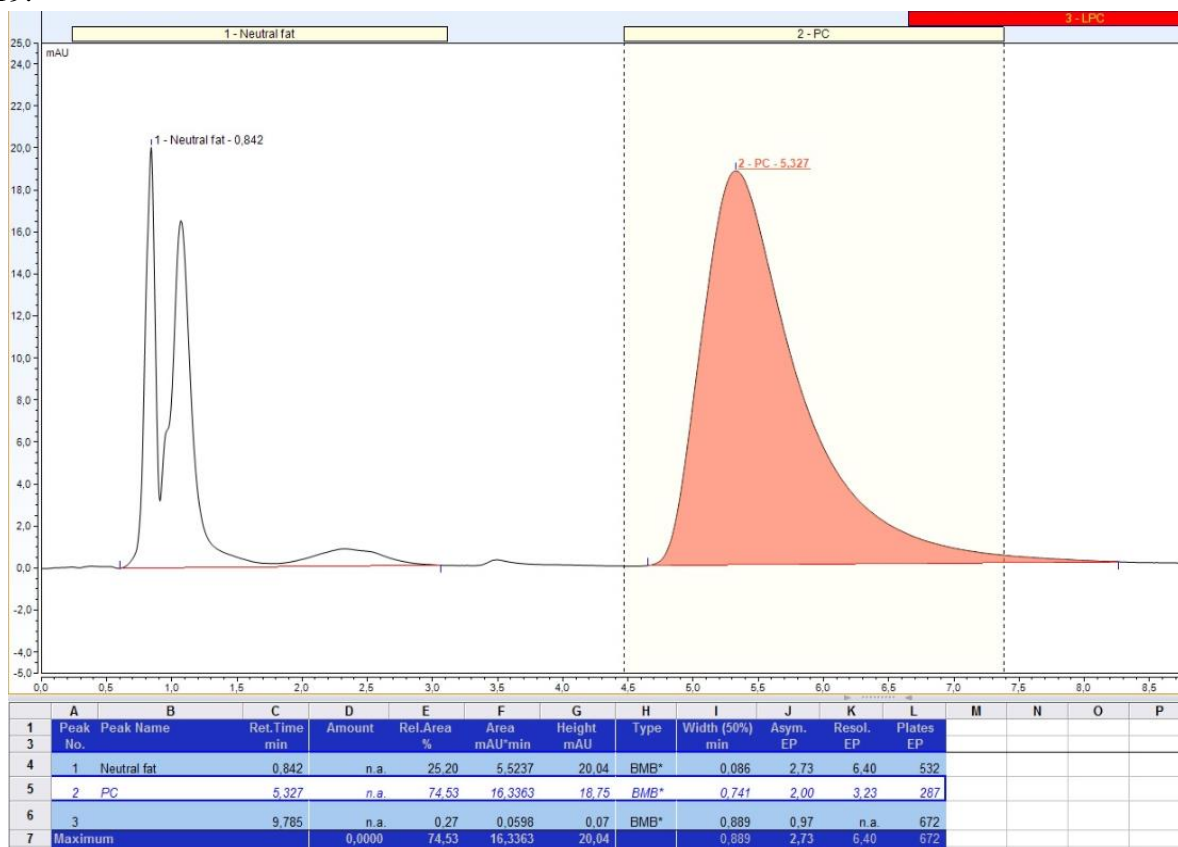


Figure 19: Example of an analysis result of UHPLC.

The mass fractions used for calculation were substituted with the area of the desired type of molecule in [mAU\*min]. Each sampling included a sample of the permeate and a sample of the feed at the sampling time. With this, two data areas, one for the permeate and one for the feed,

could be obtained. These values were put into Formula 9-4 and were used for calculating the rejection factor.

#### 10.1.6.2 Permeate flux

The permeate flux was calculated with the measurement of the permeate mass flow divided by the membrane area used (see Formula 9-1). Before starting the measurement, the valve V1.4 was open for five minutes to ensure a constant mass flow. While taking a sample the sampling vessel was covered with an aluminum foil in order to reduce the evaporation of the permeate. The mass of the permeate was measured with a high precision balance.

#### 10.1.6.3 Mixing solvent

To manufacture the solvent used, water and pure ethanol were taken and mixed together in order to obtain a tank content of 21 kg. The calculations in mass units were taken in order to avoid measurement mistakes due to volume contraction (see Chapter 10.1.4.1). To obtain a solvent with 30 wt.% water in ethanol, 6.3 kg of water and 14.7 kg of ethanol were needed. They were mixed carefully at the same temperature and were then shaken to ensure a homogenized mixture.

#### 10.1.6.4 Mixing feed

The solvent and the extract of the fish roe were used to produce the feed mixture. In order to measure the dry matter content of the fish roe extract, it was analyzed in the dry matter tester. Depending on the number of this sample, the mass was calculated which had to be put inside a certain amount of solvent to create a feed with the desired dry matter content of 0.3 % or 0.5 %. For example, 10 kg of feed with a dry matter content of 0.5 % from the fish roe batch number A are desired. Then calculation was done according to the Formula 10-1:

$$\text{Mass of dry matter in feed} = 0.005 * 10,000 \text{ g} = 50 \text{ g} \quad (10.1)$$

The feed should consist of 9,950 g solvent and 50 g dry matter. But the fish roe extract not only consists of dry matter. Therefore, three fish roe extract samples were analyzed in the dry matter tester and it calculated a dry matter content of 40.41 % on average. Then the following calculation was used:

$$\text{Mass of fish roe extract} = \frac{0.5 \% * 10 \text{ kg}}{40.41 \%} = 123.8 \text{ g} \quad (10.2)$$

This formula gives the result that 9,876.2 g solvent should be mixed with 123.8 g fish roe extract to achieve a feed mass of 10,000 g with a dry matter content of 0.5 %.



## 10.2 Experimental plan

In this chapter an overview over the performed experiments is given. Table 12 lists the data for the test series. They are structured in series name, period in date, test duration and initial dry matter content. All tests were performed with 6.01 L/min and 25 bar TMP. A subdivision into the first and second test module was done. The series designations include the following abbreviations:

RC – Recirculation test

DF – Diafiltration test

T – Temperature test

S – Solvent test

In the recirculation test, the settings for the recirculation mode (see Chapter 10.1.3.1) are applied. In the diafiltration test, the settings for the diafiltration mode (see Chapter 10.1.3.2) are applied. The normal condition (NC) for recirculation and diafiltration were set to:

LPM:                    6.01 L/min

TMP:                    25 bar

Temperature:        30 °C

In the temperature test, the system is used in recirculation mode and the desired temperature setting is made. The solvent test series are used for a cleaning test in NC and are carried out in recirculation mode with previous, pressure-reduced flushing.

An experimental plan overview in Figure 20 shows the basic order of the tests split into solvent and feed over time. For more information in detail see Table 12.

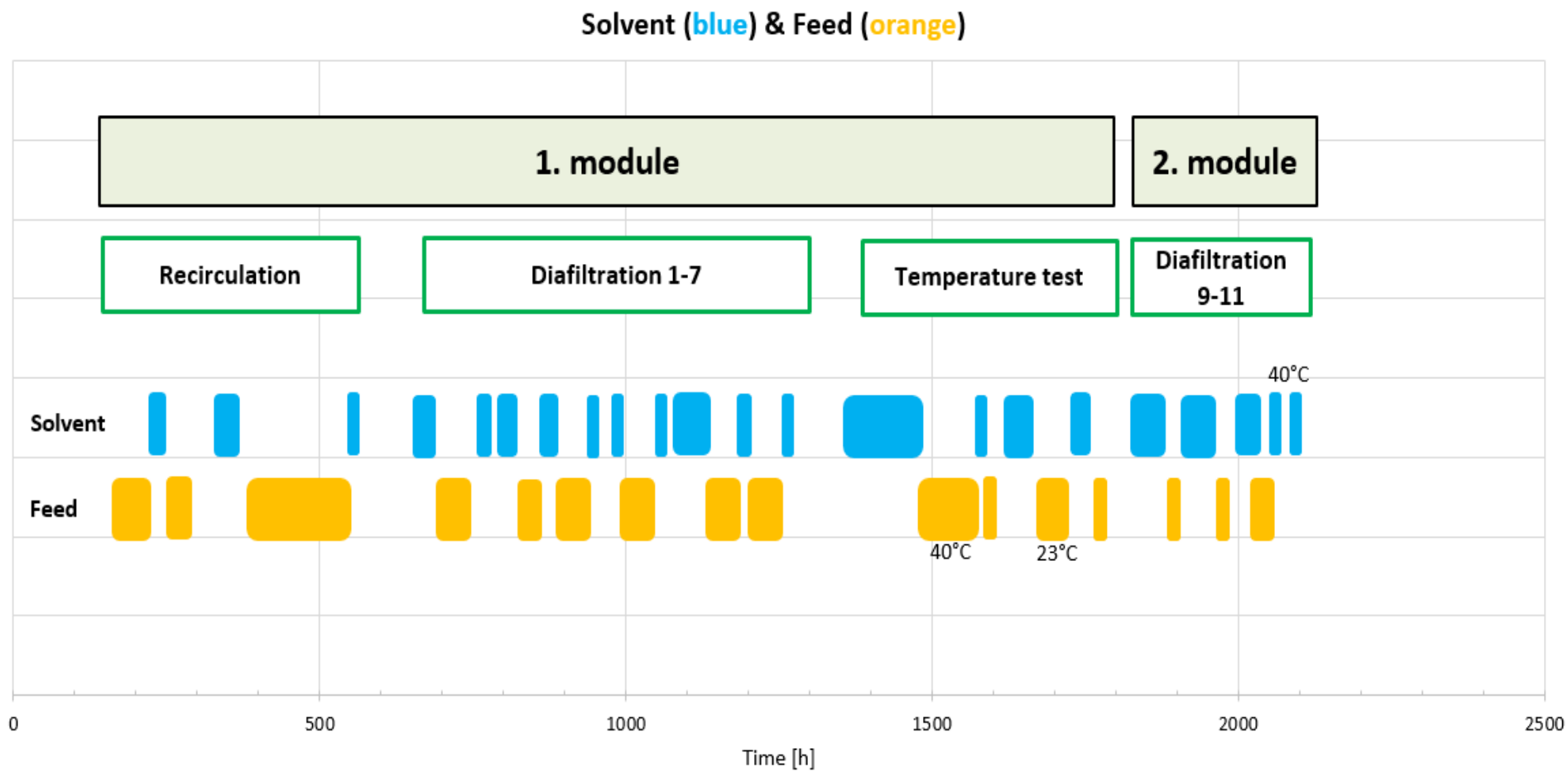


Figure 20: Schematic illustration of experimental plan under NC (25 bar, 30 °C, 6.01 L/min).

Before starting the recirculation test the module was conditioned in pure solvent. The recirculation test was chosen at the beginning of the tests in order to observe the flux performance of the module without significant influence of the progressively concentrating retentate. After this test, diafiltration was performed to analyze the membrane behavior in industry-related conditions. DF01-DF04 were used to adjust the parameters of injection pump and TMP to the concentrated mixture during the process. The first diafiltration step is simulated with DF05-DF07, which were replicates of each other. Between the diafiltration and temperature test there was a longer cleaning phase to reach a new plateau of permeate flux, before starting analyzing the influence of temperature on the module. After the temperature test, the second module was inserted into the equipment. It was cleaned with solvent and used for the DF09-DF10 (second stage) and DF11 (third stage).

### **10.3 Sampling and analytical methods**

In this chapter, the method of sampling will be explained together with the methods of analysis.

#### **10.3.1 Sampling points and schedule**

In each test the system was operated long enough until the normal condition for the specific test was reached – this took between 30 and 60 minutes, depending on the kind of test. Until normal conditions were reached, the first sample of feed and permeate were taken. The sampling valve for the permeate flow was opened and left open for about 5 minutes in order to achieve a stable permeate mass flow before the sample was taken. The feed sample was taken from the feed tank with a pipette (1 ml). Before taking the final sample for analysis the pipette tip takes three times the feed and removes it again. This is done for the inside of the pipette tip to acquire the partial pressure of the liquid and thus increase the accuracy of the liquid collection. To protect the sample against free evaporation, the sampling vessel was closed immediately after sampling. Then, a vessel was put under the permeate outlet to collect the permeate mass flow while taking the time of collection. Normally, the permeate sampling time was 2 minutes. These samples were taken in two replicates.

The liquid mass was measured by a precision balance. The UHPLC analysis of the permeate samples were done by direct injection of 1  $\mu$ l into the column. The feed samples were diluted with a 1 to 10 ml ratio before the UHPLC.

### 10.3.2 UHPLC

A UHPLC Dionex Ultimate 3000 with a silica column from Resteck called Pinnacle DB Silica 1.9  $\mu\text{m}$ , 100x2.1 mm (10 cm long and 2.1 mm of cross section) was used. The program was run with isocratic solvent, of 10 % water (v/v) in ethanol, with a flux of 0.31 ml/min and temperature of 30 °C. The detector was UV with a wavelength of 210 nm.

In general, the theory of Beer-Lambert Law was used. It states that the amount of absorbed radiation energy of a laser passing through a sample is proportional to the corresponding concentration of molecules interacting with that specific frequency (Bouguer, 1729).

It should be noted that a highly concentrated sample is diluted with a solvent before it is sent for analysis to ensure not reaching the limit of quantification, otherwise some molecules may hide behind others and the laser cannot detect them and integrate them into the calculation. Investigations for error deviation of the UHPLC analysis can be found in Chapter 10.4.1.3 and Table 35.

### 10.3.3 Dry matter analysis

The dry matter analysis was performed on samples dried with a rotary evaporator under reduced pressure. The dried samples weighed initially between 180 and 250 g, the final results were calculated using a high precision mass balance. In the first stage a vacuum of 100 mbar, a temperature of 49 °C and a rotation per minute of 130 rpm were applied. For the final evaporation phase the pressure was decrease to about 28 mbar and the temperature of the water bath set to 70 °C.

After removing the liquid from the flask, its mass was measured again, and the dry matter left inside the flask was calculated. With these numbers the dry matter content of a certain sample could be given.

Example for calculating dry matter of DF07 is given:

The mass of a 250 ml flask is 125.192 g. For the rejected retentate of DF07 180.075 g was filled in this flask. After using the rotary evaporator 125.946 g was measured for the flask with dry matter inside. The subtraction of flask mass after evaporating and the initial flask, mass results in 0.754 g dry matter. Dividing this number by the initial mass of liquid filled inside the flask a dry matter of 0.419 % for the retentate of DF07 can be obtained.

### **10.3.4 Solvent test – cleaning approach**

After every test with feed a cleaning procedure with pure solvent was performed. The solvent was filled into the tank after the removal of the feed. The equipment was then operated for one hour with 80 % pump capacity (8.01 L/min), 30 °C and no pressure (0.6 bar). During this phase no measurements of the permeate mass flow were taken due to the low-pressure conditions. The high cross flow was applied in order to increase the shear forces on the membrane surface. After this first cleaning approach, the solvent was removed, and fresh solvent was filled inside the system. This time the system was run under normal condition (25 bar, 30 °C, 6.01 L/min) until the flux tend to reach a plateau. This step was performed to stabilize the module in the given conditions. Thereafter, the solvent was removed again and the feed for the next test was filled inside the tank.

This cleaning procedure with pure solvent was applied regularly after each test. In some cases, the cleaning procedure was prematurely interrupted or extended to further investigate the effectiveness of the cleaning method.

### **10.4 Source of error**

Here possible sources of error are to be pointed out, which could have had influence on the measuring results. In the following chapter, the most important sources of error are quantified.

There are errors that cannot be detected or eliminated by repeating individual measurements – these are the so-called systematic errors (Maul & Dammeyer, 2012). These have a constant value when a measurement is repeated under identical measuring conditions. When performing physical-chemical measurements, these must be taken into account. This includes environmental influences such as the deviation of the measuring temperature from the calibration temperature or the air-generated buoyancy during weighing. Another systematic source of error may be caused by the measuring instruments. Possible non-linearities, age-related changes of the measuring instrument or calibration errors can lead to further undesired measurement inaccuracies. Furthermore, there may be a lack of objectivity on the part of the experimenter (so-called "wish observations"). Parallax errors can also occur when reading scales or vector instruments.

## 10.4.1 Error analysis of important measurement methods

In this chapter, possible errors due to inaccuracy of measurement devices will be valued.

### 10.4.1.1 Errors during solvent production

First, the precision of solvent mixing will be evaluated. Therefore, an example of a mixing phase is given in Table 1.

**Table 1: Error deviation of mixing solvent used.**

	Water		Ethanol		Solvent
	in [kg]	in [%]	in [kg]	in [%]	in [kg]
<b>Tank 1</b>	6.31	30.00	14.71	70.00	21.01
<b>Tank2</b>	6.30	30.00	14.70	70.00	21.00
<b>Tank3</b>	6.31	30.03	14.70	69.97	21.01
<b>Average</b>	6.30	30.01	14.70	69.99	21.01

In this example, three tanks were mixed for solvent production. The desired relation between water and ethanol was 30:70 % or 6.3:14.7 kg. A difference from the ideal value of 0.01 kg can be observed. For weighting, the PCE-TB15 mass balance (S/N:255) from the company PCE-Deutschland GmbH was used with a given inaccuracy of 0.5 g. The required environmental conditions were fulfilled. Further inaccuracies from human factor can be neglected due to display indication. The open fluid surface during the operation was about 30 cm<sup>2</sup>. At a measured solvent evaporation rate of  $0.0003 \frac{g}{min \cdot cm^2}$  at 24.7 °C (Artic Nutrition AS, 2018), the mass lost by evaporation during a maximum operation time of 10 minutes was 0.09 g. Summing up the possible sources of error leads to a maximum absolute error of 10.6 g during solvent production. In percentage terms, this corresponds to an error of 0.05 %. This result can also be applied to the feed production.

### 10.4.1.2 Error of using pipette

Sampling and diluting for the UHPLC-samples were done with a pipette (1 ml) and the Mettler Toledo mass balance (Model XP404S, SNR: B324437342) with a given inaccuracy of 0.1 mg. To value the real precision of the pipette using pure water, the data in Table 13 (see Appendix) were measured.

It can be observed that the average measurement result has a value of 0.999 ml. This results in an absolute difference to 1 ml of 0.001 ml. Adding the inaccuracy of the mass balance of 0.1 mg (=0.1002 ml), this corresponds in percentage terms to a maximum error of 10 %.

### 10.4.1.3 UHPLC reproducibility

In order to assess the reproducibility of the UHPLC analysis results, three different tests were randomly selected, and the respective standard deviation determined. The results are presented in Table 2 based on Table 35 (see Appendix).

**Table 2: Standard deviation of UHPLC analysis exemplified with DF07, RC02 and T02.**

	Test DF7		Test RC02		Test T02	
	SD (-)	SD (%)	SD (-)	SD (%)	SD (-)	SD (%)
<b>Sample 1</b>	0.13	1.45	0.96	0.70	0.12	0.47
<b>Sample 2</b>	0.09	0.58	0.02	0.83	0.11	0.36
<b>Sample 3</b>	0.05	0.61	0.06	2.01	0.00	0.01
<b>Sample 4</b>	0.02	0.13	0.00	0.09	0.05	0.69
<b>Sample 5</b>	0.08	0.83	0.03	1.10	0.77	2.95
<b>Sample 6</b>	0.06	0.33	0.01	0.22	0.50	6.31
<b>Sample 7</b>	0.05	0.50	0.02	0.51	0.39	4.96
<b>Sample 8</b>	0.12	0.58	0.52	0.36	1.14	4.34
<b>Sample 9</b>	0.07	0.59	-	-	0.41	5.04
<b>Sample 10</b>	0.08	0.32	-	-	0.41	5.16
<b>Sample 11</b>	0.04	0.30	-	-	0.08	2.81
<b>Average</b>	<b>0.07</b>	<b>0.57</b>	<b>0.20</b>	<b>0.73</b>	<b>0.36</b>	<b>3.01</b>

The average of all three tests is 1.43 % SD. The maximum percentage standard deviation is 6.31 %. Thus, the average as well as the minimum accuracy of the analysis was determined from the UHPLC results regarding the machine reproducibility and manual integration reproducibility. According to Artic Nutrition AS (2018) the working range of UHPLC was not at the limit of quantification and close to linearity of this method.

### 10.4.1.4 Error distribution of methods – overview

In the following Table 3, the error distribution of the used measuring methods is shown. It should serve as a rough overview for error estimation and substantiate the quality of the interpreted results. The human factor includes inaccuracies in operation – e.g. inaccuracy of reading scales – and is neglected in this calculation.

**Table 3: Error distribution of methods.**

	<b>Error (should-is- deviation)</b>	<b>PCE balance PCE-TB15</b>	<b>Mettler Toledo XP404S</b>	<b>Evaporation</b>	<b>Result of inaccuracy</b>
<b>Solvent mixing</b>	10 g	0.5 g	Not used	0.09 g	10.6 g (0.05 %)
<b>Use of pipette (1 ml)</b>	0.001 ml	Not used	0.1 ml	N/A	0.1 ml (10 %)
<b>Dry matter</b>	N/A	Not used	0.1 mg	N/A	0.1 mg

*N/A: Not applicable because of different kind of performance or due to negligibility.*



# 11 Results and discussion

In the following chapter, the results of the test series are presented and discussed. First, membrane module behavior in binary ethanol-water solution will be explored and rejection and permeate flux performance in different conditions will be evaluated.

Additional aspects such as membrane fouling during the test series will be analyzed and an investigation of cleaning procedure for the module will be performed. Furthermore, the results of a case study for production of concentrate will be presented and evaluated. Finally, energy consumption and cost estimation will be discussed briefly.

## 11.1 Stability analysis

Investigation of stability in rejection of omega-3 and stability of permeate mass flow in function of process parameter such as temperature and solution composition will be performed in the next sections. Three types of tests were used for this investigation: 1. recirculation tests, 2. diafiltration tests and 3. temperature tests.

### 11.1.1 Stability of rejection

A high and stable rejection of the desired components is one of the most important properties a membrane module such as DuraMem®300 should accomplish. In the following sections, the results for the rejection of the polar lipids under the corresponding operating conditions generated during the test series will be presented.

Rejection is calculated as defined in Formula 9-4. This definition is based on a process, during which feed streams into the module and retentate and permeate were pumped out again. The process considered in this work recirculates the retentate back into the feed tank. It is then named feed again.

#### 11.1.1.1 Rejection of polar lipids in recirculation mode

The recirculation test gives a first impression of rejection of polar lipids (such as phospholipids). After a mixing phase of at least 30 minutes, a sample was taken from feed and permeate at the beginning of each recirculation test series. Polar lipids concentration in the feed and permeate were measured by UHPLC. The same procedure was repeated at the end of the corresponding test series. The results of rejection are shown over the amount of material filtrated to the module in Figure 21.

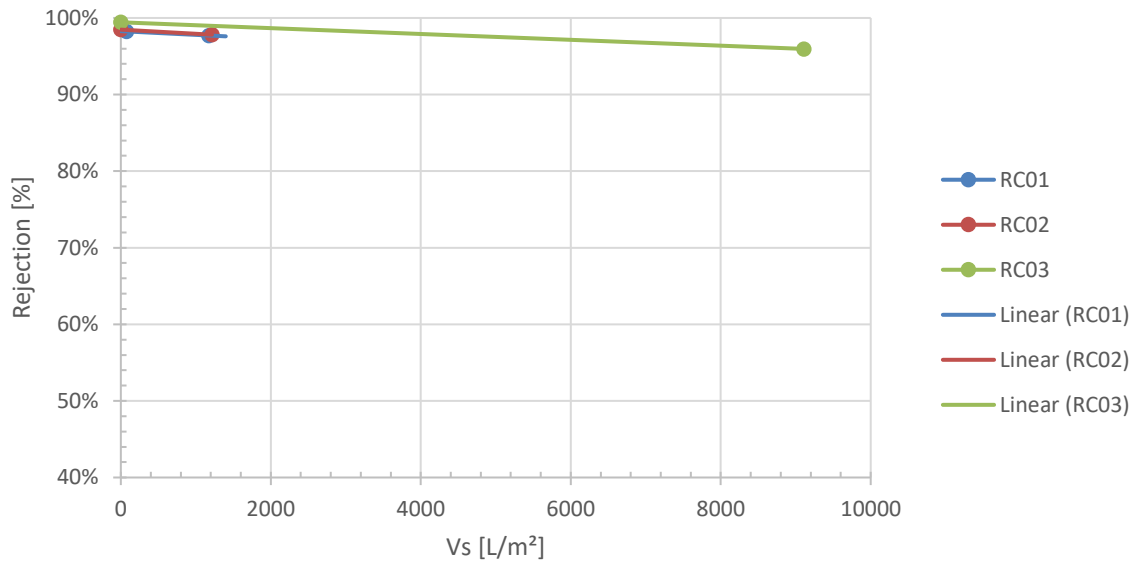


**Figure 21: Results of rejection in recirculation mode with feed.**

These three recirculation tests (RC01, RC02 and RC03) were performed under normal condition (TMP = 25 bar, TT1.1 = 30° C and LPM = 6.01 L/min) and with a dry matter concentration of 0.5 % in feed. By applying these conditions, rejection of phospholipids above 96.0 % could be obtained, even during a test period of 166.7 h as shown in RC03. At least, it is above 90 % as stated in Toh et al. (2007). During all three tests, a slight rejection decline is observed.

### 11.1.1.2 Rejection – Diafiltration first stage

Three diafiltration tests were performed (DF05, DF06 and DF07) under normal condition (TMP = 25 bar, TT1.1 = 30° C and LPM = 6.01 L/min) and are shown in Figure 22. Each test was started with a dry matter concentration of 0.3 % in 9 kg feed. During this test, ethanol injection started at a  $V_s$  of 175 L/m<sup>2</sup> and was continued until a  $V_s$  of 1118 L/m<sup>2</sup>. During this period, ethanol was added in the feed tank at a rate of 73.5 g/h.

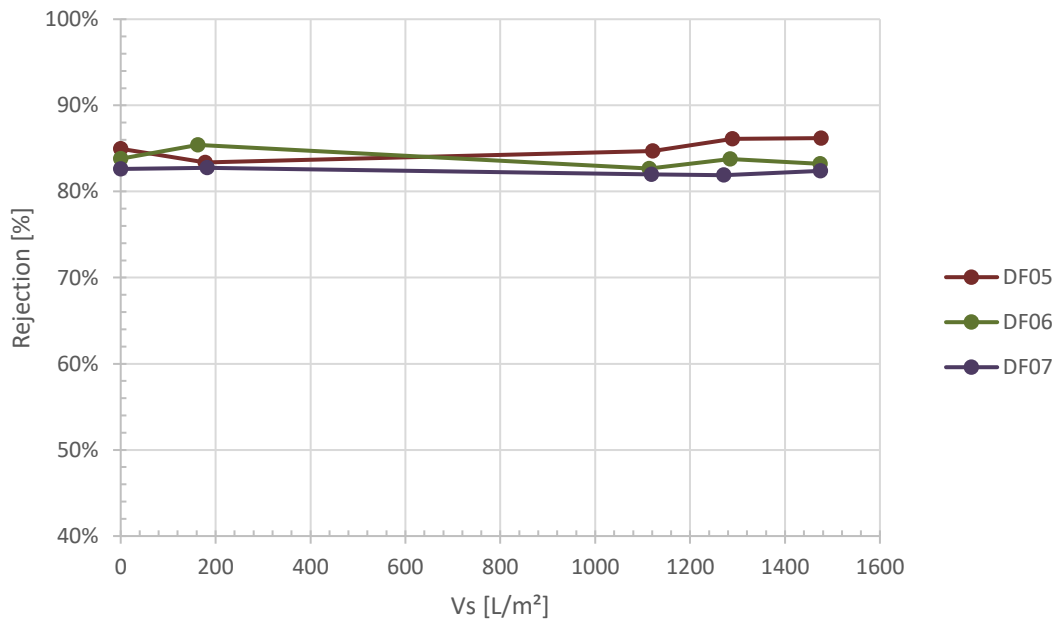


**Figure 22: Results of rejection in the first stage diafiltration mode with feed.**

The rejection observed for the three tests range between 81.9 % and 86.2 %. In DF05 a slight increase of rejection after ethanol injection is seen. For the test DF07, a slight decrease in rejection is observed. However, for the DF06 test the influence of ethanol injection seems to be negligible, the rejection varies between 85.4 % to 82.0 %.

In general, these results show that the phospholipids rejection in diafiltration mode is at 84.1 %  $\pm$  2.2 %. The concentration of dry matter increased from 0.30 % to 0.42 %. That results in a concentrating factor of 40 % while filtering 1475.2 L/m<sup>2</sup>.

### 11.1.1.3 Temperature test

The temperature tests were performed using the recirculation mode at a TMP = 25 bar and LPM = 6.01 L/m<sup>2</sup>. The results are illustrated in Figure 23. Dry matter concentration of the feed was 0.3 %. The feed temperature of the first test (T01) was set to 40 °C, the second test (T02) was set to 30 °C and the third test (T03) was set to 23 °C.

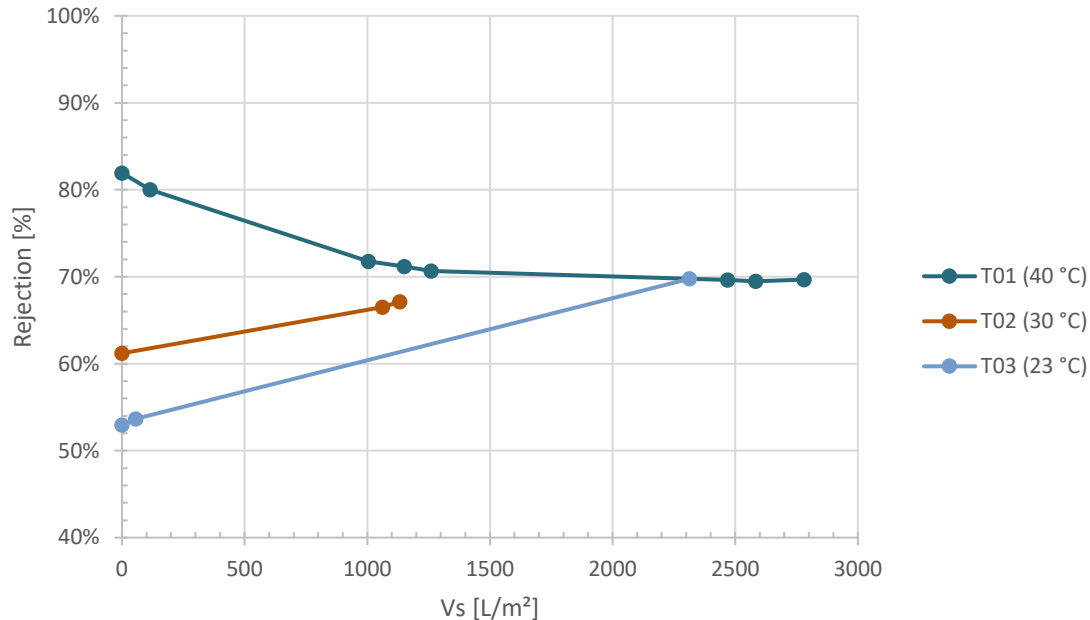


**Figure 23: Results of rejection in temperature tests with feed in recirculation mode.**

Results show that in recirculation mode at a temperature of 40 °C the rejection of PL declines over time and stabilizes at 70.0 % after a  $V_s$  of 1260 L/m<sup>2</sup>.

The second temperature test (T02) starts at a lower rejection point of 61.2 % and increases over time up to 67.1 %. The same pattern can be seen in the third temperature test (T03), with the exception that initial rejection value is 53.0 % and increased to 70.0 %.

These tests demonstrate the temperature influence on rejection. At 40 °C, a decrease of rejection over time is observed while at lower temperature (i.e. 30 °C and 23 °C) the rejection increased over time. This could be caused by a small adjustment of the pores of the membrane. At higher temperature, the pores tend to expand and open more. This increases the permeability of the module and the rejection decreases. At the same time the flux will be higher than in lower temperature test. At lower temperature the pores tend to close more and therefore the permeability decreases, a lower flux results (Figure 30) and the rejection increases.

Each rejection values seem to tend to plateau at approximately 70 %. This leads to the assumption, that the rejection of the module is in long term independent from the temperature applied. To confirm this assumption, more work is needed.

#### 11.1.1.4 Rejection – Multi-stage diafiltration

A second module of DuraMem®300 was operated in diafiltration mode and the normal condition  $TMP = 25 \text{ bar}$ ,  $TT1.1 = 30^\circ \text{ C}$  and  $LPM = 6.01 \text{ L/min}$ .

The feed for DF09 and DF10 is the concentrate from the previous diafiltration tests DF05 to DF07. The corresponding feed concentration was therefore 0.42 %. To prevent precipitation due too high dry matter concentration, ethanol was added from the beginning of the filtration experiment. The concentrate of experiments DF9 and DF10 were used as feed for DF11 (third stage test) with a dry matter concentration of 0.63 %. The final concentrate obtained in DF11 experiment had a dry matter concentration of 1.24 %.

Figure 24 presents the rejection of phospholipid in function of the specific volume for experiments DF09, DF10 and DF11.

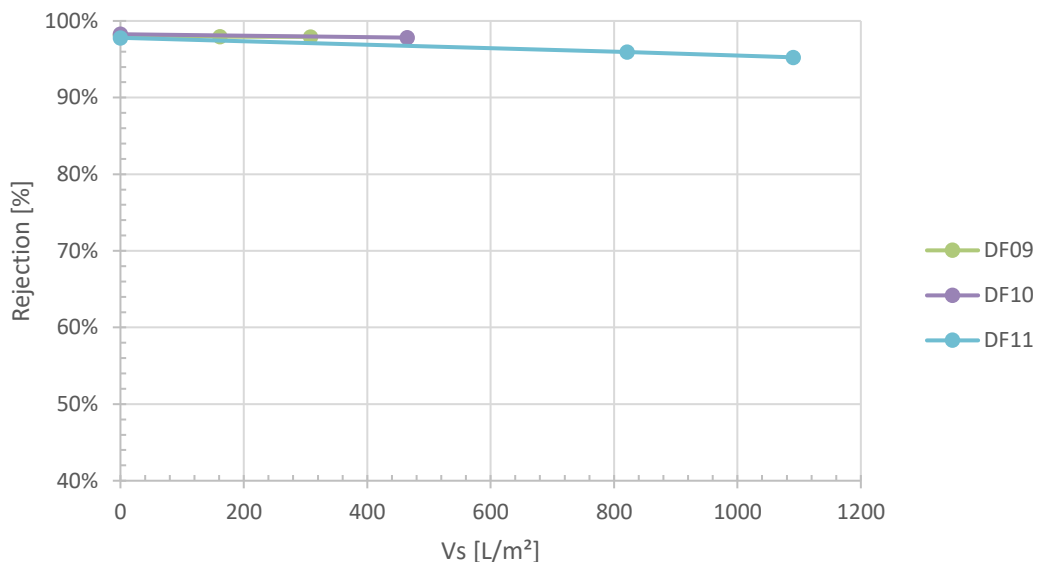


**Figure 24: Results of rejection in diafiltration mode for multi-stage diafiltration.**

Initial rejection value for 97.8 % were measured for all experiments. A small and gradual decrease of rejection can be seen over time down to 95.3 % (in DF11). However, rejection of PL stays stable over an amount of filtrated material of 1091 L/m<sup>2</sup> above 95.3 %.

The rejection performance in diafiltration mode is comparable to the performance in recirculation mode given in Figure 21 at the beginning of the first module. In DF11 experiment the rejection decrease at a rate of  $2.29 \cdot 10^{-3} \% \frac{m^2}{L}$  while in recirculation mode (RC02) the rejection rate decrease is evaluated at  $0.58 \cdot 10^{-3} \% \frac{m^2}{L}$ . This difference can be used as a supportive argument that a higher concentration of the feed reduces the rejection more at the beginning of a module.

### 11.1.2 Stability of permeate flux

First, the flux of DuraMem®300 operated in recirculation mode with pure solvent will be investigated. Then the flux of the membrane operated in recirculation and defiltration modes with feed solution will be determined. Finally, the influence of feed temperature on the membrane flux is evaluated.

#### 11.1.2.1 Conditioning of DuraMem®300 module

Main objective of the module conditioning is to get the membrane compacted with pressure, expose the membrane to solvent and remove preservatives before starting filtration tests. The conditioning condition were 25 bar, 30 °C and 6.01 L/min (NC). The conditioning period varies between 45 minutes to 6 hours. Figure 25 shows the flux over time during the conditioning period.

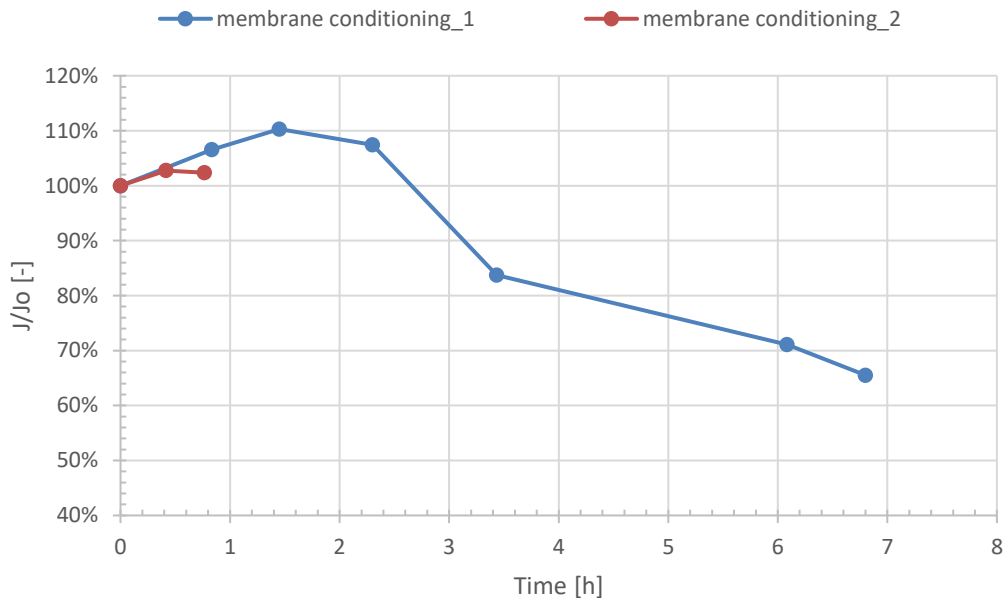


**Figure 25: Results of flux conditioning in recirculation mode with solvent.**

In this figure, the mass flux  $J$  divided by the initial mass flux  $J_0$  is plotted over time, to visualize the change of mass flux over the test period. The data for "membrane condition\_1" was taken from the first module. For "membrane conditioning\_2" the data belongs to the second module. For the second module a short interval was chosen to start early with production.

Considering "membrane conditioning\_1" an increase of up to 10 % occurs in the first 1.5 h. A pale-yellow colored liquid (preservatives) was observed at this time flowing out of the permeate pipe while operating the plant with pure solvent. After 1.5 h a slight decrease in flux occurs until 2.3 h. the flux changes over time due to applied parameters and due to removing preservatives at the beginning of using the first module. After 1.5 h the flux decreases strictly

over the remaining test duration. Tsibranska & Tylkowski (2012) point out that solvent (in their experiments pure ethanol) flux converges towards a constant final flux of the DuraMem®300 at pressure 20 bar and 30 bar in dead-end filtration. Furthermore, their results state that the measured ethanol fluxes in dead-end and cross-flow are comparable. Therefore, it can be indicated that “membrane conditioning\_1” will tend to plateau on a final flux value.

A stable permeate flux is not necessary, because in industrial processes it will not be waited for days or weeks until a stable flux occurs. This time would be an expensive loss of production. It is more economical to have a production during falling flux than no production.

### 11.1.2.2 Flux – Recirculation

These recirculation tests (Figure 26) were made under normal conditions (TMP = 25 bar, TT1.1 = 30° C and LPM = 6.01 L/min) and with a concentration of 0.5 % dry matter in the feed.

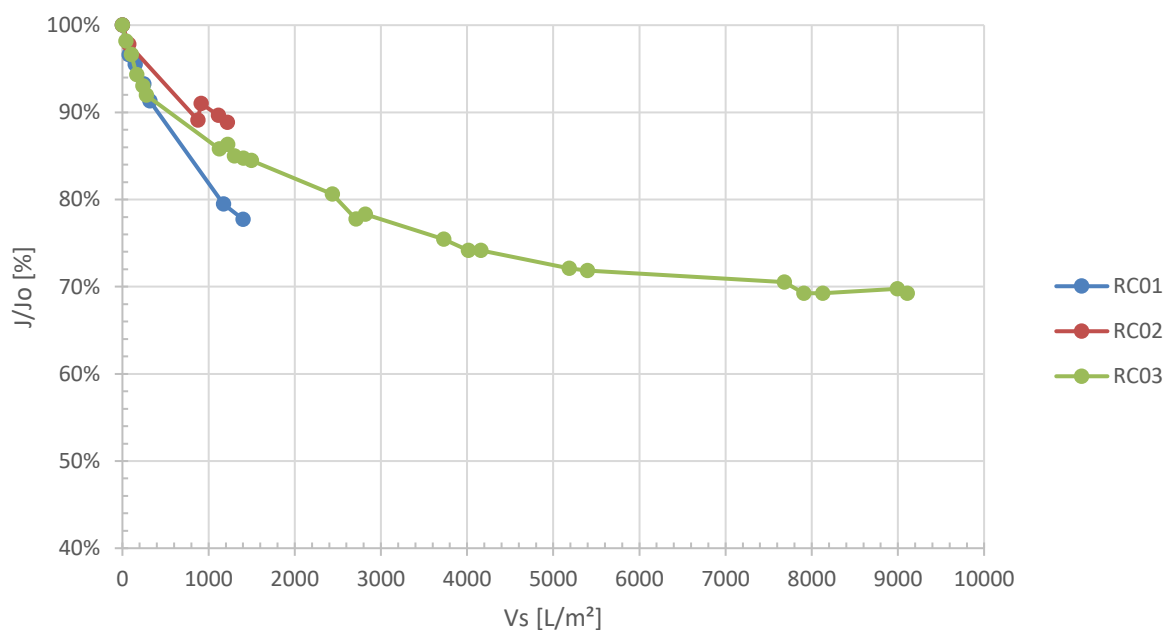


**Figure 26: Results of flux in recirculation mode with feed (0.5 %).**

These three tests give a first impression of how the module will behave in recirculation mode. Shapes of them are comparable. It seems that the permeate flux decreases at the beginning more strictly and reaches a plateau over the amount of filtrated material of around 70 % of the initial flux; especially in a longer period of time (see RC03). A comparable result is described in Siddique (2013): “[...] the flux profile of Duramem™300 clearly exhibited compaction (30 % decrease in flux) over time, [...]”. Differences between RC01, RC02 and RC03 can be traced back to pressure variation, flow variations, slightly different feed compositions, amount of filtrated material or other fluctuations based on the uncertainty of the instruments for measuring.

Figure 27 uses a power function to average the three tests in recirculation mode and represents an approximate curve “RC” over the amount of filtrated material.

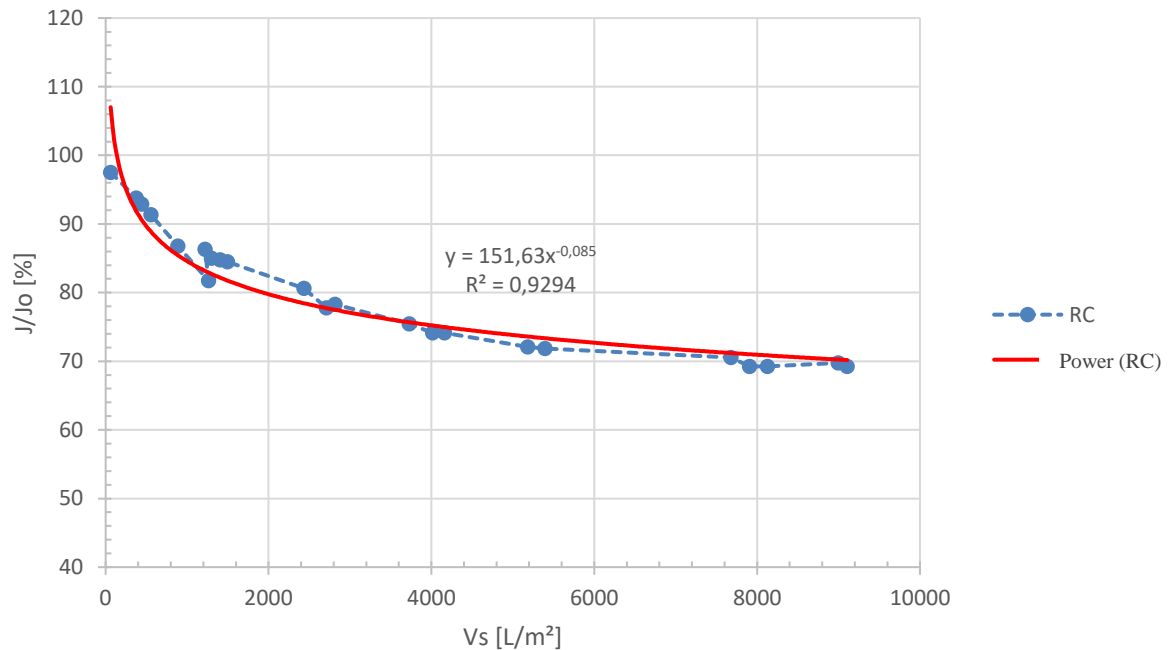


**Figure 27: Results of flux in average in recirculation mode with feed (0.5 %).**

This kind of function performance was identified in previous works (Tsibranska & Tylkowski, 2012), where the essential decrease of permeate flux in OSN is explained by the osmotic pressure increase combined with concentration polarization phenomena (Huang & Zhang (2011), Silva & Livingston (2006)). It is stated that the first quick decrease in permeate flux can be related to the concentration change. Usually it will be explained by the formation of a concentration polarization layer (Zhang et al. (2009); Shi et al. (2006)), which causes a decrease of mass transfer due to an increase of osmotic pressure. The affiliating slight decrease of permeate flux may be traced back to layer formation (Kilduff et al. (2004)), due to insufficient shear forces on top of the membrane surface. Tsibranska & Tylkowski (2012) indicate also a second explanation for layer formation on top of the membrane surface. Components of lower solubility may reach saturation and cause cake formation at a higher concentration. This can happen especially in multi-component solutions, like the feed used in this thesis.

Peeva, et al. (2004) state that regarding to the mass transfer film theory model the flux decreases exponentially with increasing feed concentration. This statement can be confirmed by the data



of this survey, see Figure 27 and Figure 28. In the beginning and at the end of each recirculation test a feed sample was taken and analyzed for concentration.

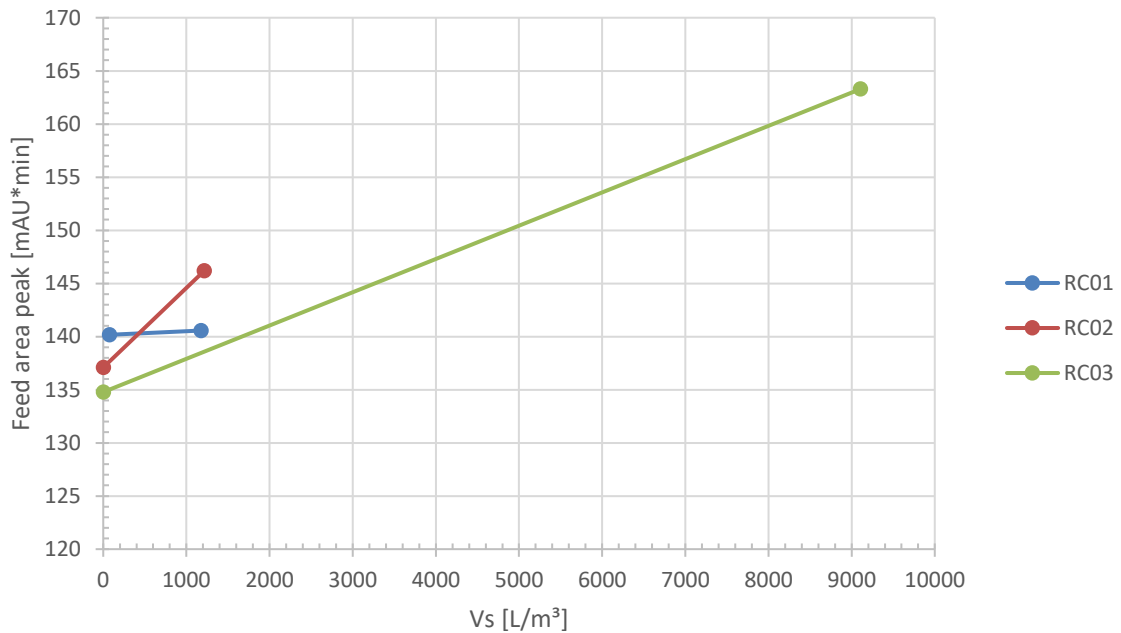


**Figure 28: Increased feed concentration during recirculation mode with feed.**

While feed concentration increases slightly even during the recirculation test, flux decreases over test duration exponentially. In RC01 the concentrating is neglectable. RC02 and RC03 show a higher increase of concentration during filtration.

All in all, the flux decreases at the beginning more intensively and seems to plateau over the amount of filtrated material to a stable value, even if there is still a slight decrease over time, explained by concentration polarization and minor layer formation.

### 11.1.2.3 Flux – Diafiltration (DF05-DF07)

The first three diafiltration tests were made under normal conditions (TMP = 25 bar, TT1.1 = 30° C and LPM = 6.01 L/min) and with a dry matter concentration of 0.3 % in the feed. The results of flux in the first stage diafiltration are shown in Figure 29.

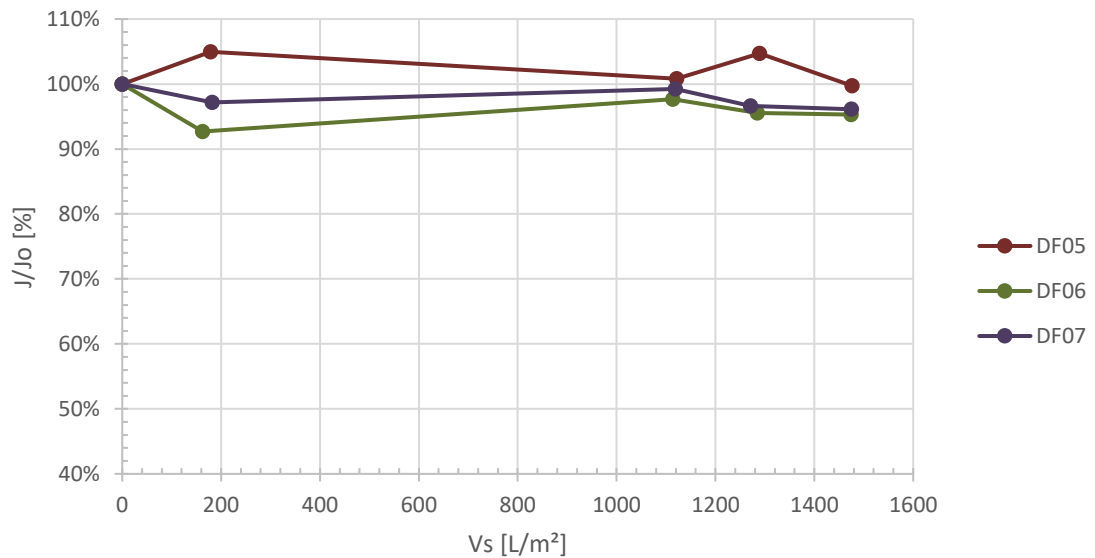


**Figure 29: Results of flux in first stage diafiltration with feed.**

These tests are replicates from each other – they contain the same experimental conditions. Differences are given by the time of operation in the experimental plan. This can be seen in DF05. It has a different pattern than DF06 and DF07. This may be traced back to the previous experiment DF04 with a dry matter concentration of 0.5 % (see Table 12). DF06 and DF07 exhibit a comparable pattern of the flux. While concentrating, the flux decreases (Peeva, et al., 2004). After  $V_s \approx 180$  L/m<sup>2</sup> ethanol was injected and injection was stopped after  $V_s \approx 1120$  L/m<sup>2</sup>. While injecting pure ethanol, the flux seems to increase between 2 % and 5 % – except for DF05, here ethanol injection decreases the flux by 4.2 %.

The flux increase can be drawn down to the fact, that injecting pure ethanol dilutes the concentrate. Subsequently, an apparent concentration polarization effect will be reduced, the osmotic pressure decreases, and the driving force increases slightly.

Zhang & et al. (2016) report an increase of flux due to swelling by using methanol as a solvent and STARMEM membranes. Ethanol is both hydrophilic and lipophilic. Therefore, it can interact with the cross-linked polyimide membrane. If a membrane in the active layer is free to expand during swelling, its pores will enlarge and thus the permeability will increase. This argument can be supported by the characteristics of DF06 and DF07.

On the other hand, a decrease of flux is reported by Labanda, et al. (2012) due to an increase in feed ethanol volume fraction. If the support layer does not expand as much as the active layer of the membrane, the pores will shrink inward producing the opposite effect and decrease the permeability

However, Tylkowski, et al. (2010) state that “[i]n the case of Duramem<sup>TM</sup>300, there is no change in the active layer thickness after nanofiltration and no observed influence of the applied pressure on the degree of concentration”. According to this statement, resulting out of flat sheet experiment with ethanol, a significant change of flux due to swelling of the active layer thickness in ethanol can be assessed as negligible.

All in all, the change in permeate flux with a deviation maximum of 7.3 % (DF06) over the test duration can be assumed as stable and even with ethanol injection no significant and permanent change in flux occurs.

#### 11.1.2.4 Temperature test (T01-T03)

The temperature tests were performed under TMP = 25 bar and LPM = 6.01 L/m<sup>2</sup> in recirculation mode. The dry matter concentration was 0.3 % in the feed. The first test (T01) was set to 40 °C, the second test (T02) to 30 °C and the third test (T03) to 23 °C. The influence of temperature on permeate flux is shown in this chapter.

Figure 30 illustrates the change of permeate flux over the time of filtrated material.

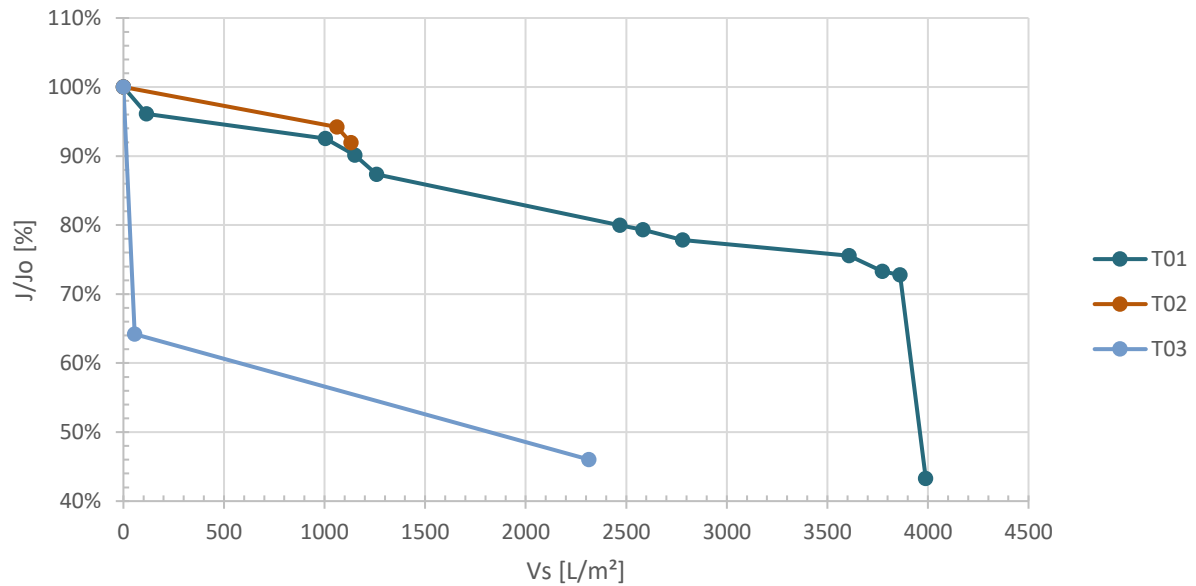


Figure 30: Results of flux in temperature tests with 0.3 % dry matter in feed.

T01 (40 °C) shows a gradual and continuous flux decline about 27 % from the initial flux. After 3,860 L/m<sup>2</sup> the temperature was changed to 30 °C. From this point on, a large decrease of flux down to 43 % from the initial flux occurred.

T02 was tested under 30 °C to observe how the flux changed in normal condition temperature, after applying 40 °C on the membrane. It can be seen, that the initial pattern is comparable to the first temperature test. The last temperature test started at 30 °C and was then cooled down to 23 °C. A significant flux decline was monitored. Even reaching 23 °C, the flux continued decreasing over time. After reaching a decrease of 54 % from the initial flow, the test was stopped.

It can be observed, that a decrease of temperature causes a decrease of permeate flux. The same correlation can be found in Siddique, et al. (2013) and Peeva, et al. (2013). This is explained by a decreasing permeability of the membrane material and lower solution viscosity.

A decrease of temperature causes also a decrease of solubility of fat. The precipitated fat can accumulate on the membrane, increases the concentration polarization and therefore the osmotic pressure. This results in an increase of rejection (see Figure 23) and in a decrease of flux (see Figure 31).

In Figure 31, it can be observed, that higher temperatures result in a higher permeate mass flow.

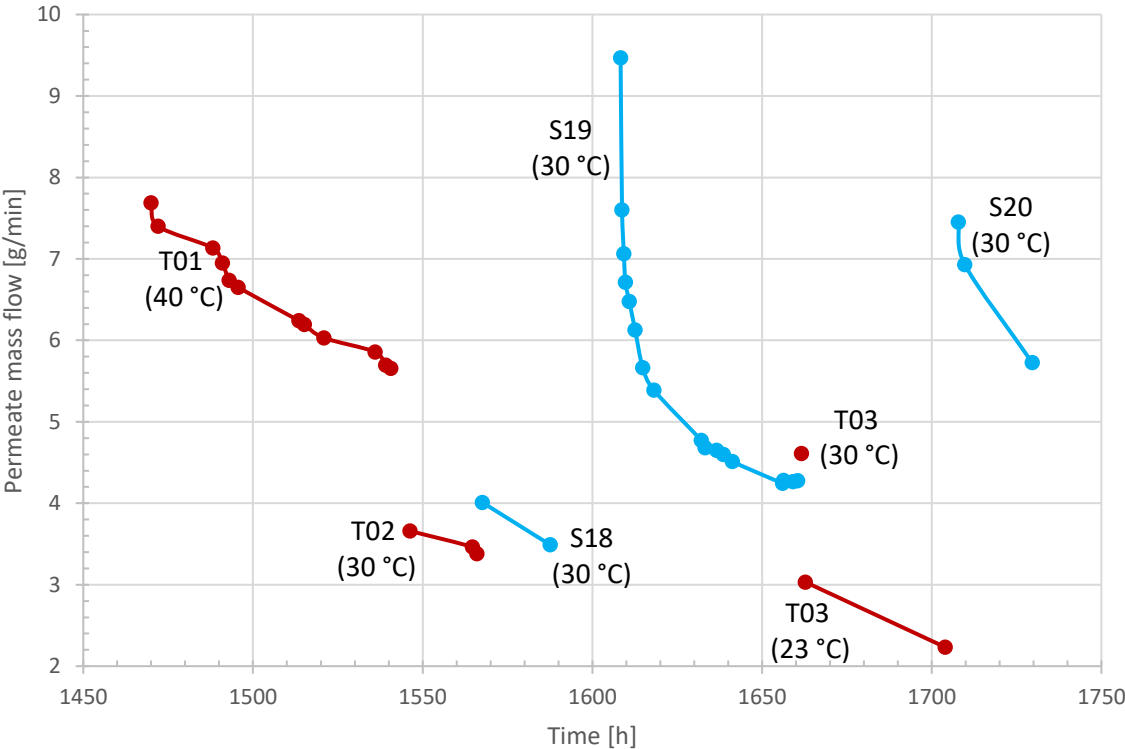
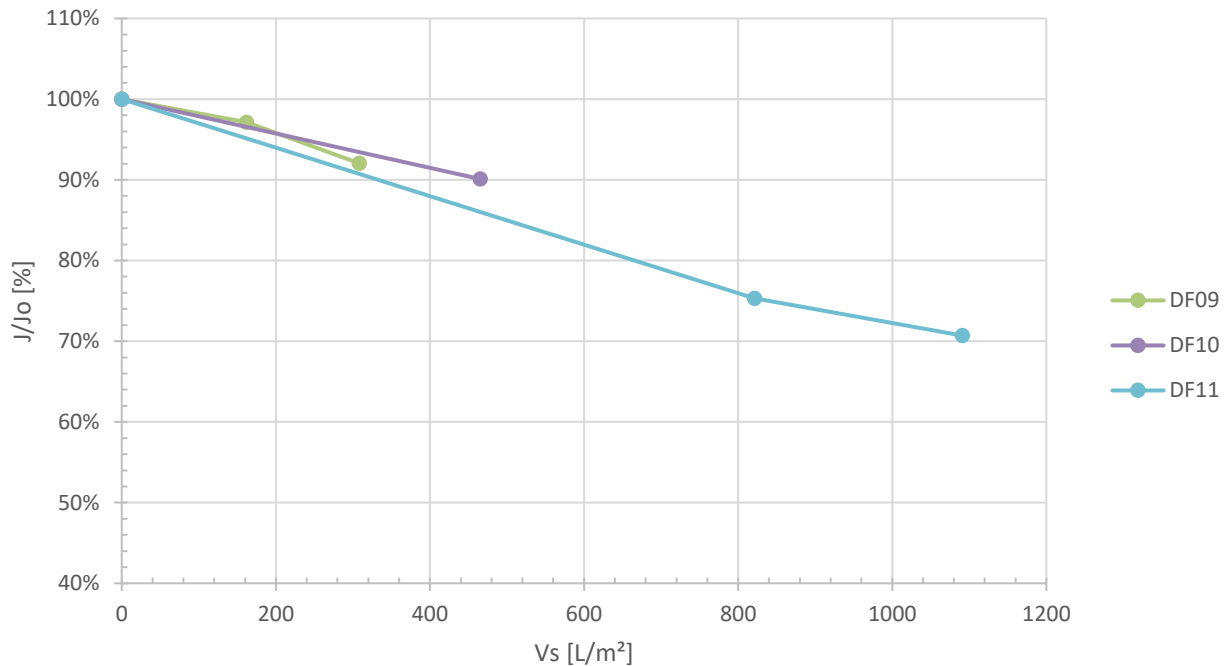


Figure 31: Results of permeate mass flow over time in temperature tests with feed.

### 11.1.2.5 Multi-stage diafiltration (DF09-DF11)

With the second module the multi-stage diafiltration was tested under normal conditions (TMP = 25 bar, TT1.1 = 30° C and LPM = 6.01 L/min). The results of flux performance are given in Figure 32.



**Figure 32: Flux performance of multi-stage diafiltration with feed.**

The three multi-stage diafiltration tests show a decreasing flux with the increase in filtrated material. DF11 has a flux of 70% of the initial flux at  $V_s \approx 1100$  L/m<sup>2</sup>. At a lower dry matter concentration in the feed (i.e. RC03) the flux at  $V_s \approx 1100$  L/m<sup>2</sup> was 86 % of the initial flux. This observation can be used to confirm the presumption, that a higher concentration causes a higher impact of slope decrease. For DF09 and DF10, the concentration was increased from 0.42 % to 0.63 %. This concentrate was used for the feed of DF11. In the last DF-test it was then increased to a concentration of up to 1.24 % dry matter. This difference can be seen in a slightly higher decrease of DF11 compared with DF09 and DF10 – even though much more ethanol was injected and therefore diluted the feed in DF11.

## 11.2 Lifespan analysis

In this chapter, the lifespan of the membrane module will be examined.

On one hand, the results from the recirculation mode will be investigated, which are predominantly concerned with the modification of the module itself – without the influence of a strong increase in concentration. On the other hand, the results of the diafiltration tests are considered, in which the influence of intentional concentration on the lifespan of the module is taken into account. For the following illustrations, the absolute value permeate mass flow over time is plotted. Figure 33 shows the permeate mass flow of RC01-RC03 and DF01-DF07 over time.

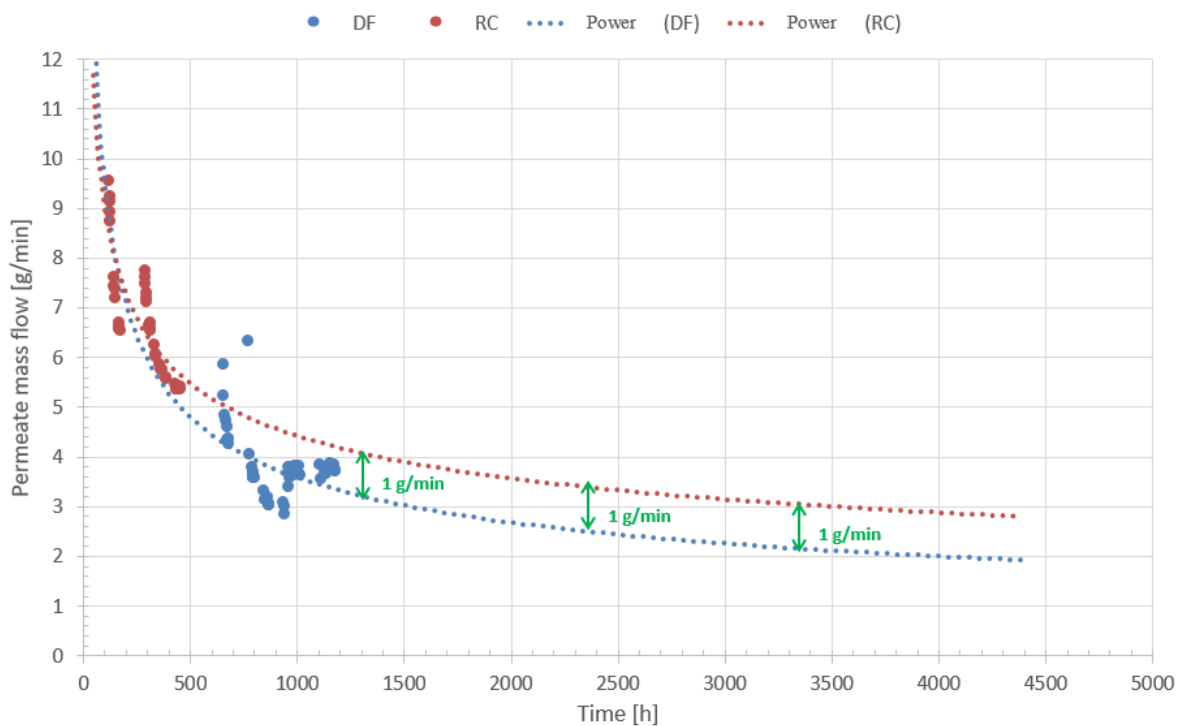


**Figure 33: Approximated lifespan of the first module in recirculation and diafiltration mode with feed.**

Through the recirculation test series and the diafiltration test series, a trend function (power) was applied in each case in order to illustrate the expected functional course. The selection of this approximation is based on Figure 9 – it shows a typical course of permeate flow for cross flow operation, which can be assumed in the following discussion.

In the approximations shown here, the functional decrease is less pronounced after about 500 h.

From this point on, the functions begin to stabilize. After about 1300 h the curve stabilized. After about 300 h, the two trend functions are separated from each other. The trend function for recirculation tests flattens slightly earlier than the trend function for diafiltration. After an operating time of about 1300 h, a stationary permeate flow difference of 1 g/min between the

two trend lines appears to be established. With this difference, both trend lines continue to flatten over time.

As described in Chapter 8.2.5.1, in reality there is usually always a further reduction of the permeate flux over time (Kraume M., 2012), which is also shown in this approximation. Nevertheless, the approximations seem to approach a final value greater than zero.

Figure 34 shows four (power) approximations. Two of them for the 1. module and two of them for the 2. module. One of them represents the performance exclusively with feed. The other represents the performance exclusively with solvent.

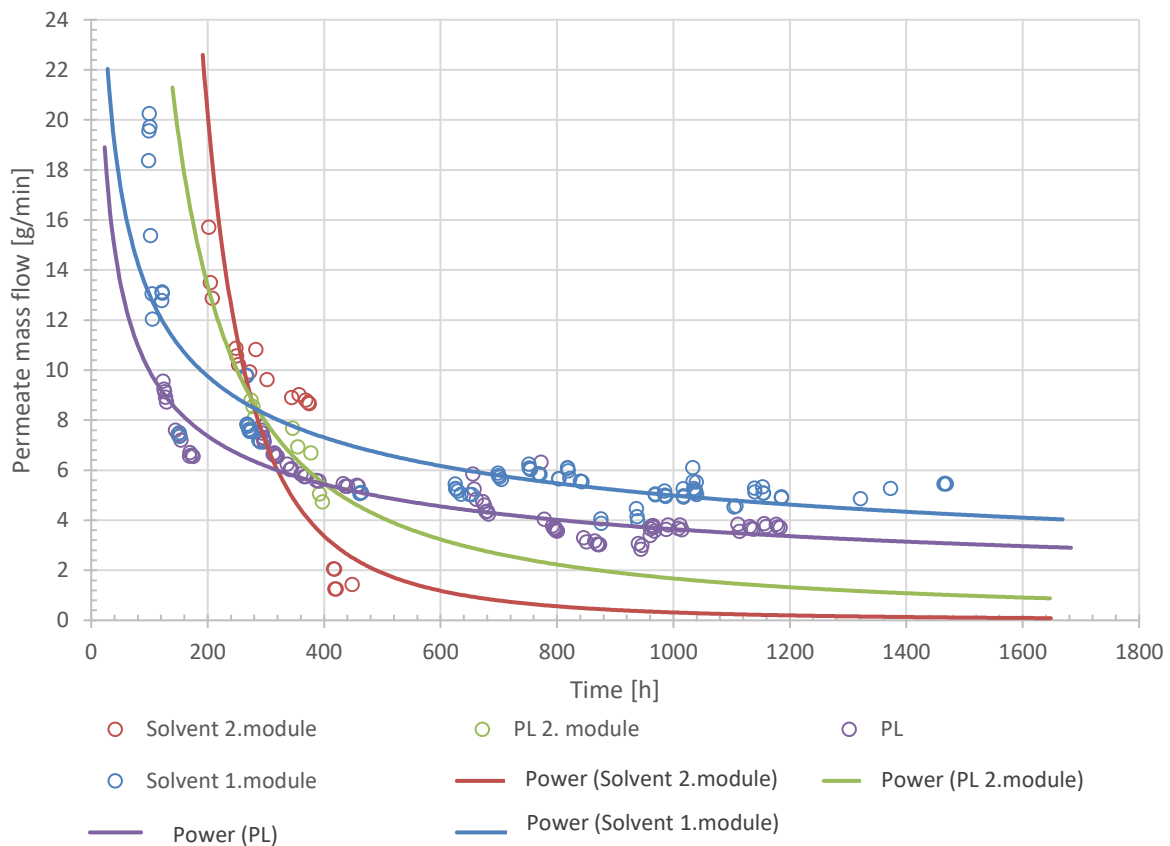


**Figure 34: Lifespan analysis of 1. & 2. module based on permeate mass flow of PL and solvent.**

When operating with pure solvent (without previous use of feed) the permeate production decreases strongly from 20.3 g/min to 12.0 g/min – means a loss of 59.1 % – within 4.5 hours; shown in “Solvent 1.module”. This cannot be attributed to the formation of a top layer as a result of the dry matter. Thus, the permeate mass flow is reduced due to adjustments of solvent properties, pressure conditions, temperature and other operating properties.

The time axis in Figure 34 depends on the operating time of the respective module. At time  $t = 0$ , the module was inserted and conditioned in pure solvent. The first two trend lines ("power PL" and "power solvent 1. module") belong to the first module. The subsequent trend lines are



assigned to the second module. All graphs have the same characteristics but have different gradients. From this figure it can be seen that a relatively long membrane conditioning is required – and thus correspondingly long measurement periods for a significant result – in order to reach an approximately stationary range.

As expected, the first module for the solvent has a higher MF than the mixture with dry matter. For this module, 172 measured values were recorded, and an operating time of 1469 h was used for this observation. Thus, the power function graphically stabilizes over time rather than using the measured values for this trend function only at the beginning.

In the second module, 27 measured values of the solvent and PL mixture were taken during a considered operating time of 448 h. Apparently, the test duration of the second module was not long enough to make a realistic statement about the further course of the permeate mass flow using this approximation. An indication of this is the fact that the trend function for the solvent has a lower MF than the trend function for the actual mixture. This results of the measured values at the beginning, i.e. during the first hours, still show a strong dependence on the membrane adaptation and thus the slope is overinterpreted by the power function. As can be seen with the first module, the slope decreases significantly after the adjusting phase. Accordingly, the influence of the values following after the adjustment could not be integrated into the approximation for the second module.

The trend function of the PL mixture of the second module (power (solvent 2. module)) decreases more strongly and is below the PL approximation of the first module when the stationary area is reached. Since in the second module the retentate from the diafiltration tests of the first module was used as feed for the diafiltration tests of the second module, it could be concentrated more strongly than before. This increases the total flow resistance.

Moreover, a loss of rejection can be observed in the course of the operating time (Figure 35).

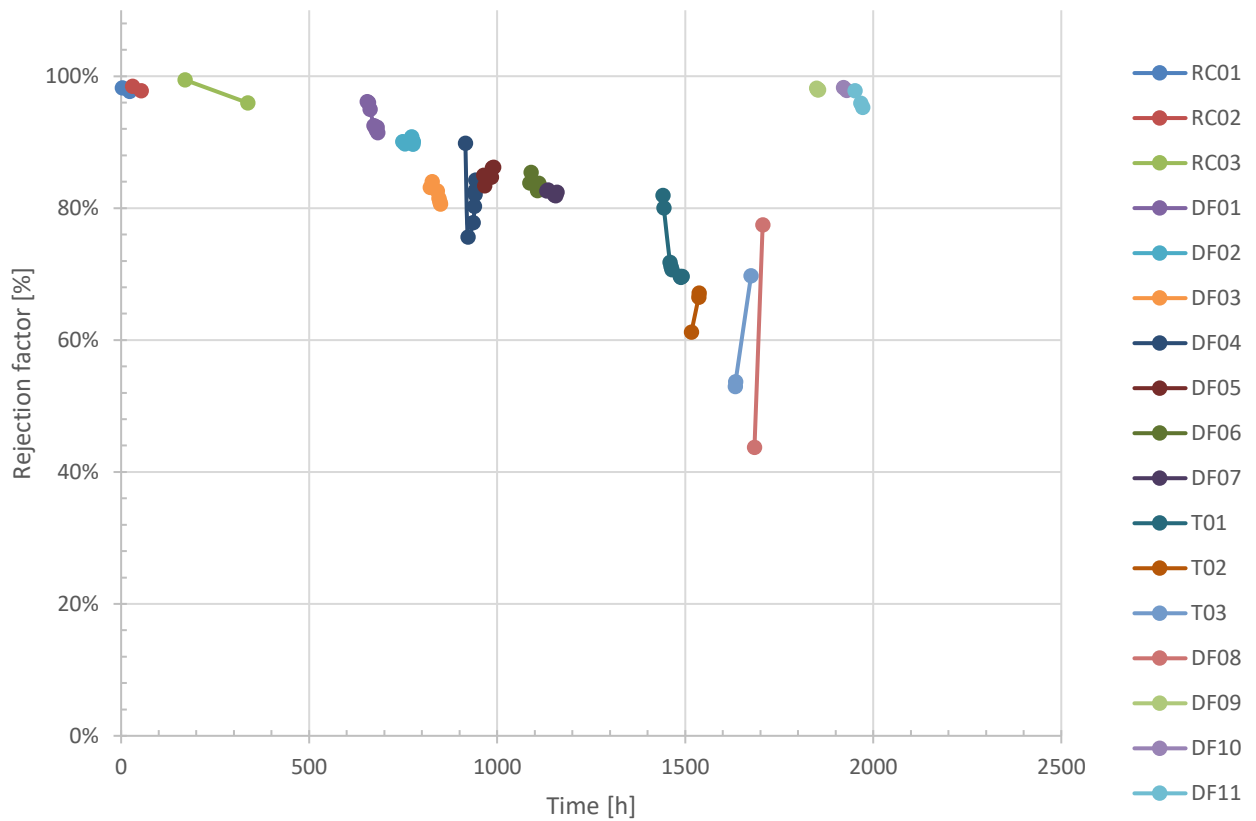


**Figure 35: Decrease of rejection in lifespan of both moduls with feed.**

This diagram shows a stable rejection at the beginning of both modules. The results for the first module show a decrease in rejection during the diafiltration tests. In the first 300 h a rejection of more than 95 % could be achieved. After about 850 h, a rejection of slightly more than 80 % could be achieved.

Since the following temperature tests caused a strong fluctuation of the rejection, it can be concluded that the temperature has an influence on the rejection and thus on the lifespan of the module. Further investigations are required.

In the following Figure 36 the rejection factor is plotted as a function of the flux divided by the initial flux.

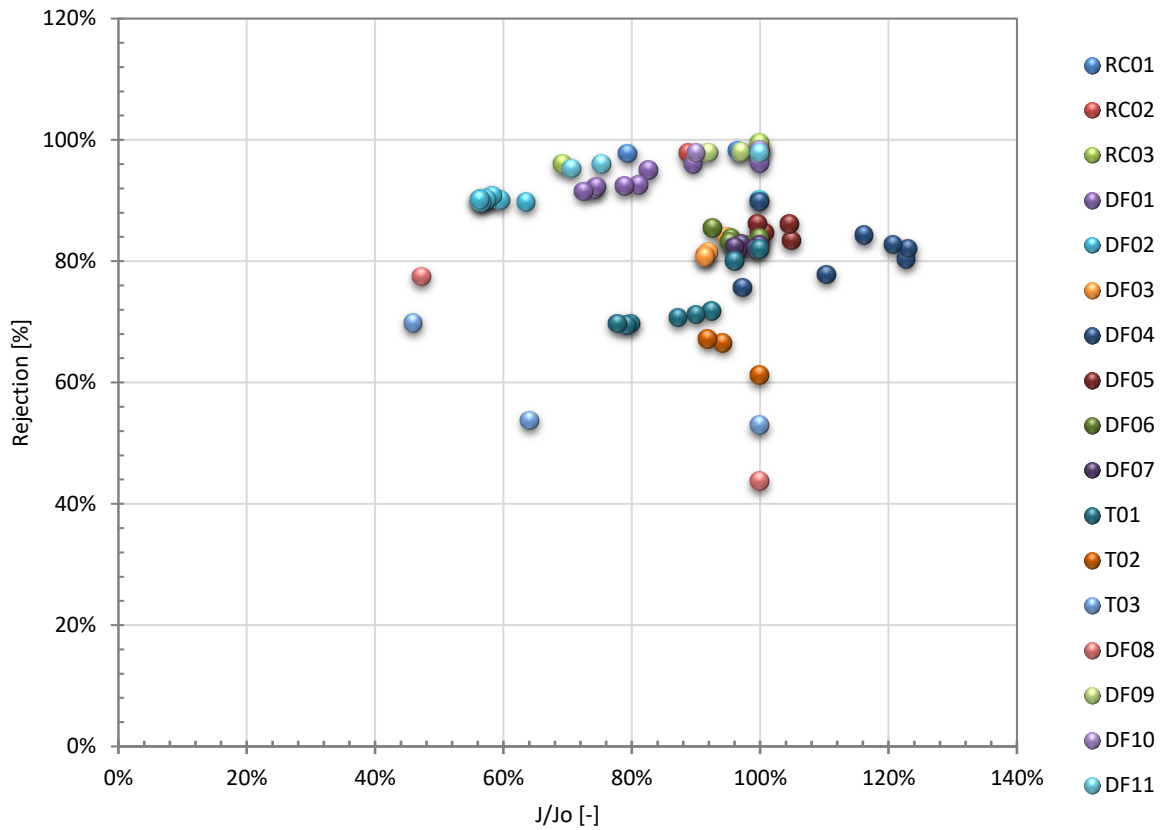


**Figure 36: Rejection over flux change in the lifespan of both moduls with feed.**

This figure shows the tendency that the loss of flux is also accompanied by a loss of rejection. A similar tendency can be seen in Figure 43 (see Appendix).

### 11.3 Membrane fouling and cleaning

Figure 37 shows the permeate flow from the pure solvent and the combined tests (RC & DF) with the feed.

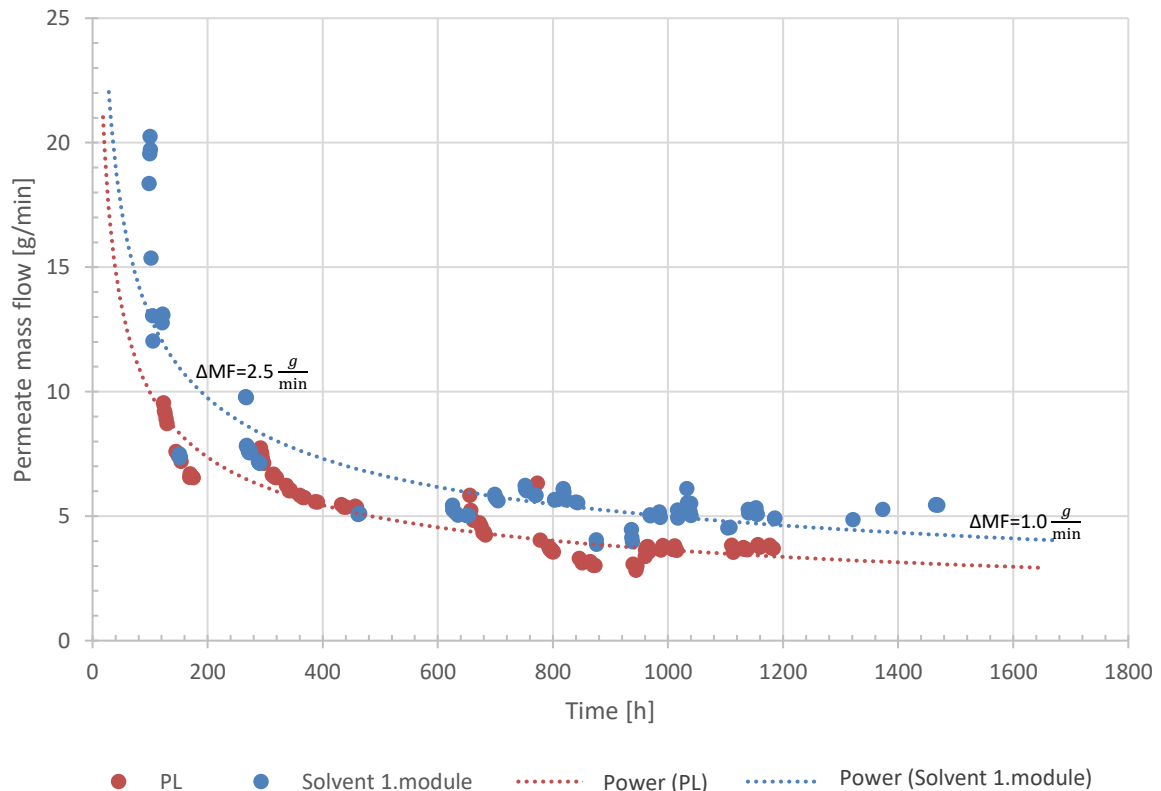


**Figure 37: Permeate mass flow over lifespan of the 1. module (solvent and feed).**

The approximation using the power function is reused. The upper trend function shows the development of the permeate flow with pure solvent. Below this, the trend function is averaged over all PL tests in order to estimate the influence of feed usage.

It can be seen from Figure 37 that the permeate flow of the solvent is higher than of the feed. Due to dry matter in the feed, a top layer could form on the membrane if the shear forces of the flow are not high enough to remove them. In pure solvent, there are few up to no particles in the fluid (it cannot be excluded that dust or other small particles may enter the system when filling the tank). This would result in the formation of the top layer being much less significant than in the feed tests. Furthermore, ethanol has an antibacterial effect and can therefore protect the membrane surface against biofouling.

Despite the cleaning measures used, the decrease of the permeate mass flow with PL could not be prevented. Furthermore, it can be seen that even the mass flow (MF) of the solvent continues to decrease over time, although scarcely any particles can be assumed in the filled solvent. After 170 h, the functional processes show a difference of 2.5 g/min. After 1,600 h, this difference

drops to a value of 1.0 g/min, as the trend function for the solvent approaches the trend function for the PL.

Such behavior is typical of irreversible layer formation (Kraume M., 2014, pp. 2-8). A surface layer builds up on the membrane surface which cannot be removed with the cleaning measure used here and which also appears to obstruct the permeate flow of the solvent. It should be noted that despite numerous cleaning measures in the period from 600 h to 1,200 h, there was no significant improvement in the MF.

It can therefore be summarized that even with regular cleaning measures, the permeate mass flow could not be prevented from further decreasing. So, it can be concluded that the cleaning methods used were inadequate. A closer examination of the individual cleaning tests will be carried out in the following chapter.

## 11.4 Cleaning approaches

The positive change in the permeate mass flow according to the selected cleaning method is selected as the parameter for the cleaning effectiveness.

The cleaning method applied between RC01 and RC02 and DF05 to DF07 is used to evaluate their effectiveness. Figure 38 shows the recirculation test. Between RC01 and RC02 the first cleaning test was carried out.

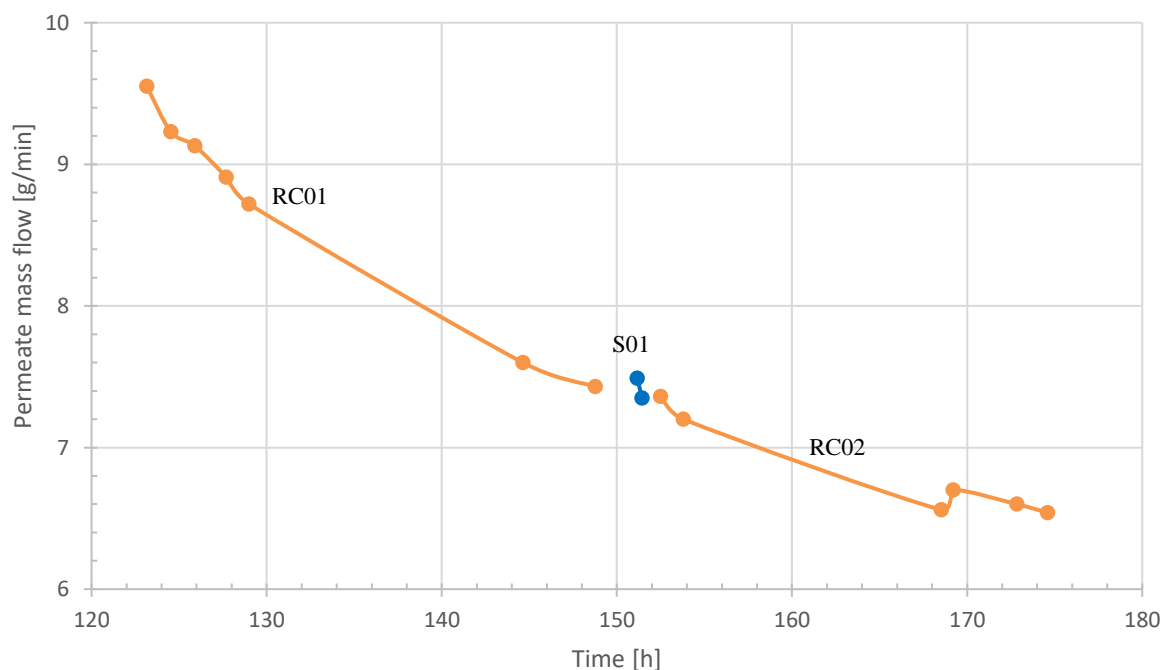
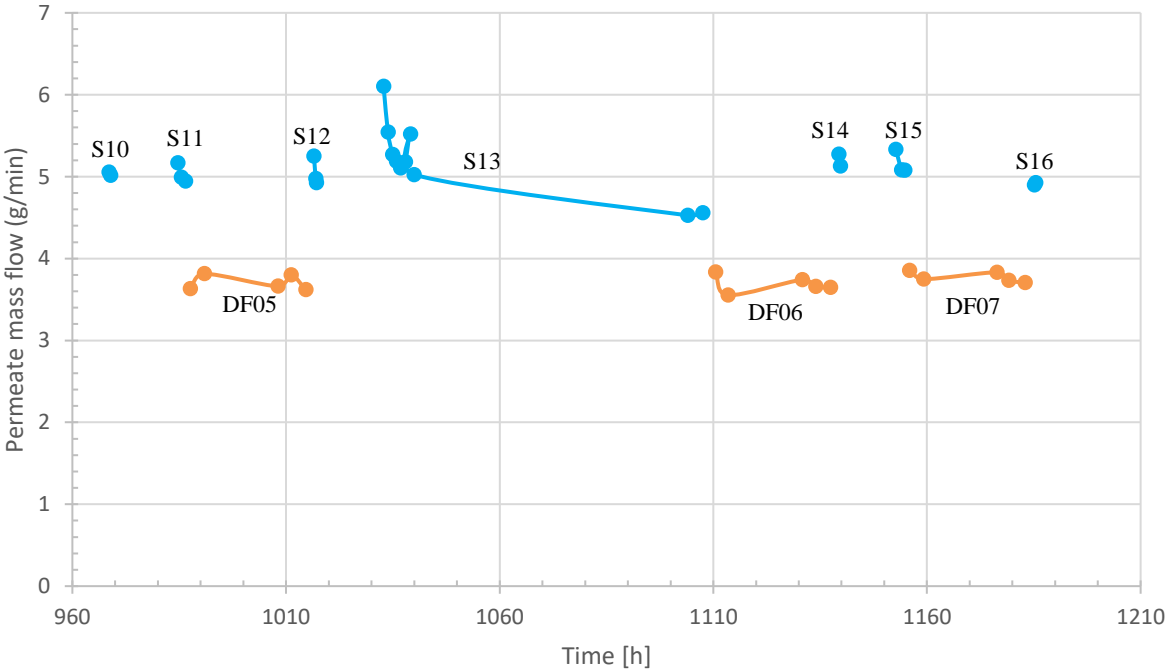


Figure 38: Example of cleaning performance in recirculation test.

After RC01 was completed, the system was flushed for 1 h with solvent at 30 °C and 8.01 L/min without applying pressure. This process was intended to remove the compact top layer – that might have formed – on the membrane surface by applying high shear forces. Furthermore, the compressed pore structure should relax again if possible and thus exhibit a higher flow rate for a short time in order to flush out possible particles present in the pores. After this process, the system was cleaned under NC (25 bar, 30 °C, 6.01 L/min) with new solvent for 20 min to find out whether a short washing was sufficient.

As can be seen in Figure 38 the measurement results of the permeate mass flow give no indication that this cleaning method has led to an improvement in flux performance with feed. Before and after cleaning, the permeate mass flow was 7.4 g/min. Furthermore, it can be stated that this method has not caused any deterioration in flux performance.

During the diafiltration tests, the selected cleaning measures were also used to confirm the previous results. Figure 39 shows the cleaning tests S10 – S16 and DF05 – DF07.



**Figure 39: Cleaning performance during first stage diafiltration test.**

It can be confirmed that the short cleaning cycles do not result in any significant improvement of the permeate mass flow with feed – as can be seen between DF06 and DF07.

With S13 a longer cleaning (74.7 h under NC) was performed to investigate the influence of the cleaning time under the selected conditions. No significant change in the permeate mass flow from DF05 (3.6 g/min) to DF06 (3.8 g/min) was observed. The 5.5 % increase can be attributed to the difference in concentration at the beginning and end of the diafiltration tests.

The fact that the concentration has an influence on the flux can be seen from the comparison of solvent and feed mass flow. Furthermore, a decrease in permeate mass flow with solvent of 24.6 % can be observed. This confirms the results given by Siddique et al. (2013).

From these results it can be concluded that the cleaning methods used were insufficient to achieve a significant recovering of permeate mass flow.

This can be due to insufficient flushing of the system among several reasons. Unnecessary corners, edges and dead spaces cannot be cleaned without leaving residues simply by flushing (clean-in-place). To improve this property, the process components in Hygienic Design can be constructed according to the guidelines of the European Hygienic Engineering & Design Group (EHEDG) (European Hygienic Engineering & Design Group (EHEDG), 2018). In certain food industries, cleaning can require up to 25 % of production time, so such a design can reduce the amount of cleaning effort (Krause, 2018).

## **11.5 Swelling**

Solvent and polymer membrane can interact with each other. This interaction – the slow diffusion of the solvent into the polymer chains – can lead to a swelling of the membrane surface and change the properties of the membrane (Gugliuzza, 2015). The structure of DuraMem®300 is mainly apolar. The modified polyimide membrane is composed by small polar zones - the connections between the molecules of the polymer – and apolar chains – which constitute the bulk of the polymer (Evonik Resource Efficiency GmbH, 2017). The binding of water is limited to the polar zones, the ethanol on the other hand can bind and fit itself to polar and apolar zones. Since the polymer-polymer interaction forces are superior to the polymer-solvent forces, expansion of the polymer network is sustained, and the membrane is prevented from completely dissolving (Billeyer, 1971). Swelling and “deswelling” of polymeric membranes can already be investigated with optical technique (Izak et al., 2007).

A hint for the occurrence of a swelling behavior can be found in Figure 40.

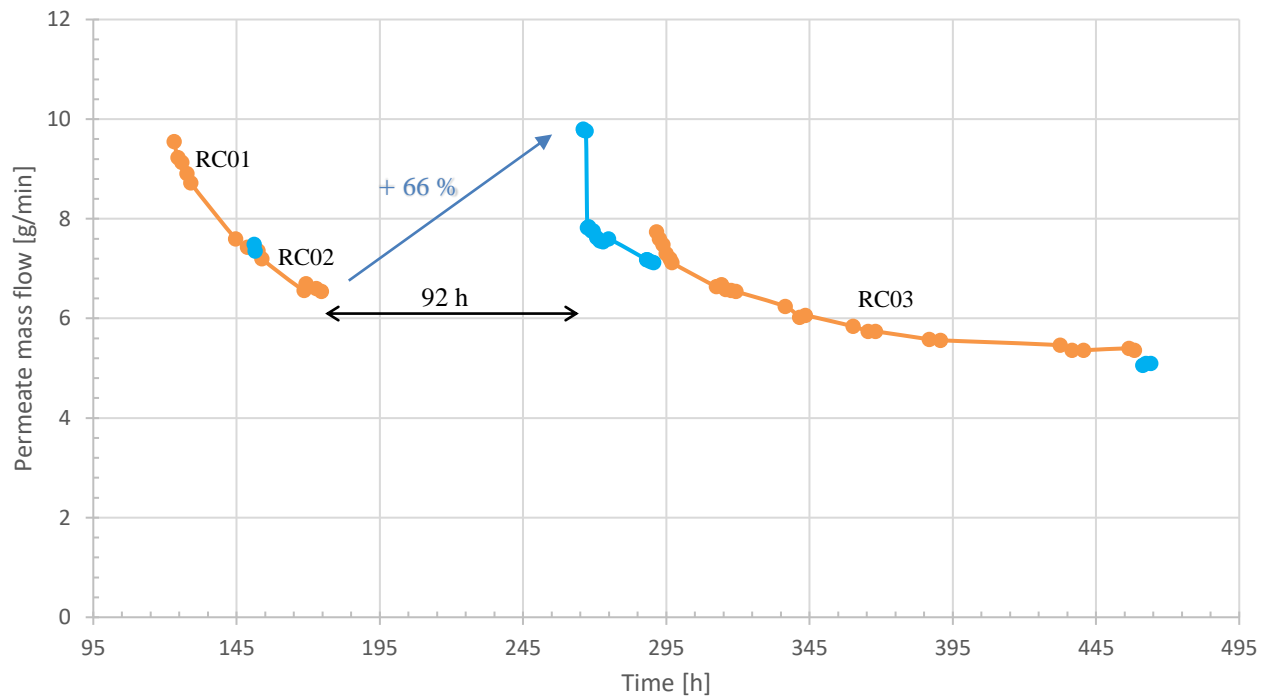


**Figure 40: Swelling effect observed in permeate mass flow performance.**

This figure shows the permeate mass flow over the first module's time of use during the recirculation tests RC01 – RC03. After the second recirculation test RC02, the module was left in solvent for 92 h before the solvent test was performed. It was found that this rest period caused a short permeate mass flow increase from 6.5 g/min (feed) to 9.8 g/min – what is similar to an increase of 66 %. This value dropped abruptly within 2 hours to 7.8 g/min and then steadily further. This drop of 20 % in permeate flux is inside the range of up to 30 % as described by Siddique et al. (2013).

From this it can be assumed that the rest phase (without pressure) caused the membrane to swell. The solvent has further diffused into the membrane and has enlarged the pore network. This is indicated by the fact that the permeate mass flow showed a strong increase during the following use – thus more permeate could flow through the membrane, which suggests enlarged pores. The strong decline of the permeate flux during the application of pressure can be attributed to the compression of the membrane again. The expanded pores are compressed and reduce their pore diameter so that less permeate can flow through the membrane. The solvent that has penetrated into the polymer structure is forced out of the network and an equilibrium corresponding to the pressure is achieved.



## 11.6 Case study for production (multi-stage test)

In this case study a multi-stage diafiltration was made. The study includes three diafiltration stages for the laboratory scale (see Table 4). The target of this case study is to show the concentrating of the feed amount in three diafiltration stages (also see Table 36 in Appendix).

**Table 4: Multi-stage test – designation.**

Stage	Test
1	DF05 – DF07
2	DF09 – DF10
3	DF11

The concentrate of stage 1 was used as feed for stage 2. The concentrate of stage 2 was used as feed for stage 3. The starting material for each diafiltration test in laboratory scale in the first stage was 9 kg feed with a dry matter content of 0.3 %.

### 11.6.1 Calculation of starting material (9 kg) – first stage

Starting material used in laboratory scale for one batch is presented in the following calculations.

One batch (for one diafiltration test) shall contain 9 kg feed with 0.3 % dry matter content. Fish roe extract used has a dry matter content of 40.4 % (Artic Nutrition AS, 2018). The mass fraction of fish roe extract inside 9 kg feed can be calculated as followed.

$$\text{Amount of fish roe extract} = \frac{0.003 * 9000 \text{ g}}{0.404} = 66.8 \text{ g} \quad (11.1)$$

From this follows the proportion of solvent in the feed.

$$\text{Amount of solvent} = 9000 \text{ g} - 66.8 \text{ g} = 8933.2 \text{ g} \quad (11.2)$$

This leads to the proportion of ethanol and water.

$$\text{Amount of ethanol} = 8933.2 \text{ g} * 0.7 = 6253.2 \text{ g} \quad (11.3)$$

$$\text{Amount of water} = 8933.2 \text{ g} * 0.3 = 2680.0 \text{ g} \quad (11.4)$$

These results are summarized in Table 5 .

**Table 5: Overview – material calculations for laboratory scale in multi-stage diafiltration mode.**

		Feed	Extract	Solvent	Ethanol	Water
Laboratory scale	<b>Amount [g]</b>	9000.0	66.8	8933.2	6253.2	2680.0
	<b>Percentage [%]</b>	100.00	0.74	99.26	69.48	29.78

Out of this batch starting material the multi-stage diafiltration test was done. In the following the results of these tests will be analyzed.

### 11.6.2 Product analysis

In the following section, the product produced in the multistage test will be analyzed according to ions content and conductivity. An external analysis laboratory (Eurofins Food & Feed Testing Norway, 2018) tested samples of product produced. The results of DF11 are given in Table 6.

**Table 6: External analysis results of the last diafiltration stage.**

Component	Concentrate	Permeate	Rejection	Atom radius	Polarity in Pauling Scala
[-]	[mg/kg]	[mg/kg]	[%]	[pm]	[-]
<b>Cu</b>	2.2	3.3	40.0	135	1.90
<b>Mg</b>	2,600	530	83.1	150	1.31
<b>Ca</b>	200	230	46.5	180	1.00
<b>K</b>	380	2,000	16.0	220	0.82
<b>Na</b>	6,700	28,000	19.3	180	0.93
<b>Zn</b>	7.3	3.1	70.2	135	1.65
<b>P</b>	7,800	1,500	83.9	100	2.19
<b>As</b>	1.8	0.3	85.7	115	2.18

*Data for Pauling-Scala were taken from (David R., 2010).*

A large proportion of magnesium is retained by the membrane in the retentate. This confirms the statement given in Chapter 8.1.3 that divalent ions like magnesium with 83.1 % are more retained from nanofiltration membranes than monovalent ions like sodium, which is only retained by 19.3 % (Crittenden, et al., 2012, p. 822). That shows the efficiency of desalination effect with nanofiltration membranes – over 80.7 % of sodium have been removed from the extract.

Furthermore, phosphorus is largely rejected, too. Phospholipid contains phosphorus, so they are retained by membrane used. Even arsenic is more rejected than permeated.

### 11.6.3 Conductivity

Conductivity is a sign for salt concentration in the sample (Bock, 2019). It was measured at 30 °C. The obtained data out of the experiments are shown in Figure 41 and in Table 34 in the Appendix.

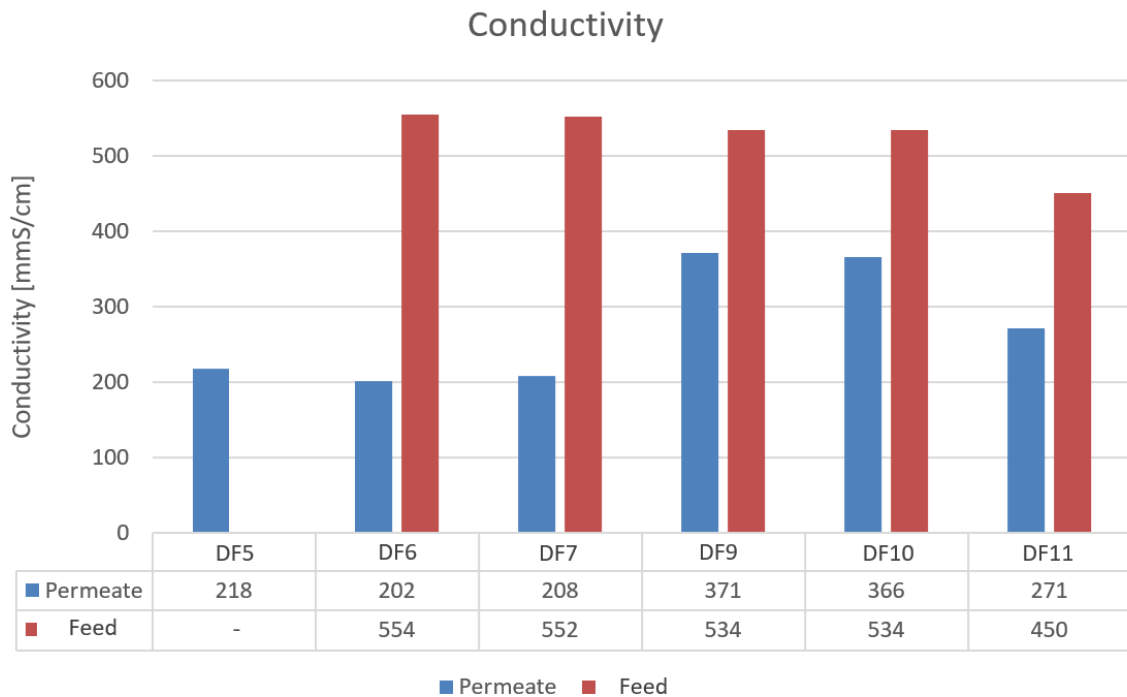


**Figure 41: Conductivity results of multi-stage diafiltration test (case study) with feed.**

It can be seen, that in the feed a higher conductivity occurs than in the permeate. This is due to the rejected ions. In the more concentrated samples of DF09 and DF10 an increase of permeate conductivity can be observed. More ions will be forced through the membrane, because of concentration polarization. For this reason, in DF11 the permeate conductivity would be higher again, too. But in this case the ethanol injection was increased to 53.4 % of feed amount to prevent substances from precipitation. Ethanol dilutes the concentrate. Therefore, the conductivity decreases as shown in Table 7.

**Table 7: Data for conductivity analysis of multi-stage diafiltration tests with feed in laboratory scale.**

	DF5	DF6	DF7	DF9	DF10	DF11
<b>Feed amount [g]</b>	8,918.6	9,000	9,000	6,032.4	7,275.3	6,754.5
<b>Ethanol amount [g]</b>	2,083	2,051.1	2,102.3	654.2	1,150	3,607
<b>Ethanol/feed [%]</b>	23.36	22.79	23.36	10.84	15.81	53.40
<b>Conductivity_Permeate [mmS/cm]</b>	218	202	208	371	366	271
<b>Conductivity_Feed [mmS/cm]</b>	No data	554	552	534	534	450
<b>Conductivity ratio permeate [%]</b>	No data	26.72	27.37	40.99	40.67	37.59
<b>Conductivity ratio feed [%]</b>	No data	73.28	72.63	59.01	59.33	62.41

As the data show, a higher conductivity was always measured in the feed than in the permeate. Among other factors, this can be attributed to the retained salts such as magnesium. A conductivity value of over 200 mmS/cm can also be measured in the permeate, which can largely be attributed to the sodium removed from the feed. This is another point in support of removing salts from the feed.

#### **11.6.4 Calculations for simulation – 100 kg assumed start material per batch**

To understand the performance of the system even more, a simulation for a scale up with calculated numbers is performed. The laboratory test serves as the basis for the evaluation of the case study for scale-up simulation. The results of the laboratory scale were used to calculate the same process with a starting material of 100 kg per batch in the first stage. In Table 8 this calculation is summarized. The percentage value of the scale up is similar to the percentage value of the laboratory scale (see Table 5).

**Table 8: Overview – material calculations for assumed scale up in multi-stage diafiltration mode.**

		Feed	Extract	Solvent	Ethanol	Water
Scale up	<b>Amount [kg]</b>	100.00	0.74	99.26	69.48	29.78
	<b>Percentage [%]</b>	100.00	0.74	99.26	69.48	29.78

The results of the diafiltration tests in laboratory scale (see Appendix) were transferred to the values of scale up, which are shown in Table 9.

**Table 9: Calculated results for the scale up simulation of multi-stage diafiltration tests.**

<b>DF-stage</b>	<b>Feed</b>	<b>Retentate</b>	<b>Permeate</b>	<b>Ethanol injected</b>
<b>[-]</b>	<b>[kg]</b>	<b>[kg]</b>	<b>[kg]</b>	<b>[kg]</b>
<b>1.1</b>	100.0	43.6	69.5	23.36
<b>1.2</b>	100.0	44.0	68.7	22.79
<b>1.3</b>	100.0	42.9	70.5	23.36
<b>2.1</b>	65.3	29.8	39.3	7.08
<b>2.2</b>	65.3	29.6	41.3	10.31
<b>3.1</b>	59.3	18.6	62.4	31.68

This table shows the results of concentrating in the first stage (1.1, 1.2, 1.3), second stage (2.1, 2.2) and third stage (3.1) when 100 kg per batch was chosen as starting. The column “Ethanol injected” shows the amount of injected ethanol during each test.

Figure 42 illustrates the results of the calculated case study with a starting amount of 100 kg per batch in the first stage.

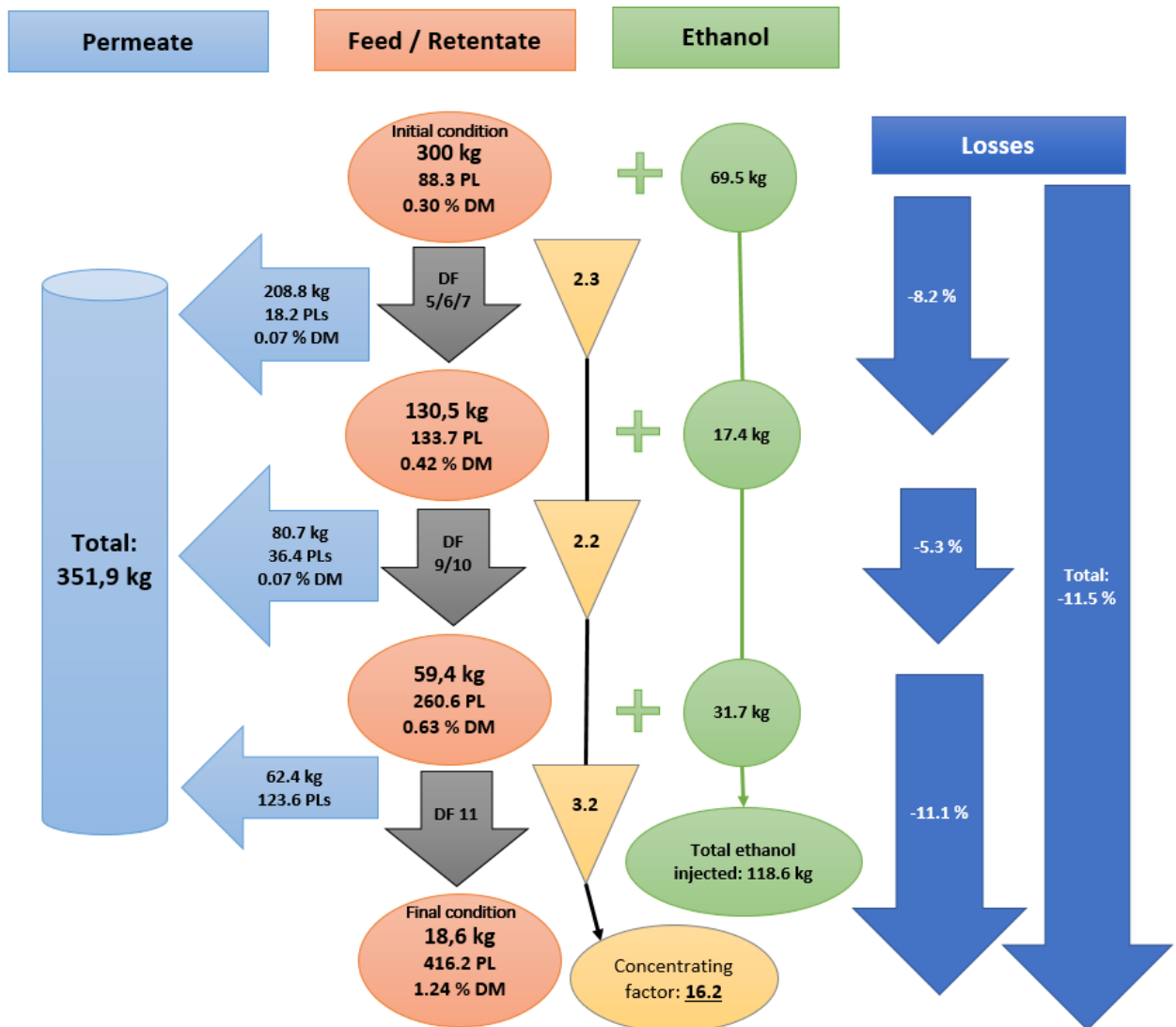


Figure 42: Calculated results of case study with assumed starting material of 100 kg per batch in the first stage of diafiltration.

The calculations show, that in a multi-stage diafiltration test with a starting material of 300 kg feed the process would produce 18.6 kg of concentrate. This indicates a concentrating factor of 16.2. During operation 118.6 kg ethanol were injected. The dry matter content increases from 0.30 % up to 1.24 %, which corresponds to a fourfold increase in the dry matter concentration. The increase of the polar lipid concentration can be confirmed by the values of the average area peaks of polar lipids (PL), which are abbreviated as "PL" in this figure. This value increases from 88.3 mAU\*min to 416.2 mAU\*min. The extracted permeate has an amount of 351.9 kg. An integral mass balance can be used to determine the proportion of loss that can occur for example during transfers, sampling, evaporation or residues in the vessel.

$$Mass\ loss = \frac{300.0\ kg + 118.6\ kg - (18.6\ kg + 351.9\ kg)}{300.0\ kg + 118.6\ kg} = 11.5\ \% \quad (11.5)$$

In this example, the mass loss of the process has a value of 48.1 kg.

### 11.6.5 Energy consumption and cost estimation for laboratory scale

Following analysis of energy consumption and cost estimation is only made for the laboratory scale. The energy consumption of the MMS Membrane System is given by the manufacturer with 4 kW (MMS AG Membrane Systems, 2016). The most energy is used by the heat exchanger E1.1 with 2.5 kW and the HYDRA-CELL Pump with 1.5 kW (MMS AG Membrane Systems, 2018). The energy consumption of display, balance or other measuring devices can be neglected in this range of value.

According to Melin & Rautenbach (2007), the selectivity and the efficiency of the membrane are of central importance for the economic efficiency of a membrane process. Performance is understood to mean the permeate flow achieved under certain operating conditions. It should be noted that this is of secondary importance for economic efficiency, since lower performance can be compensated by more membrane area. A low degree of selectivity, on the other hand, can often not be compensated cost-effectively. In most cases, multi-stage processes are required that would not be competitive with existing alternative processes.

Firstly, electricity costs will be estimated for an operation period of 24 h. Cleaning approaches will not be included into this calculation because of insufficient cleaning results. It is therefore assumed that continuous operation is carried out without further cleaning intervals – the shear forces caused by the flow are assumed to be sufficient enough for cleaning.

The average electricity price in Europe in 2017 was 20.4 cents/kWh (1-Stromvergleich.com, 2019). A continuous operation (24 h) would result in electricity costs of 19.58 €/day.

$$Electricity\ cost\ for\ one\ day = \frac{20.4\ cent}{kWh} * 24\ h * 4\ kW = 19.58\ € \quad (11.6)$$

The usability of this membrane module will now be investigated based on the cost of the treated amount while the diafiltration case study.

The basic material data of the test series in laboratory scale (starting material for the first stage test was 9 kg per batch) are listed in Table 10.

**Table 10: Overview over the operation effort for case study in laboratory scale.**

Test [-]	Feed (start) [kg]	Feed (end) [kg]	Ethanol injected [kg]	Time of operation [h]
<b>DF05</b>	9.0	4.6	2.1	28.2
<b>DF06</b>	9.0	4.7	2.1	28.4
<b>DF07</b>	9.0	4.2	2.1	28.2
<b>DF09</b>	6.0	3.0	0.7	7.4
<b>DF10</b>	7.3	3.8	1.2	10.5
<b>DF11</b>	6.8	2.6	3.6	22.5

The total amount of feed used is the sum of the amount submitted in DF05-DF07. These 27 kg feed consist of 18.8 kg ethanol, 8.0 kg water and 0.2 kg fish roe extract.

Ethanol costs are estimated at 0.30 €/L (finanzen.net, 2019). Assuming a density of 0.79 kg/L (Baum, 2006), this results in a cost factor of 0.38 €/kg ethanol. During operation 11.8 kg ethanol was added to the mixture. This gives the following calculation for the ethanol costs.

$$\text{Case study cost for ethanol} = (18.8 \text{ kg} + 11.8 \text{ kg}) * 0.38 \frac{\text{€}}{\text{kg}} = 11.63 \text{ €} \quad (11.7)$$

The costs for the water are neglected. For the production of 0.2 kg extract 1.89 kg fish roe are needed. It had a price of 15 NOK/kg (Artic Nutrition AS, 2018). From this, the costs for the used amount of fish roe can be determined.

$$\begin{aligned} \text{Case study cost for extract (0.2 kg)} &= 1.89 \text{ kg} * 15 \frac{\text{NOK}}{\text{kg}} * \frac{1 \text{ €}}{9.73 \text{ NOK}} \quad (11.8) \\ &= 2.91 \text{ €} \end{aligned}$$

The basis for the currency translation is provided by (finanzen.net, 2019). The total electricity costs for the assumed continuous operation of the case study amount to the following amount.

$$\text{Case study cost for electricity} = 125.2 \text{ h} * 4 \text{ kW} * 20.4 \frac{\text{cent}}{\text{kWh}} = 102.16 \text{ €} \quad (11.9)$$

As a result, the material costs are as shown in Table 11.



**Table 11: Cost overview of the case study in laboratory scale.**

Type	Amount	Cost
<b>Ethanol</b>	30.6 kg	11.63 €
<b>Water</b>	8.0 g	0.00 €
<b>Extract</b>	0.2 kg	2.91 €
<b>Electricity (125.2 h)</b>	0.5 MW	102.16 €
<b>Total</b>	-	<b>116.70 €</b>

At the end of DF11 in laboratory scale, 2.6 kg concentrate with 1.2 % DM could be obtained from this test series. This results in the following price per treated amount:

$$\text{Cost of product (1.2 \% DM)} = \frac{116.7\text{€}}{2.6 \text{ kg}} = 44.89 \frac{\text{€}}{\text{kg}} \quad (11.10)$$

According to the use of materials and electricity, these are estimated costs per kilogram of product of 1.24 % DM. Additional costs such as storage costs, investment costs for the plant, maintenance costs, labor costs and if necessary additional cleaning costs for longer operating periods must be added. In addition, the use of solvent recycling can be investigated in order to reduce costs. Due to the limited comparability with these pilot studies, no industry-related cost estimates are made here. Further investigations for this topic must be done.

## 12 Conclusion and recommendation

During operation of the plant, it was found that the desired concentration was achieved in diafiltration mode. Since even in recirculation mode a slight concentration could be detected, an accumulation of the PL on or in the module can be assumed. A concentration does not seem to have a high influence on the flux or the rejection.

At the beginning of the operating phase of a module there is a strong drop in flux. This indicates an adaptation phase of the module to the ambient conditions. This flux stabilizes over time. A flatter drop can also be detected during rejection over time. These two parameters seem to converge to a range of values. Even with the cleaning methods used, no detectable improvement could be achieved in flux or rejection. The applied cleaning methods seem to have been insufficient. Further investigations, e.g. by chemical cleaning, should be carried out. Furthermore, the resistance of the module to the solvent and the influence of ethanol should be investigated in a long-term test.

The temperature tests showed that as the temperature increases, the flux increases and the rejection decreases. At lower temperatures the flux decreases and the rejection increases. An increase in temperature could also be detected during concentration. This can be attributed to the higher density of the mixture and the associated friction.

Desalination (of sodium at 81 %) of the extract could be verified by external analysis and conductivity measurement. Desired salts such as magnesium could be retained in the extract.

In summary, the hypotheses set out in the introduction can be answered as follows:

- The permeate mass flow is not stable over the operating time of the module, but drops sharply, especially at the beginning. Only at the end does the flux seem to stabilize.
- The rejection is not stable over the operating time of the module and decreases steadily. At the beginning, a rejection of more than 95 % could be determined. However, this dropped further to below 80 %. Thus, the results of Toh, et al. (2007) could only be confirmed for certain tests.
- Sodium predominantly passed the membrane, so that a desalination effect occurred. The product quality also increased due to the retention of magnesium and calcium in the extract.
- The module can work for an estimated period of about 9 weeks with a rejection of over 80 % and a flux of about 30 % of the initial flux (see Figure 34 & Figure 35). In this time, despite applied shear forces, fouling seems to occur – at least a change of the membrane, which leads to a reduction of flux and rejection. Further investigations are recommended and should be carried out.

## 13 Future work

Further work can be carried out in the area of cleaning. If necessary, longer cleaning cycles or even other methods or substances for cleaning the module are required. Furthermore, stronger concentration tests can be carried out to observe the limit for an appropriate flux. Scale up and long-term tests with the module under the proven conditions are the next steps required for industrial use. The influence of solvent, temperature and other pressures can be studied. A combination of several modules as well as an improved component distribution of the plant must also be tested in order to make this process marketable.

The following measuring setup can be used to investigate the softening effect of ethanol. The flat membranes are placed in water, ethanol and solvent for one month. They are then removed and tested for elasticity using a stretch test. Depending on when or at what force the membrane tears, a softener effect can be inferred.

In order to reduce the possible influence of the ethanol-water mixture on the membrane material, a sintered material made of PTFE (polytetrafluoroethylene) may be used. This is a hydrophobic, chemically resistant and inert polymer which is suitable for the filtration of highly aggressive media in a wide temperature range (-200 °C to +260 °C) and into whose pores neither water nor electrolytes can penetrate (RCT Reichelt Chemietechnik GmbH + Co., 2018).

Dynamic modelling can also be considered for more detailed investigation. Either a physical model with corresponding physical correlations can be created (white box) or a phenomenological model with input and output can be created (black box). The latter is easier to generate on the basis of the measurement data.

Other methods may be applied to this process to achieve improved performance of flux or rejection while treating the membrane with ammonia or certain alkylamines as described for example in the patent no. 5,755,964 according to Midland (1998).

## 14 List of references

- 1-Stromvergleich.com. (2019). *www.1-stromvergleich.com*. Retrieved from <https://1-stromvergleich.com/strompreise-in-europa/>
- Artic Nutrition AS. (2018, 07 22). Industrievegen 42, NO-6155 Ørsta, Norway.
- Baum, M. (2006, March). Ethanol. Georg Thieme Verlag KG. Retrieved 01 22, 2019, from <https://roempp.thieme.de/roempp4.0/do/data/RD-05-01878>
- Billeyer, F. W. (1971). *Textbook of polymer science* (2d ed.). New York: Wiley-Interscience.
- Bock, P. (2019). Leitfähigkeit (EC) und gelöste Feststoffe (TDS). (E. Umwelttechnik, Ed.) Retrieved 01 12, 2019, from [http://www.eurotronik.de/dateien/Definition\\_Leitfaehigkeit.pdf](http://www.eurotronik.de/dateien/Definition_Leitfaehigkeit.pdf)
- Bouguer, P. (1729). *Essai d'optique sur la gradation de la lumière*. Paris: Claude Jombert.
- Bundestag. (2005, April 6). Drucksache 15/5231 Umfassende und wirksame Bekämpfung der Fehlernährung in Deutschland. (G. Bundestag, Ed.) Berlin, Germany. Retrieved 10 24, 2018, from <http://dip21.bundestag.de/dip21/btd/15/052/1505231.pdf>
- Crittenden, J. C., Trussell, R. R., Hand, D. W., Howe, K. J., & Tchobanoglous, G. (2012). *MWH's Water Treatment: Principles and Design, Third Edition*. New Jersey; Canada: John Wiley & Sons, Inc.
- David R., L. (2010). Molecular Structure and Spectroscopy . In *CRC Handbook of Chemistry and Physics* (90 ed., pp. 9-98). CRC Press/Taylor and Francis.
- Elstrodt, J. (2018). *Maß- und Intergrationstheorie* (Vol. 8). (U. Münster, Ed.) Münster, Deutschland: Springer Spektrum. doi:10.1007/978-3-662-57939-8
- Eurofins Food & Feed Testing Norway. (2018, 06 19). Analytical report. Moss, Norway.
- European Hygienic Engineering & Design Group (EHEDG). (2018). *European Hygienic Engineering & Design Group (EHEDG)*. Retrieved 09 21, 2018, from [www.ehedg.org](http://www.ehedg.org)
- Evonik Resource Efficiency GmbH. (2017, March). Technical Information DuraMem Products. Germany.
- finanzen.net. (2019, 01 22). *www.finanzen.net*. Retrieved from [www.finanzen.net: https://www.finanzen.net/rohstoffe/ethanolpreis](https://www.finanzen.net/rohstoffe/ethanolpreis)
- finanzen.net. (2019, 01 22). *www.finanzen.net*. Retrieved from [www.finanzen.net: https://www.finanzen.net/waehrungsrechner/norweg-krone\\_euro](https://www.finanzen.net/waehrungsrechner/norweg-krone_euro)
- Goethe-University (Ed.). (2018, 06 18). *www.wiwi.uni-frankfurt.de*. Retrieved 12 28, 2018, from [https://www.wiwi.uni-frankfurt.de/fileadmin/user\\_upload/dateien\\_pruefungsamt/Formulare\\_Merkblaetter/Ehrenwoertliche\\_Erklaerung.pdf](https://www.wiwi.uni-frankfurt.de/fileadmin/user_upload/dateien_pruefungsamt/Formulare_Merkblaetter/Ehrenwoertliche_Erklaerung.pdf)

- Goss, K.-U., & Schwazzenbach, R. P. (2003, April 1). Rules of Thumb for Assessing Equilibrium Partitioning of Organic Compounds: Successes and Pitfalls. *Journal of Chemical Education*, 80(4), p. 450. doi:10.1021/ed080p450
- Gugliuzza, A. (2015, December 07). Membrane Swelling. *Drioli E., Giorno L. (eds.) Encyclopedia of Membranes*. doi:https://doi.org/10.1007/978-3-642-40872-4
- Huang, J., & Zhang, K. (2011, September 30). The high flux poly (m-phenylene isophthalamide) nanofiltration membrane for dye purification and desalination. *Dentoscope*, pp. 19-26.
- Izak, P., Hovorka, S., Bartovsky, T., Bartovska, L., & Crespo, J. (2007, June 15). Swelling of polymeric membranes in room temperature ionic liquids. *Journal of Membrane Science*(Volume 296, Issues 1-2), pp. 131-138. Retrieved from https://doi.org/10.1016/j.memsci.2007.03.022
- Karger, R., & Hoffmann, F. (2013). *Wasserversorgung - Gewinnung - Aufbereitung - Speicherung - Verteilung* (14 ed.). Wiesbaden: Springer Vieweg. doi:10.1007/978-3-8348-2096-9
- Kilduff, J., Mattaraj, S., & Belfort, G. (2004, May 6). Flux decline during nanofiltration of naturally-occurring dissolved organic matter: effects of osmotic pressure, membrane permeability and cake formation. *J. Membr. Sci.*(239), pp. 39-53.
- King, P. D.-I. (2012). *Grundlagen der Mess- und Regelungstechnik*. 102. Berlin, Berlin, Deutschland: Technische Universität Berlin - Institut für Prozess- und Verfahrenstechnik - Fachgebiet Mess- und Regelungstechnik.
- Kraume, M. (2012). *Transportvorgänge in der Verfahrenstechnik - Grundlagen und apparative Umsetzungen*. Berlin: Springer Vieweg.
- Kraume, M. (2014). *Membranverfahren. Skript Membranverfahren*. Berlin: Technische Universität Berlin; Fachgebiet Verfahrenstechnik.
- Kraume, M. (2014). *Membranverfahren*. Berlin: Technische Universität Berlin; Fachgebiet Verfahrenstechnik.
- Krause, P. (2018, October). Ohne Ecken und Kanten - selbstreinigende Filter im Hygienic Design. (D. e.-G. GDCh, Ed.) *CITpuls - Das Praxismagazin für Verfahrens- und Chemieingenieure*, pp. 29-30.
- Labanda, J., Sabate, J., & Llorens, J. (2012, 10 30). Permeation of organic solutes in water-ethanol mixtures with nanofiltration membranes. *Desalination*(315), pp. 83-90.
- Larsen, R. (1999). *Anästhesie und Intensivmedizin in Herz-, Thorax- und Gefäßchirurgie*. Berlin/Heidelberg/New York: Springer.
- Li, F.-Y., Chaigne-Delalande, B., Kanellopoulou, C., Davis, J. C., Matthews, H. F., Douek, D. C., . . . Lenardo, M. J. (2011, July 27). Second messenger role for Mg<sup>2+</sup> revealed by human T-cell immunodeficiency. *Nature - international journal of science*, 475, pp. 471-476. doi:doi:10.1038/nature10246
- Loeb, S., & Sourirajan, S. (1964, May 12). *California Patent No. 3,133,132*.

- Maul, C., & Dammeyer, T. (2012). *www.tu-braunschweig.de*. Retrieved from <https://www.tu-braunschweig.de/Medien-DB/pci/fehlerrechnung.pdf>
- Melin, T., & Rautenbach, R. (2007). *Membranverfahren - Grundlagen der Modul- und Anlagenauslegung*. Berlin - Heidelberg: Springer-Verlag.
- Mickels, W. E. (1998, May 26). *Midland, Mich. Patent No. 5,755,964*.
- MMS AG Membrane Systems. (2016). SW18 Rental System. Switzerland.
- MMS AG Membrane Systems. (2018, 01 17). Equipment List. Urdorf.
- MUNKTELL. (2018). Quantitative Filter Paper. *Art.no: 100003, Grade 00H, Batch: 2773, Size 110 mm*. Norway.
- Otterlei, I. (2018, November 17). Medisinen har effekt. *SUNNMØRSPOSTEN*, 11.
- Parment, S. (2019, 01 08). Technique boosts omega 3 fatty acid levels. (U. o. Chicago, Ed.) Chicago. Retrieved 01 09, 2019, from <https://medicalxpress.com/news/2019-01-technique-boosts-omega-fatty-acid.html>
- Peeva, L., Arbour, J., & Livingston, A. (2013, June 11). On the Potential of Organic Solvent Nanofiltration in Continuous Heck Coupling Reactions. *Organic Process Research & Development*(17), pp. 967-975.
- Peeva, L., Gibbins, E., Luthra, S., White, L., Stateva, R., & Livingston, A. (2004, March 1). Effect of concentration polarisation and osmotic pressure on flux in organic solvent nanofiltration. *J. Membr. Sci.*(236), pp. 121-136.
- Pike, I., & Jackson, A. (2010). *Fish oil: production and use now and in the future*. Lipid Technology. doi:10.1002/lite.201000003
- RCT Reichelt Chemietechnik GmbH + Co. (2018, October). Sinterwerkstoffe aus PTFE zur Filtration und Separation. (D. e.-G. GDCh, Ed.) *CITplus - Das Praxismagazin für Verfahrens- und Chemieingenieure*(10), p. 44.
- Reisman, H. B. (2008, September 27). Problems in Scale-Up of Biotechnology Production Processes. *Critical Reviews in Biotechnology*, 13(3), pp. 195-253. doi:10.3109/07388559309041319
- Schrader, M. (2016). *Prinzipien und Anwendungen der Physikalischen Chemie*. Berlin: Springer Spektrum.
- Shi, D., Kong, Y., Yu, J., Wang, Y., & Yang, J. (2006). Separation performance of polyimide nanofiltration membranes for concentrating spiramycin extract. *Dentoscope*(191), pp. 309-317.
- Siddique, H., Rundquist, E. B., Peeva, L., & Livingston, A. (2013, October 29). Mixed matrix membranes for organic solvent nanofiltration. *Journal of Membrane Science*(452), pp. 354-366.
- Silva, P., & Livingston, A. (2006, March 5). Effect of solute concentration and mass transfer limitations on transport in organic solvent nanofiltration - partially rejected solute. *J. Membr. Sci.*, 280, pp. 889-898.

- Toh, Y., Loh, X., Li, K., Bismarck, A., & Livingston, A. (2007, March 15). In search of a standard method for the characterisation of organic solvent nanofiltration membranes. *Journal of Membrane Science*(291), pp. 120-125.
- Tsibranska, I., & Saykova, I. (2013, 05 25). Combining nanofiltration and other separation methods (review). *Journal of Chemical Technology and Metallurgy*(48), pp. 333-340.
- Tsibranska, I., & Tylkowski, B. (2012, September 17). Concentration of ethanolic extracts from *Sideritis* ssp. L. by nanofiltration: Comparison of dead-end and cross-flow modes. *Food and Bioproducts Processing*, pp. 169-174.
- Tylkowski, B., Tsibranska, I., Kochanov, R., Peev, G., & Giamberini, M. (2010, November 4). Concentration of viologically active compounds extracted from *Sideritis* ssp. L. by nanofiltration. *Food and Bioproducts Processing*(89), pp. 307-314.
- Ulrih, N. P., Gmajner, D., & Raspor, P. (2009). *Structural and physicochemical properties of polar lipids from thermophilic archaea*. Springer-Verlag.
- Zefikj, M. U. (2017). *Performance of Organic Solvent Nanofiltration Membrane for Purification of Omega-3*. Trondheim: NTNU - Norwegian University of Science and Technology - Department of Civil and Environmental Engineering.
- Zhang, H., & et al. (2016). Comparison Between Polydimethylsiloxane and Polyimide-Based Solvent-Resistant Nanofiltration Membranes. *Chemical Engineering Communications*(203(7)), pp. 870-879.
- Zhang, L., Wang, L., Zhang, G., & Wang, X. (2009). Fouling of nanofiltration membrane by effluent organic matter: characterization using different organic fractions. *J. Environ. Sci.*(21), pp. 49-53.

# 15 Appendix

## 15.1 Tables/Data

Table 12: Overview of the experimental plan.

	Name	Date	Duration	Dry matter (start)
	[-]	[dd.mm.yyyy]	[h]	[%]
1.module	RC01	13.03.-14.03.18	25.62	0.50
	S01	14.03.2018	0.26	0
	R02	14.03.-15.03.18	22.10	0.50
	S02	19.03.-20.03.2018	24.65	0
	RC03	20.03.-27.03.2018	166.77	0.50
	S03	27.03.2018	2.82	0
	S04	03.04.-04.04.2018	28.28	0
	DF01	04.04.-05.04.18	27.15	0.50
	S05	06.04.2018	5.35	0
	S06	08.04.-09.04.18	18.95	0
	DF02	09.04.-10.04.18	28.06	0.50
	S07_1	10.04.2018	0.29	0
	S07_2	11.04.-12.04.18	24.73	0
	DF03	12.04.-13.04.2018	27.39	0.50
	S08	13.04.2018	0.39	0
	S09	16.04.2018	1.80	0
	DF04	16.04.-17.04.2018	27.57	0.50
	S10	17.04.2018	0.36	0
	S11	18.04.2018	1.85	0
	DF05	18.04.-19.04.2018	27.03	0.30
	S12	19.04.2018	0.57	0
	S13	20.04.-23.04.2018	74.67	0
	DF6	23.04.-24.04.2018	26.94	0.30
	S14	24.04.2018	0.40	0
	S15	25.04.2018	2.06	0
	DF7	25.04.-26.04.2018	27.01	0.30
	S16	26.04.2018	0.28	0
	S17	02.05.-08.05.2018	147.54	0
T01+T02	08.05.-12.05.2018	96.02	0.30	



	S18	12.05.-13.05.2018	20.00	0	
	S19	14.05.-16.05.2018	52.18	0	
	T03	16.05.-18.05.2018	42.33	0.30	
	S20	18.05.-19.05.2018	2.47	0	
	DF08	19.05.-20.05.2018	21.77	0.50	
	2.module	S21	22.05.-25.05.2018	70.64	0
		DF09	25.05.2018	5.72	0.42
S22		25.05.-28.05.2018	61.67	0	
DF10		28.05.2018	8.52	0.42	
S23		28.05.-29.05.2018	17.55	0	
DF11		29.05.-30.05.18	19.95	0.63	
S24		31.05.-01.06.2018	4.08	0	

**Table 13: Pipette accuracy (1 ml) with pure water.**

06.04.2018		Fluid:	Pure water
Time: 11:51		Density (20 °C):	0.998 [g/ml]
Pipette:		1ml	(blue)
Number		Mass	Volume
[-]		[g]	[ml]
1		1.0097	1.0117
2		0.9990	1.0010
3		0.9994	1.0014
4		0.9961	0.9981
5		0.9959	0.9979
6		0.9933	0.9953
7		0.9935	0.9955
8		0.9950	0.9970
9		0.9947	0.9967
10		0.9929	0.9949
11		0.9924	0.9944
Average			<b>0.9985</b>

**Table 14: Measurement results from sampling – RC01.**

RC 01				
Permeate [mAU*min]	Retentate [mAU*min]	Time [h]	Permeate Flux [g/min]	Rejection
3.5611	-	1.22	9.55	-

2.47	140.17	2.60	9.23	98.24 %
2.6805	-	3.93	9.13	-
2.5970	-	5.75	8.91	-
2.5989	-	7.05	8.72	-
3.2186	140.5688	22.70	7.60	97.71 %
2.8605	-	26.83	7.43	-

**Table 15: Measurement results from – RC02.**

<b>RC 02</b>				
<b>Permeate</b>	<b>Retentate</b>	<b>Time [h]</b>	<b>Permeate Flux</b>	<b>Rejection</b>
2.0896	137.0947	30.57	7.36	98.48 %
2.9975	-	31.87	7.20	-
5.4173	-	46.60	6.56	-
3.1761	-	47.27	6.70	-
3.0680	-	50.90	6.60	-
3.1933	146.1956	52.82	6.54	97.82 %

**Table 16: Measurement results from sampling – RC03.**

<b>RC 03</b>				
<b>Permeate</b>	<b>Retentate</b>	<b>Time [h]</b>	<b>Permeate Flux</b>	<b>Rejection</b>
0.7635	134.7783	169.97	7.74	99.43 %
1.5434	-	170.68	7.60	-
1.8602	-	171.83	7.48	-
2.2277	-	173.03	7.30	-
5.2136	-	174.30	7.20	-
2.5109	-	175.02	7.12	-
2.8635	-	190.57	6.64	-
2.8660	-	192.30	6.68	-
2.9669	-	193.73	6.58	-
2.9037	-	195.67	6.56	-
2.9966	-	197.32	6.54	-
3.3805	-	214.55	6.24	-
3.5201	-	219.60	6.02	-
3.5647	-	221.55	6.06	-
3.8951	-	238.23	5.84	-
4.1569	-	243.47	5.74	-

4.1069	-	246.10	5.74	-
4.5864	-	264.83	5.58	-
4.7916	-	268.70	5.56	-
5.6441	-	310.52	5.46	-
5.8307	-	314.68	5.36	-
6.0508	-	318.68	5.36	-
6.1985	-	334.58	5.40	-
6.5993	163.2907	336.65	5.36	95.96 %

**Table 17: Measurement results from sampling – DF01.**

DF01					
Name	Permeate	Retentate	Time [h]	Permeate Flux	Rejection
<b>P01</b>	5.1472	133.1983	654.465	5.84	96.1 %
<b>P02</b>	5.7411	143.0421	657.54	5.24	96.0 %
<b>P03</b>	7.9762	158.6901	661.465	4.83	95.0 %
<b>P04</b>	16.3373	218.5599	672.205	4.74	92.5 %
<b>P05</b>	19.1735	248.9169	675.075	4.61	92.3 %
<b>P06</b>	23.5294	289.5355	678.065	4.34	91.9 %
<b>P07</b>	27.0312	350.0348	680.295	4.36	92.3 %
<b>P08</b>	33.2375	388.6205	682.523	4.24	91.4 %

**Table 18: Measurement results from sampling – DF02.**

DF02					
Name	Permeate	Retentate	Time [h]	Permeate Flux	Rejection
<b>F01</b>	-	139.4525	747.37	-	-
<b>P01</b>	13.8709	139.8043	748.805	6.32	90.1 %
<b>P02</b>	16.1087	156.9968	754.1425	4.02	89.7 %
<b>P03</b>	22.817	229.076	768.4375	3.77	90.0 %
<b>P04</b>	24.4214	255.2135	770.3875	3.66	90.4 %
<b>P05</b>	24.9514	270.9015	772.4975	3.69	90.8 %
<b>P06</b>	27.3174	279.512	773.5925	3.63	90.2 %
<b>P07</b>	28.4445	289.8645	774.6325	3.57	90.2 %
<b>P08</b>	30.3023	293.9316	775.7725	3.58	89.7 %
<b>P09</b>	31.0028	312.4297	776.6625	3.56	90.1 %

**Table 19. Measurement results from sampling – DF03.**

DF03					
------	--	--	--	--	--

Name	Permeate	Retentate	Time [h]	Permeate Flux	Rejection
<b>F01_1&amp;2</b>	-	147.723	820.2	-	-
<b>P01</b>	25.87	153.3555	821.685	3.3	83.1 %
<b>P02</b>	25.8876	162.1658	826.55	3.13	84.0 %
<b>P03</b>	35.0731	201.5828	840.875	3.17	82.6 %
<b>P04</b>	41.3613	223.2993	845.075	3.04	81.5 %
<b>P05</b>	44.5255	234.0755	847.045	3.02	81.0 %
<b>P06</b>	47.8645	247.2133	849.075	3.02	80.6 %

**Table 20: Measurement results from sampling – DF04.**

DF04					
Name	Permeate	Retentate	Time [h]	Permeate Flux	Rejection
<b>P01</b>	14.4177	141.6538	915.415	3.07	89.8 %
<b>P02</b>	34.8009	142.7998	921.855	2.99	75.6 %
<b>P03</b>	32.4143	146.068	936.2	3.39	77.8 %
<b>P04</b>	28.8319	146.3115	939.44	3.77	80.3 %
<b>P05</b>	27.253	152.1818	940.805	3.78	82.1 %
<b>P06</b>	27.3037	157.9718	942.11	3.71	82.7 %
<b>P07</b>	25.5958	162.3448	942.978	3.57	84.2 %

**Table 21: Measurement results from sampling – DF05.**

DF05					
Name	Permeate	Retentate	Time [h]	Permeate Flux	Rejection
<b>F01_1&amp;2</b>	-	89.541	962.89	-	-
<b>P01</b>	13.753	91.497	963.65	3.63	84.97 %
<b>P02</b>	16.2466	97.7113	966.92	3.81	83.37 %
<b>P03</b>	17.8102	116.4303	984.18	3.66	84.70 %
<b>P04</b>	17.7612	127.8703	987.25	3.8	86.11 %
<b>P05</b>	19.7473	143.0485	990.67	3.62	86.20 %

**Table 22: Measurement results from sampling – DF06.**

DF06					
Name	Permeate	Retentate	Time [h]	Permeate Flux	Rejection
<b>F01_1&amp;2</b>	-	85.6035	1085.65	-	-
<b>P01</b>	13.9402	86.0538	1086.54	3.83	83.80%
<b>P02</b>	13.703	93.9043	1089.52	3.55	85.41%
<b>P03</b>	18.5572	107.058	1106.93	3.74	82.67%

<b>P04</b>	19.2067	118.4428	1110.06	3.66	83.78 %
<b>P05</b>	22.0625	131.3168	1113.53	3.65	83.20 %

**Table 23: Measurement results from sampling – DF07.**

DF07					
Name	Permeate	Retentate	Time [h]	Permeate Flux	Rejection
<b>P01</b>	14.8965	85.657	1132.02	3.86	82.61 %
<b>P02</b>	16.3510	94.7763	1135.35	3.75	82.75 %
<b>P03</b>	19.4334	107.9473	1152.49	3.83	82.00 %
<b>P04</b>	21.1415	116.754	1155.28	3.73	81.89 %
<b>P05</b>	23.6285	134.203	1159.01	3.71	82.39 %

**Table 24: Measurement results from sampling – T01.**

T01					
Name	Permeate	Retentate	Time [h]	Permeate Flux	Rejection
<b>P01</b>	15.1851	84.0885	1440.99	7.49	81.9 %
<b>P02</b>	16.1736	80.9595	1443.09	7.2	80.0 %
<b>P03</b>	23.2358	82.2913	1459.37	6.93	71.8 %
<b>P04</b>	23.7129	82.2578	1462.04	6.75	71.2 %
<b>P05</b>	24.0617	82.042	1464.04	6.54	70.7 %
<b>P06</b>	25.2842	83.291	1486.17	5.99	69.6 %
<b>P07</b>	25.2639	82.7755	1488.27	5.94	69.5 %
<b>P08</b>	25.3527	83.5845	1491.89	5.83	69.7 %
<b>P09</b>	24.9553	0	1507.03	5.66	-
<b>P10</b>	25.2650	0	1510.07	5.49	-
<b>P11</b>	24.8668	84.6035	1511.67	5.45	70.6 %
<b>T01/T02_P01</b>	25.4688	0	1514	3.24	-

**Table 25: Measurement results from sampling – T02.**

T02					
Name	Permeate	Retentate	Time [h]	Permeate Flux	Rejection
<b>P01</b>	29,1175	75.0365	1516.285	3.46	61.2 %
<b>P02</b>	26,2959	78.5318	1535.725	3.26	66.5 %
<b>P03</b>	26,2874	79.967	1537	3.18	67.1 %

**Table 26: Measurement results from sampling – T03.**

T03					
-----	--	--	--	--	--

Name	Permeate	Retentate	Time [h]	Permeate Flux	Rejection
<b>T02/T03_P01</b>	38.3989	81.6163	1632.715	4.41	53.0 %
<b>P01</b>	37.049	79.9613	1633.745	2.83	53.7 %
<b>P02</b>	23.9302	79.1515	1675.065	2.03	69.8 %

**Table 27: Measurement results from sampling – DF08.**

DF08					
Name	Permeate	Retentate	Time [h]	Permeate Flux	Rejection
<b>F01_1&amp;2</b>	-	80.4438	1682.96	-	-
<b>P01</b>	45.3575	80.5923	1684.16	5.22	43.7 %
<b>P02</b>	20.8107	92.2675	1705.91	2.47	77.4 %

**Table 28: Measurement results from sampling – DF09.**

DF09					
Name	Permeate	Retentate	Time [h]	Permeate Flux	Rejection
<b>P01</b>	2.4669	134.4258	1849.07	8.8	98.2 %
<b>P02</b>	3.4928	169.1225	1852.03	8.6	97.9 %
<b>P03</b>	4.9103	236.6433	1854.71	8.1	97.9 %

**Table 29: Measurement results from sampling – DF10.**

DF10					
Name	Permeate	Retentate	Time [h]	Permeate Flux	Rejection
<b>P01</b>	2.4282	140.2105	1920.565	7.68	98.3 %
<b>P02</b>	4.8830	224.6048	1929.075	6.92	97.8 %

**Table 30: Measurement results from sampling – DF11.**

DF11					
Name	Permeate	Retentate	Time [h]	Permeate Flux	Rejection
<b>P01</b>	5.0136	228.0613	1951.48	6.69	97.8 %
<b>P02</b>	12.3255	302.6063	1966.51	5.04	95.9 %
<b>P03</b>	19.7535	416.2025	1971.45	4.73	95.3 %

**Table 31: UHPLC-results of RC01.**

UHPLC-results for RC01			
Comment	Name	PL - Area	Average PL
[-]	[-]	[mAU*min]	[mAU*min]
<b>Permeate 01</b>	004007.2.01	3.5532	3.5611
	004007.2.01	3.5689	

<b>Permeate 02</b>	004007.2.02	2.3985	2.4694
	004007.2.02	2.5403	
<b>Feed 01</b>	004007.2.F01	138.8828	140.1692
	004007.2.F01	141.4556	
<b>Permeate 03</b>	004007.2.03	2.5272	2.6805
	004007.2.03	2.8338	
<b>Permeate 04</b>	004007.2.04	2.5969	2.5970
	004007.2.04	2.597	
<b>Permeate 05</b>	004007.2.05	2.5869	2.5989
	004007.2.05	2.6109	
<b>Permeate 06</b>	004007.2.06	3.1933	3.2186
	004007.2.06	3.2438	
<b>Permeate 07</b>	004007.2.07	2.8501	2.8605
	004007.2.07	2.8708	
<b>Feed 02</b>	004007.2.F02	139.5889	140.5688
	004007.2.F02	141.5486	

**Table 32: UHPLC-results of RC02.**

<b>UHPLC-results for RC02</b>			
<b>Comment</b>	<b>Name</b>	<b>PL - Area</b>	<b>Average PL</b>
<b>[-]</b>	<b>[-]</b>	<b>[mAU*min]</b>	<b>[mAU*min]</b>
<b>Feed 01</b>	004009.2.F03	136.1392	137.0947
	004009.2.F03	138.0502	
<b>Permeate 01</b>	004009.2.2.08	2.1069	2.0896
	004009.2.2.08	2.0722	
<b>Permeate 02</b>	004009.2.3.09	2.9374	2.9975
	004009.2.3.09	3.0576	
<b>Permeate 03</b>	004009.2.4.10	5.4222	5.4173
	004009.2.4.10	5.4124	
<b>Permeate 04</b>	004009.2.5.11	3.1411	3.1761
	004009.2.5.11	3.211	
<b>Permeate 05</b>	004009.2.6.12	3.0748	3.068
	004009.2.6.12	3.0612	
<b>Permeate 06</b>	004009.2.7.13	3.2094	3.1933
	004009.2.7.13	3.1771	

<b>Feed 02</b>	004009.2.8.F04	145.6723	146.1956
	004009.2.8.F04	146.7189	

**Table 33: UHPLC-results of RC03.**

<b>UHPLC-results for RC03</b>			
<b>Comment</b>	<b>Name</b>	<b>PL - Area</b>	<b>Average PL</b>
<b>[-]</b>	<b>[-]</b>	<b>[mAU*min]</b>	<b>[mAU*min]</b>
<b>Feed 01</b>	004014.2.1.F05	134.3771	134.77825
	004014.2.1.F05	135.1794	
<b>Permeate 01</b>	004014.2.2.29	0.7393	0.7635
	004014.2.2.29	0.7877	
<b>Permeate 02</b>	004014.2.3.30	1.5789	1.5433
	004014.2.3.30	1.5078	
<b>Permeate 03</b>	004014.2.4.31	1.8941	1.8601
	004014.2.4.31	1.8262	
<b>Permeate 04</b>	004014.2.5.32	2.2695	2.2277
	004014.2.5.32	2.1858	
<b>Permeate 05</b>	004014.2.6.33	5.2040	5.2136
	004014.2.6.33	5.2231	
<b>Permeate 06</b>	004014.2.7.34	2.5191	2.5109
	004014.2.7.34	2.5027	
<b>Permeate 07</b>	004014.2.8.35	2.97	2.8635
	004014.2.8.35	2.757	
<b>Permeate 08</b>	004014.2.9.36	2.8561	2.8656
	004014.2.9.36	2.8758	
<b>Permeate 09</b>	004014.2.10.37	2.9613	2.9669
	004014.2.10.37	2.9724	
<b>Permeate 10</b>	004014.2.11.38	2.8465	2.9037
	004014.2.11.38	2.9609	
<b>Permeate 11</b>	004014.2.12.39	2.9627	2.9966
	004014.2.12.39	3.0304	
<b>Permeate 12</b>	004014.2.13.40	3.3926	3.3805
	004014.2.13.40	3.3683	
<b>Permeate 13</b>	004014.2.14.41	3.5187	3.5201
	004014.2.14.41	3.5215	



<b>Permeate 14</b>	004014.2.15.42	3.6059	3.5647
	004014.2.15.42	3.5234	
<b>Permeate 15</b>	004014.2.16.43	3.8905	3.8951
	004014.2.16.43	3.8997	
<b>Permeate 16</b>	004014.2.17.44	4.1575	4.1569
	004014.2.17.44	4.1562	
<b>Permeate 17</b>	004014.2.18.45	4.0529	4.1069
	004014.2.18.45	4.1609	
<b>Permeate 18</b>	004014.2.19.46	4.6287	4.5864
	004014.2.19.46	4.5441	
<b>Permeate 19</b>	004014.2.20.47	4.7985	4.7916
	004014.2.20.47	4.7847	
<b>Permeate 20</b>	004014.2.21.48	5.6776	5.6441
	004014.2.21.48	5.6106	
<b>Permeate 21</b>	004014.2.22.49	5.882	5.8307
	004014.2.22.49	5.7794	
<b>Permeate 22</b>	004014.2.23.50	6.0548	6.0508
	004014.2.23.50	6.0467	
<b>Permeate 23</b>	004014.2.24.51	6.1907	6.1985
	004014.2.24.51	6.2062	
<b>Permeate 24</b>	004014.2.25.52	6.5404	6.5993
	004014.2.25.52	6.6581	
<b>Feed 02</b>	004014.2.26.F06	167.3242	163.2907
	004014.2.26.F06	159.2571	

**Table 34: Conductivity data of the diafiltration test.**

	<b>DF5</b>	<b>DF6</b>	<b>DF7</b>	<b>DF9</b>	<b>DF10</b>	<b>DF11</b>
<b>Feed amount [g]</b>	8,918.6	9,000	9,000	6,032.4	7,275.3	6,754.5
<b>Ethanol amount [g]</b>	2,083	2,051.1	2,102.3	654.2	1,150	3,607
<b>Ethanol/feed [%]</b>	23.36	22.79	23.36	10.84	15.81	53.40
<b>Permeate [mmS/cm]</b>	218	202	208	371	366	271
<b>Retentate [mmS/cm]</b>	-	554	552	534	534	450
<b>Conductivity amount in permeate [%]</b>	-	26.72	27.37	40.99	40.67	37.59
<b>Conductivity amount in retentate [%]</b>	-	73.28	72.63	59.01	59.33	62.41

**Table 35: Measurement value deviation of the UHPLC exemplified with DF07, RC02 and T02.**

DF7	Sample 1	Sample 2	Sample 3	Sample 4	Sample 5	Sample 6	Sample 7	Sample 8	Sample 9	Sample 10	Sample 11	Average
#1	8.89	14.98	8.64	16.37	9.59	19.37	10.84	21.26	11.75	23.55	13.46	-
#2	8.89	14.81	8.55	16.33	9.45	19.50	10.80	21.02	11.66	23.70	13.39	-
#3	8.63	-	8.50	-	9.49	-	10.83	-	11.72	-	13.46	-
#4	8.65	-	8.58	-	9.38	-	10.71	-	11.57	-	13.38	-
SD	0.13	0.09	0.05	0.02	0.08	0.06	0.05	0.12	0.07	0.08	0.04	<b>0.07</b>
SD (%)	1.45	0.58	0.61	0.13	0.83	0.33	0.50	0.58	0.59	0.32	0.30	<b>0.57</b>
RC02	Sample 1	Sample 2	Sample 3	Sample 4	Sample 5	Sample 6	Sample 7	Sample 8	Sample 9	Sample 10	Sample 11	Average
#1	136.14	2.11	2.94	5.42	3.14	3.07	3.21	145.67	-	-	-	-
#2	138.05	2.07	3.06	5.41	3.21	3.06	3.18	146.72	-	-	-	-
SD	0.96	0.02	0.06	0.00	0.03	0.01	0.02	0.52	-	-	-	<b>0.20</b>
SD (%)	0.70	0.83	2.01	0.09	1.10	0.22	0.51	0.36	-	-	-	<b>0.73</b>
T02	Sample 1	Sample 2	Sample 3	Sample 4	Sample 5	Sample 6	Sample 7	Sample 8	Sample 9	Sample 10	Sample 11	Average
#1	25.35	29.01	7.53	7.53	25.52	7.43	7.39	25.15	7.64	7.53	2.99	-
#2	25.59	29.22	7.53	7.42	27.07	8.43	8.16	27.43	8.45	8.35	2.82	-
SD	0.12	0.11	0.00	0.05	0.77	0.50	0.39	1.14	0.41	0.41	0.08	<b>0.36</b>
SD (%)	0.47	0.36	0.01	0.69	2.95	6.31	4.96	4.34	5.04	5.16	2.81	<b>3.01</b>

**Table 36: Test results of laboratory test - basis for calculations.**

<b>DF</b>	<b>DM-Start</b>	<b>Start</b>	<b>End Retentate</b>	<b>End Permeate</b>	<b>Ethanol input</b>	<b>Time</b>
<b>[-]</b>	<b>[%]</b>	<b>[g]</b>	<b>[g]</b>	<b>[g]</b>	<b>[g]</b>	<b>[h]</b>
<b>5</b>	0.30	8918.6	4592.9	6202.3	2083.0	28.18
<b>6</b>	0.30	9000.0	4747.5	6186.5	2051.1	28.42
<b>7</b>	0.30	9000.0	4153.9	6343.3	2102.3	28.22
<b>9</b>	0.42	6032.4	2968.6	3637.4	654.2	7.38
<b>10</b>	0.42	7275.3	3785.9	4607.8	1150.0	10.45
<b>11</b>	0.63	6754.5	2550.5	7108.3	3607.0	22.45

# 15.2 Figures

